University of Kentucky
UKnowledge

Theses and Dissertations--Mining Engineering | Mining Engineering

2017

ESTIMATING THE EFFECTS OF BLASTING VIBRATIONS ON THE HIGH-WALL STABILITY

Abhinav Sharma
University of Kentucky, abhinav42sharma@gmail.com
Author ORCID Identifier:
https://orcid.org/0000-0001-8732-4750
Digital Object Identifier: https://doi.org/10.13023/ETD.2017.467

Right click to open a feedback form in a new tab to let us know how this document benefits you.

Recommended Citation

Sharma, Abhinav, "ESTIMATING THE EFFECTS OF BLASTING VIBRATIONS ON THE HIGH-WALL STABILITY" (2017). *Theses and Dissertations--Mining Engineering*. 38.
https://uknowledge.uky.edu/mng_etds/38

This Master's Thesis is brought to you for free and open access by the Mining Engineering at UKnowledge. It has been accepted for inclusion in Theses and Dissertations--Mining Engineering by an authorized administrator of UKnowledge. For more information, please contact UKnowledge@lsv.uky.edu.

STUDENT AGREEMENT:

I represent that my thesis or dissertation and abstract are my original work. Proper attribution has been given to all outside sources. I understand that I am solely responsible for obtaining any needed copyright permissions. I have obtained needed written permission statement(s) from the owner(s) of each third-party copyrighted matter to be included in my work, allowing electronic distribution (if such use is not permitted by the fair use doctrine) which will be submitted to UKnowledge as Additional File.

I hereby grant to The University of Kentucky and its agents the irrevocable, non-exclusive, and royalty-free license to archive and make accessible my work in whole or in part in all forms of media, now or hereafter known. I agree that the document mentioned above may be made available immediately for worldwide access unless an embargo applies.

I retain all other ownership rights to the copyright of my work. I also retain the right to use in future works (such as articles or books) all or part of my work. I understand that I am free to register the copyright to my work.

REVIEW, APPROVAL AND ACCEPTANCE

The document mentioned above has been reviewed and accepted by the student's advisor, on behalf of the advisory committee, and by the Director of Graduate Studies (DGS), on behalf of the program; we verify that this is the final, approved version of the student's thesis including all changes required by the advisory committee. The undersigned agree to abide by the statements above.

Abhinav Sharma, Student

Dr. Jhon Silva-Castro, Major Professor

Dr. Zacharias Agioutantis, Director of Graduate Studies

ESTIMATING THE EFFECTS OF BLASTING VIBRATIONS ON THE HIGH-WALL STABILITY

THESIS

A thesis submitted in partial fulfillment of the
requirements for the degrees of Master of Science in
Mining Engineering in the College of Engineering
at the University of Kentucky

By
Abhinav Sharma
Lexington, Kentucky

Director: Dr. Jhon Silva-Castro
Assistant Professor of Mining Engineering
Lexington, Kentucky

December 2017

Copyright © Abhinav Sharma 2017

https://orcid.org/0000-0001-8732-4750

ABSTRACT OF THESIS

ESTIMATING THE EFFECTS OF BLASTING VIBRATIONS ON THE HIGH-WALL STABILITY

The stability of the high-walls is one of the major concerns for open pit mines. Among the various factors affecting the stability of high-walls, blast vibrations can be an important one. In general, worldwide the established respective government regulations and industry standards are used as guidance to determine the maximum recommended levels of the peak particle velocity and frequency from the blast to avoid any effects on the structures around the mining project. However, most of the regulations are meant for buildings or houses and do not concern high-walls.

This thesis investigates the response of high-walls under the effects of vibrations from mine blasting. In this research, the relationship between the high-wall response, the geometry of the slope, the frequency and the amplitude, of the ground vibration produced by blasting, is explored using numerical models in 3DEC. The numerical models were calibrated initially with data collected using seismographs installed in a surface mine operation and recording vibrations produced by an underground mine drill and blast operation. Once the calibration was accomplished, a parametric study was developed to explore the relationships between various parameters under study and its impact on the stability of high-walls.

KEYWORDS: High-walls, blasting vibrations, frequency, amplitude, 3DEC, numerical modeling

Abhinav Sharma
Student's Signature

December 4th, 2017
Date

ESTIMATING THE EFFECTS OF BLASTING VIBRATIONS ON THE HIGH-WALL STABILITY

By

Abhinav Sharma

Dr. Jhon Silva-Castro

Director of Thesis

Dr. Zacharias Agioutantis

Director of Graduate Studies

December 4th, 2017

(Date)

DEDICATION

This thesis is dedicated to my mother, father, and family.

I have been extremely fortunate to have been brought up by them, who instilled in me the desire to continue my education. Without their help and support, this research would not have been possible.

ACKNOWLEDGEMENTS

I would like to express my deepest gratitude to all those who provided insight and expertise that greatly assisted this research.

I am thankful to Dr. Jhon Silva-Castro who gave me the opportunity to join his research team. I am extremely grateful to Dr. Silva who has been a great advisor and mentor. His guidance helped me at all the stages of the project and writing of this thesis. He consistently allowed this research to be my own work but steered me in the right direction whenever I needed it.

I would like to thank Dr. Kyle Perry who accepted my application to join the Department of Mining Engineering at the University of Kentucky. I would like to thank Dr. Perry and Dr. Michael Kalinski for being part of my Thesis Committee and giving the valuable inputs.

I am thankful to The National Institute for Occupational Safety and Health (NIOSH) for having funded the research. I would like to extend my sincere thanks to the Nally & Gibson management, for facilitating us to conduct the field study at their Georgetown Limestone Quarry and for all their efforts in ensuring successful data collection.

I would like to express my sincere gratitude to my fellow graduate students especially without whom conducting the various test programs and field data collection for this project would have been impossible. Further thanks to the whole Mining engineering department for creating a wonderful atmosphere, which made my stay at the department truly memorable.

Finally, I would like to thank my family for all their support and encouragement.

TABLE OF CONTENTS

ACKNOWLEDGEMENTS iii
TABLE OF CONTENTS iv
LIST OF TABLES vi
LIST OF FIGURES vii
1 Introduction 1
1.1 Background 1
1.2 Blasting Vibrations 2
1.1 Problem Statement 4
1.2 Supplemental Tools 5
1.3 Organization of the Thesis 6
2 Literature Review 7
2.1 Blasting Vibrations 7
2.1.1 General Characteristics of Blast Vibrations 8
2.1.2 Movement of the waves 9
2.1.3 Parameters describing vibration 12
2.1.4 Vibration Amplitude 13
2.1.4 Vibration Frequency 15
2.2 Slope Stability 17
2.2.1 General modes of Slope failure 20
2.2.2 Mechanical approach to Stability Analysis 22
2.3 Attempts at studying and preventing effects of vibration on Slope Stability 24
2.3 Numerical Modeling 33
2.3.1 Numerical Modeling application in Slope Stability Analysis 36
2.4 Vibration Standards 37
3 Experiment 42
3.1 Experiment Stages 42
3.1.1 Field data collection 43
3.1.1.1 Seismograph Setup 44
3.1.1.2 Site Scanning 44
3.1.2 Data Processing 45
3.1.2.1 Scanner Data Processing 46

3.1.2.2 Vibration Data assessment 46
3.1.3 Numerical Modeling 47
3.2 Calibration of the Model 49
3.3 Parametric Study 50
3.3.1 Establishing the natural frequency of the 100ft model 53
3.3.2 Effect of height of the high-wall on natural frequency 60
3.3.3 Effect of slope of the high-wall on natural frequency 61
3.3.4 Effect of the amplitude of the vibration on natural frequency of high-wall 65
4 Results 67
5 Conclusions and Recommendations 70
5.1 Future Course of Action 71
Appendix 72
A. Variation in the natural frequency with the height of high-wall 72
A1. Model: 300ft and 90 degrees 72
A2. Model: 500ft and 90 degrees 75
B. Variation in the natural frequency with the slope of high-wall 78
B1. Model: 100ft and 65 degrees 78
B2. Model: 100ft and 30 degrees 82
C. Variation in high-wall natural frequency with the amplitude of vibration 85
C1. Model: 100ft and 3 in/s Amplitude 85
C2. Model: 100ft and 5 in/s Amplitude 88
Bibliography 91
VITA 95

LIST OF TABLES

Table 1-1: High-wall fatalities compared with total surface mining fatalities (MSHA, 2017) 2

Table 2-1: Range of typical blast parameters 13

Table 2-2: DGMS prescribed permissible limits for ground vibration in India 41

Table 3-1: Properties of Limestone assigned in model 47

Table 3-2: Various parameters considered for the study and their variations 51

Table 3-3: Variation in Natural Frequency with Height of the High-wall 61

Table 3-4: Variation of the Natural Frequency of the high-wall with Slope angle 65

Table 3-5: Effect of change in amplitude on Natural Frequency of High-wall 66

LIST OF FIGURES

Figure 1-1: Typical high-wall mining operation (contourmining.com, Sep 20, 2017)..... 1

Figure 1-2: USBM RI 8507 Safe Blasting Levels 3

Figure 1-3: High-wall under study at Nally & Gibson, Limestone Quarry, Georgetown, Kentucky..... 5

Figure 2-1: A typical seismograph (Source: Glossary, Blasting Training International)... 8

Figure 2-2: A seismograph record measured in the field with all the three dimensions 9

Figure 2-3: Movement of the body waves from the blast-hole (M.S. Far et. al, 2016) 10

Figure 2-4: A general distinction of the three wave types monitored at large distance from blast-hole (Geological Digressions, Archives Geophysics) 11

Figure 2-5: Particle motion variation with wave type (Weebly, Earthquakes)..... 12

Figure 2-6: Sine wave with repetitive motion with time (Introduction to Waves, Wordpress) 14

Figure 2-7: FFT of a signal giving a frequency distribution curve..... 16

Figure 2-8: Slope Configuration (Arteaga et. al, 2014)..... 18

Figure 2-9: Orientation of a plane (Engineering 360, Geotechnical Services Information) 19

Figure 2-10: Different modes of slope failure in rock masses (R.Rai, Slope Lecture)..... 21

Figure 2-11: Block on an inclined plane at limiting equilibrium (Rock Slope Stability, C.A. Kliche)..... 23

Figure 2-12: Pre-split formation through instantaneous initiation of closely spaced holes (P.Dunn, 1995) 26

Figure 2-13: Approximate Powder Factor in Cushion Blasting (C.J. Konya, 1980)..... 28

Figure 2-14: Section-view of Non-Pre-Split Final Design 29

Figure 2-15: Design for the third trial..... 30

Figure 2-16: East Ramp High-Wall of the mine..... 32

Figure 2-17: Single hole blast vibration Power Spectrum..... 32

Figure 2-18: Transient vibration guide values for the cosmetic damage BS 5228-2:2009 38

Figure 2-19: DIN-4150 (3) Vibration velocity levels for the evaluation of the short term and long-term impact 39
Figure 2-20: Building categories, SN 640312 40
Figure 2-21: Frequency range for the various building types 40
Figure 3-1: Experimental setup process of the research 42
Figure 3-2: High-wall under study at Nally & Gibson, Limestone Quarry, Georgetown, Kentucky 43
Figure 3-3: Setting up seismograph in field for data collection 44
Figure 3-4: Maptek I-Site 8800 Scanner used to scan high-wall in field 45
Figure 3-5: Model generated by I-Site software from scan data collected in field 46
Figure 3-6: Vibration data accessed using Seismograph Data Analysis 47
Figure 3-7: 3D model with boundary conditions for the numerical model in 3DEC 48
Figure 3-8: Schematic 2D diagram of a 100ft model for the analysis 49
Figure 3-9: Velocity record data collected in the field 50
Figure 3-10: Calibration of the model by using the field vibration data 50
Figure 3-11: An artificial ground vibration sine wave with a frequency of 5 Hz 52
Figure 3-12: Output Displacement at the crest on various Input Shear Wave Frequencies 53
Figure 3-13: The X-displacement time history for the 5 Hz stress wave on 100ft model 54
Figure 3-14: The X-displacement contour for the 5 Hz stress wave on 100ft model 54
Figure 3-15: The X-displacement time history for the 20 Hz stress wave on 100ft model 55
Figure 3-16: The X-displacement contour for the 20 Hz stress wave on 100ft model 55
Figure 3-17: The X-displacement time history for the 30 Hz stress wave on 100ft model 56
Figure 3-18: The X-displacement contour for the 30 Hz stress wave on 100ft model 56
Figure 3-19: The X-displacement time history for the 30 Hz stress wave on 100ft model 57
Figure 3-20: The X-displacement contour for the 38 Hz stress wave on 100ft model 57
Figure 3-21: The X-displacement time history for the 50 Hz stress wave on 100ft model 58

Figure 3-22: The X-displacement contour for the 50 Hz stress wave on 100ft model 58
Figure 3-23: The X-displacement time history for the 60 Hz stress wave on 100ft model 59
Figure 3-24: The X-displacement contour for the 60 Hz stress wave on 100ft model 59
Figure 3-25: Displacement vs Frequency, with 38 Hz natural frequency of the 100ft high-wall 60
Figure 3-26: The X-displacement time history for the 20 Hz stress wave on 100ft model 61
Figure 3-27: The X-displacement contour for the 20 Hz stress wave on 100ft model 62
Figure 3-28: The X-displacement time history for the 28 Hz stress wave on 100ft model 62
Figure 3-29: The X-displacement contour for the 28 Hz stress wave on 100ft model 63
Figure 3-30: The X-displacement time history for the 44 Hz stress wave on 100ft model 63
Figure 3-31: The X-displacement contour for the 44 Hz stress wave on 100ft model 64
Figure 3-32: The X-displacement time history for the 55 Hz stress wave on 100ft model 64
Figure 3-33: The X-displacement contour for the 55 Hz stress wave on 100ft model 65
Figure 4-1: Line Graph between Natural Frequency and High-Wall Height 67
Figure 4-2: Variation of Natural Frequency with Slope of High-Wall for various heights 68
Figure 4-3: Comparison of Displacement and Frequency with Amplitude of 1 in/s & 3 in/s 69

1 Introduction

1.1 Background

Usually, after an open-pit mine excavation, a high-wall remains which is either abandoned or covered. But with the development of high-wall miners, they are sometimes left to recover the precious mineral in the future to justify the ever-increasing high stripping cost in open-pit mining or in some cases support the underground excavation. These two facts have resulted in larger high-walls that are left standing for increased periods of time prior to reclamation. These long-standing high-walls with constant exposure to wear and tear of mining operations, natural processes like rain, snow etc. have resulted in greater exposure to the risk for miners and an elevated probability of serious accidents, which have sometimes turned out to be fatal. Figure 1-1 shows a typical high-wall mining operation in the Appalachian region in the USA.

Figure 1-1: Typical high-wall mining operation (contourmining.com, Sep 20, 2017)

The total number of surface mining fatalities has always been a concern and remains the top priority for the mines. The modernization, improved studies, increased focus on safety has helped in reducing the numbers as compared to past, but it is still high from the coveted target of zero fatalities. Since 2005, the fatalities related to high-wall failures are close to 9.5% (Table 1-1) of the total fatalities in surface mining. Most of the modern surface mining fatalities are associated with machinery and haulage.

Table 1-1: High-wall fatalities compared with total surface mining fatalities (MSHA, 2017)

Year	High-wall Failure Fatalities	Total Surface Fatalities	Year	High-wall Failure Fatalities	Total Surface Fatalities
2017	1	10	2010	0	3
2016	1	10	2009	0	4
2015	0	12	2008	1	5
2014	0	14	2007	2	7
2013	1	10	2006	1	6
2012	0	3	2005	0	2
2011	2	8	**Total**	**9**	**94**

The high-wall stability is a problem that is affected by various factors like, geology, discontinuities in the rock mass, stresses, mining operations, standing time, weathering due to surroundings and many others. But of them all, one of the important factors that is relatively less talked or emphasized upon is the blasting induced stress, which over the period can result in devastating outcomes when least expected.

The current study aims to delve into the forefront of understanding the effects of these blast -induced stresses on a high-wall and determine the extent to which and how these stresses affect the stability of high-wall.

1.2 Blasting Vibrations

Blasting of rocks using explosives remains the cheapest, simplest and most widely used method to fragment and heave rock for the construction and mining industries. Part of the energy released in the process of blasting is used for fragmenting or moving the rock, and a part of the energy released during the chemical process is wasted in the form of heat, vibration, sound, etc. Out of these various parts of energy that are not utilized for the rock fragmentation and movement, vibrations and sounds are the most studied and observed

parameters. Sounds and vibrations effects of a mining blast are more perceptible to humans and can have significant damaging effects on both humans and structures.

Based, on the damaging effects and human perception studies, various leading government organizations across the countries established maximum recommended levels of vibrations and sound generated from mining and construction operations to operate and to safeguard structures. One of such organizations was the United States Bureau of Mines (USBM). After years of research, a Report of Investigation (RI) 8507 was released by USBM, which the main contribution to the mining industry is shown in Figure 1-2 and is known as the Z curve.

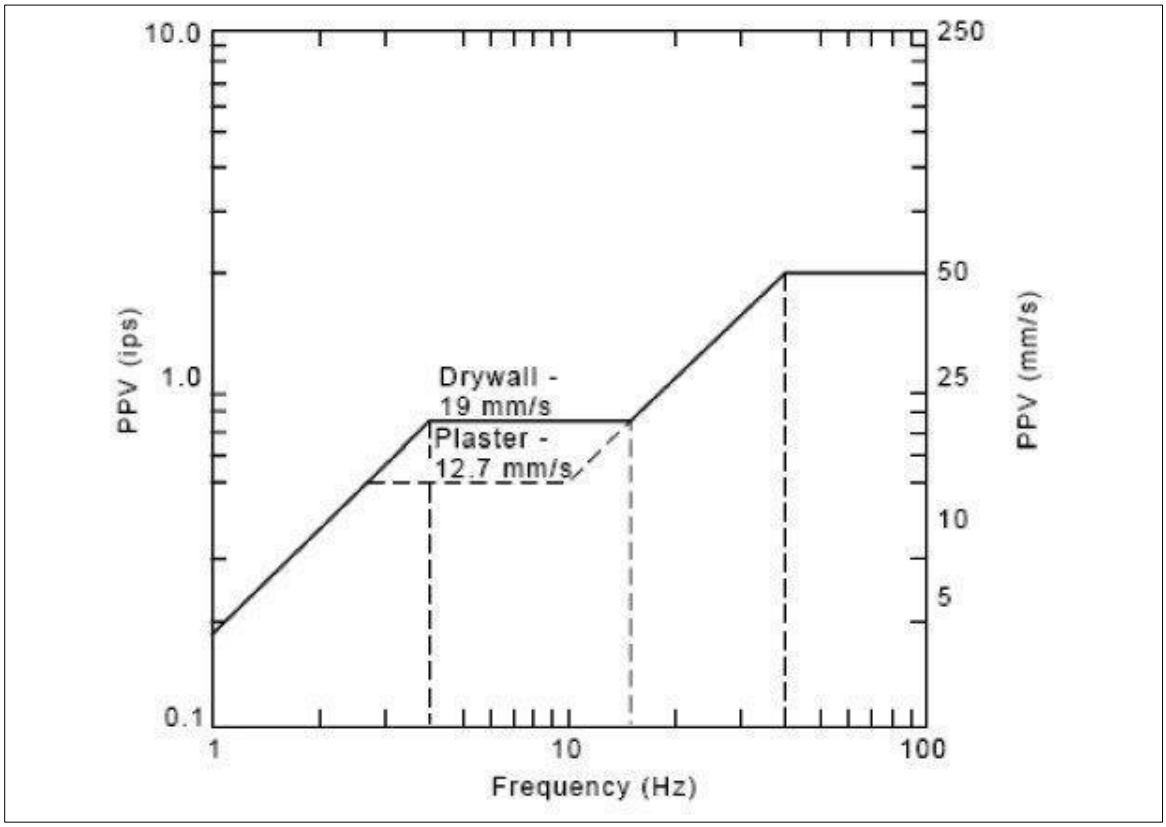

Figure 1-2: USBM RI 8507 Safe Blasting Levels

According to the Z curve, any ground vibration (the peak particle velocity or PPV) produced by a mining operation above the solid line will generate damage to the structures. If the PPV is below the line, the safety of the structure without damage is assured. Another important concept as per the Z curve is that the mining operations can operate at higher PPV values if the generated blast vibration is composed of a high-frequency content. So,

usually, it is a general practice in mining to “shift” the ground vibration frequencies produced by blasting to higher levels to prevent damage to structures. However, as mentioned before, the Z curve was developed for the safety of structures (one story rural houses) under certain blasting conditions and cannot be applied to high-walls. The levels of vibrations and frequencies which affect high-walls could be different from mine to mine, and damaging effects might not govern from the usual blasting standards set for human structures.

1.1 Problem Statement

The current research investigates the impacts of the dynamic stresses generated due to blasting on the high-walls and tries to correlate its damage to blasting vibration, frequencies, amplitude, and duration.

The research is divided into two phases, where in Phase 1, the focus is the on collection of the field data by setting up seismographs to record blasting vibrations and use of a scanner to collect the scan data of walls. Phase 2, of the research, is the parametric study based on the calibrated numerical model to understand the relationship between parameters like frequency, geometry on the stability of high-walls.

Phase 1

The first part of the research concentrates on studying high-wall as shown in Figure 1-3 and the case under study is Nally and Gibson, Georgetown Limestone Quarry located in Georgetown Kentucky, where the underground excavation of limestone is done using drill and blast.

Phase 1 was carried out in two stages with field data collection of vibration histories and scan data of the high-walls at various stages. The vibration histories collected from the field were used as an input to calibrate the model in Phase 2 of the project. The scanned data collected using the Maptek I-Site 8800, is used to design surfaces and could be used as an input for the Three-Dimensional Discrete Element Code (3-DEC) for further numerical simulation. In the present research, due to time constraint, this was not utilized, but it can be a further course of the study for the future work.

Figure 1-3: High-wall under study at Nally & Gibson, Limestone Quarry, Georgetown, Kentucky

Phase 2

Usually, the mines look for the established government regulations for guidance to determine the peak particle velocity and frequency levels. But most of the regulations around the globe are meant for the structures surrounding mine and does not concern high-walls.

The parametric study in this phase explores numerical models in 3DEC to understand the impact of parameters like the geometry of the slope, the frequency, the amplitude, and the duration of the blasting vibrations on high-wall stability. The models in use were calibrated initially with data collected from seismographs in the first phase of the research. The study also tries to explore if the any of the outcomes can help the mines to design their blast more prudently.

1.2 Supplemental Tools

Various tools were the key to achieving the outcome of the research. They were important in various stages of the research.

In the primary stage of the field data collection, following tools made the basis for it:

1. Seismographs

The seismograph was set up to collect the vibration, frequency, amplitude of the blast vibrations. The data collected by the seismographs is accessed remotely using a modem used to transmit data.

2. Maptek-I-Site Laser Scanner

The high-wall under study was scanned using Maptek I-Site 8800. The scanner is set up in the field at multiple locations, usually three, to cover the high-wall from all the angles. The scanner takes a 360° picture of the area and the picture is divided into multiple sections to scan as per the requirement. The scanned data is stored in a portable hand-held controller which can be later imported to a personal computer for further processing.

3. Three-Dimensional Discrete Element Code (3DEC)

3DEC is a three-dimensional numerical program based on the distinct element method for discontinuum modeling from Itasca. This numerical program allows finite displacements and rotations of discrete bodies, including complete detachment (User's Guide 3DEC version 5.0). It has a command driven structure for programming. The various numerical models for the parametric study were generated using the 3DEC.

1.3 Organization of the Thesis

The thesis is divided into five main chapters. Chapter 1 provides the background leading to the research. It also discusses the purpose of the project. Chapter 2 is focused on the literature review and discusses the previous attempts to study the high-wall stability. Chapter 3 focuses on the experiments and the setup for the research. Chapter 4 discusses the outcomes of the results of the study. Finally, chapter 5 summarizes the results and conclusions.

2 Literature Review

2.1 Blasting Vibrations

Vibrations can be described as a passage of the energy which oscillates the particles of the material about an average position. The vibrations at a point could be of the low intensity or the high intensity depending on the various parameters like the source of energy, distance from the source, mode of transportation of energy etc.

Ground vibrations due to blasting are a similar passage of the energy, released from the blasting operations in mines, quarries, and other construction activities. Vibrations need a medium to travel, which is different from light and electromagnetic waves that can travel within the vacuum. As the name suggests, ground vibrations propagate through the earth and are sometimes termed as seismic waves as their propagation properties are similar to the ground motions produced by earthquakes (David Siskind, 2005). But blasting vibrations are primarily different with their low peak amplitude and high dominant frequencies than earthquakes due to the source of energy and lower distance of propagation.

To understand these ground vibrations, they are measured in terms of velocity, displacement or acceleration at the point of interest. The seismograph as shown in Figure 2-1 is an instrument that records vibrations of the particle in all the three directions i.e. vertical, transverse and longitudinal to understand the complete movement. The time history recorded by these seismographs is a waveform, a continuous representation of the particle movement.

Figure 2-1: A typical seismograph (Source: Glossary, Blasting Training International)

2.1.1 General Characteristics of Blast Vibrations

The passage of the ground vibrations makes the ground to move in an elliptical manner in three dimensions. To understand and measure this movement the motion is recorded in all the three dimensions, longitudinal, transverse and vertical as shown in the Figure 2-2. In the given figure, the X-axis is time and Y-axis is the velocity measured continuously at all point of times on the curve. Longitudinal component is usually along the horizontal direction of explosion and other two components are perpendicular to it with, vertical being vertical and transverse being in the radial direction.

The three wave types are divided into two varieties:

1. Body Waves

2. Surface Waves

Body waves are the waves that travel through the body of the rock and soil, whereas surface waves propagate along a surface-air interface.

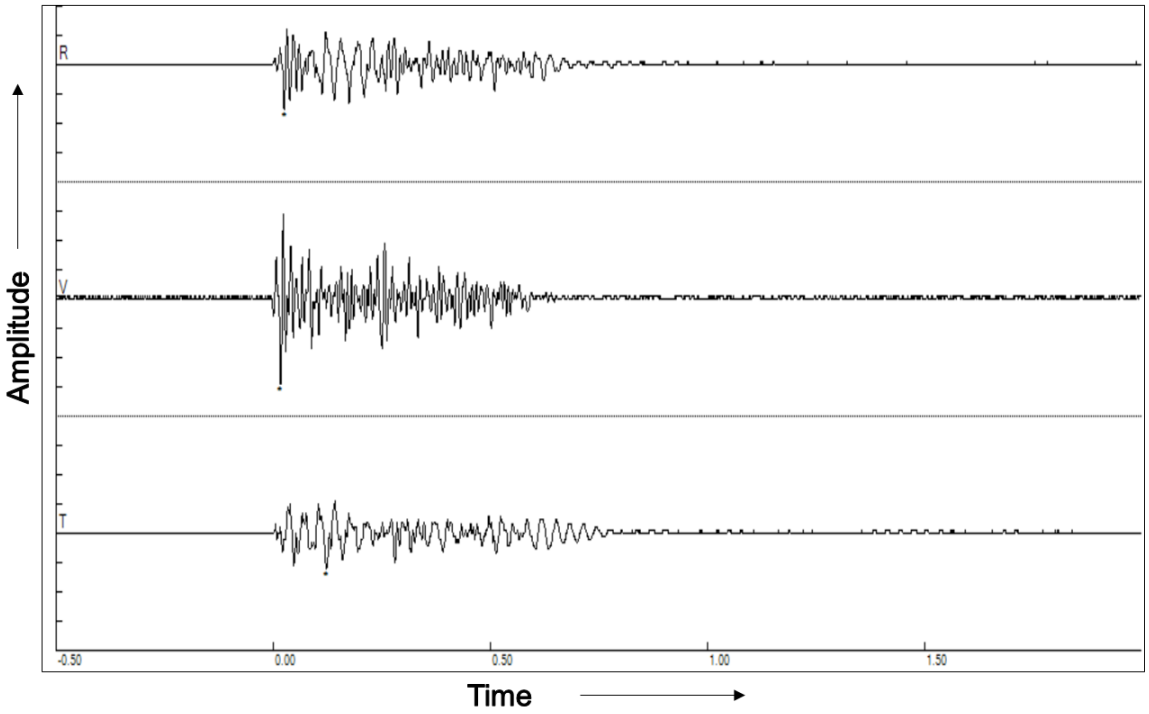

Figure 2-2: A seismograph record measured in the field with all the three dimensions

Body waves are further divided into two types:

1. Primary waves (P-wave)

2. Shear waves (S-wave)

Primary waves are compressive in nature and the shear waves are distortional in nature. The surface waves are more commonly known as Rayleigh waves and become significant usually at a distance from the source of the blast.

2.1.2 Movement of the waves

A blast hole explosion results in the generation of the body waves at small distances. These waves propagate in a spherical manner as shown in the Figure 2-3, are pre-dominantly the P-waves, which on intersection with a crack or fracture or any other rock type results into the generation of the shear and surface waves.

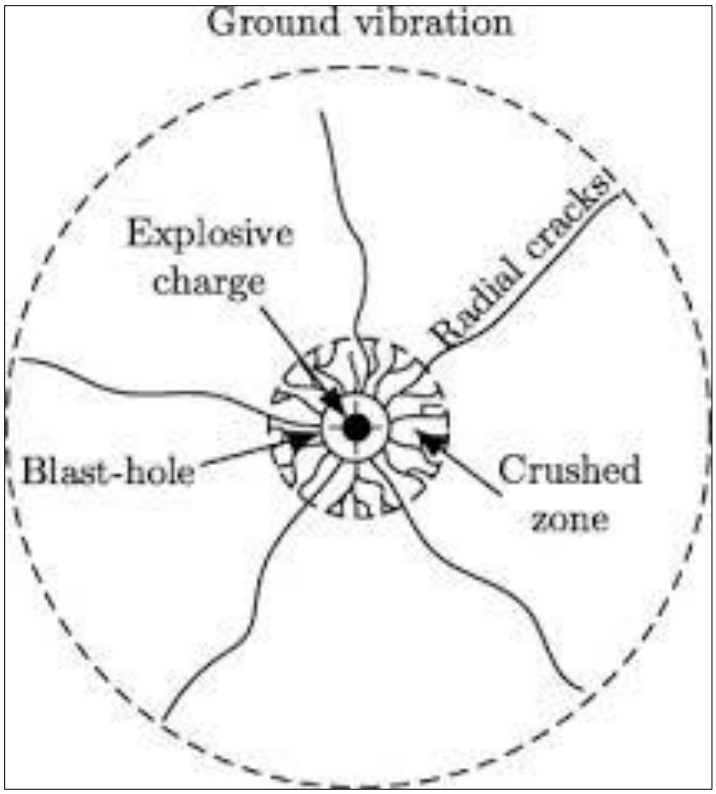

Figure 2-3: Movement of the body waves from the blast-hole (M.S. Far et. al, 2016)

At small distances, usually, all the three wave types reach at the same time and it is difficult to identify them. But at large distances, the shear wave and the surface waves which are relatively slow as compared to the compressive waves are easy to distinguish as shown in Figure 2-4.

In blasting operations, the blast-holes fire in a sequence of few milliseconds resulting in overlapping of the waves and makes it a difficult phenomenon to understand. But single hole shots study (Reihart, 1975) gave a better understanding of the effects of the blasting vibrations.

Usually, the blasting personnel are not concerned about the individual types of the waves and focus on measuring and analyzing the highest amplitude for the purpose of blast design. But sometimes the wave type is also of concern when the generation mechanism is relevant.

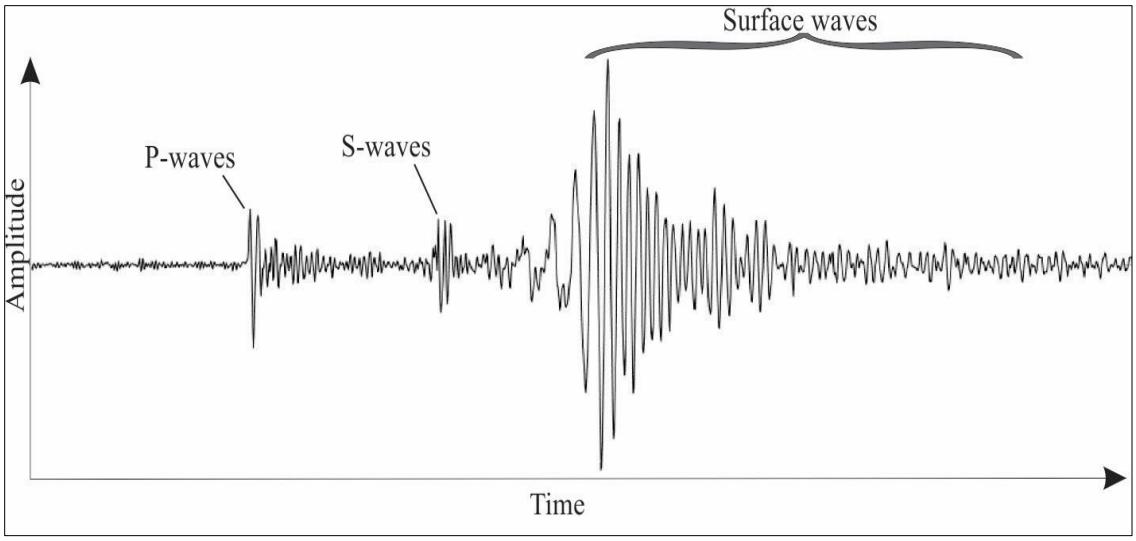

Figure 2-4: A general distinction of the three wave types monitored at large distance from blast-hole (Geological Digressions, Archives Geophysics)

The three waves create a completely different movement of the particle when they pass through rock or soil as shown in the Figure 2-5. Thus, they have the different effect on the structure concerned. The longitudinal wave (P-wave) generates motion of the particle in the direction of propagation, the shear wave (S-wave) produces motion perpendicular to the direction of propagation. The surface wave (Rayleigh wave) generates motion of the particle both in the perpendicular and parallel direction of propagation.

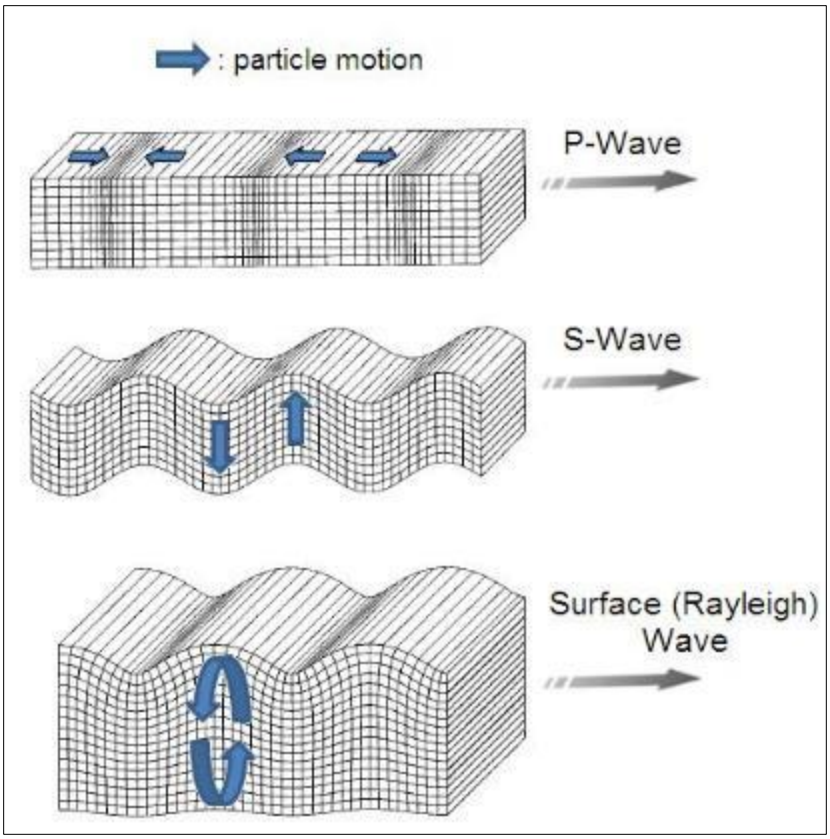

Figure 2-5: Particle motion variation with wave type (Weebly, Earthquakes)

2.1.3 Parameters describing vibration

A typical particle motion time history graph i.e. a vibration plot is described mainly by the following:

1. Peak amplitude
2. Principal frequency
3. Duration of the motion

These parameters are dependent on various properties such as the strength of the rock, propagation medium, and the blasting sequence or blast timing. The range of parameters determining the characteristics of the vibration for general mine blasting, quarrying, and construction operations are presented in the Table 2-1 (Cording et al. 1975).

Table 2-1: Range of typical blast parameters

Parameter	Range
Displacement	10^{-4} to 10 mm
Particle Velocity	10^{-4} t 10^{3} mm/s
Particle Acceleration	10 to 10^{5} mm/s^{2}
Pulse Duration	0.5 to 2 s
Wavelength	30 to 1500 m
Frequency	0.5 to 200 Hz

The two important characteristics that make a blast vibration different from the earthquake are:

1. The vibrations occur at relatively higher frequencies as compared to earthquake

2. The energy contained in the motion is minute as compared to an earthquake

2.1.4 Vibration Amplitude

The particle motion is most commonly measured in the form of displacement, velocity or acceleration. Most of the current seismographs measure velocity and the major safety regulations set up by the countries also have velocity limits.

To study blasting vibrations they are approximated as sine waves varying in time or distance. The approximation helps in simple conversions in between the velocity, acceleration, and displacement.

The general form of sine wave used in blasting vibrations can be understood with equation for the displacement, *u*,

$$u = U \sin (Kx + \omega t) \qquad (2.1)$$

where;

U is maximum displacement

K is constant know as wave number

ω is circular natural frequency

t is time

If the location and wavelength are constant, the variation of displacement with time can be written as;

$$u = U \sin (\text{constant} + \omega t) \tag{2.2}$$

As can be seen from the Figure 2-6, the wave repeats itself after a certain fixed time called as the period T, ω must be equal to $2\pi/T$ to make the function repeat when time moves by a period. As frequency is the number of times waves repeats itself in a second, so frequency is equal to 1/T. So, the circular natural frequency can be given as,

$$\omega = 2\pi/T \tag{2.3}$$

$$f = 1/T \tag{2.4}$$

$$\omega = 2\pi f \tag{2.5}$$

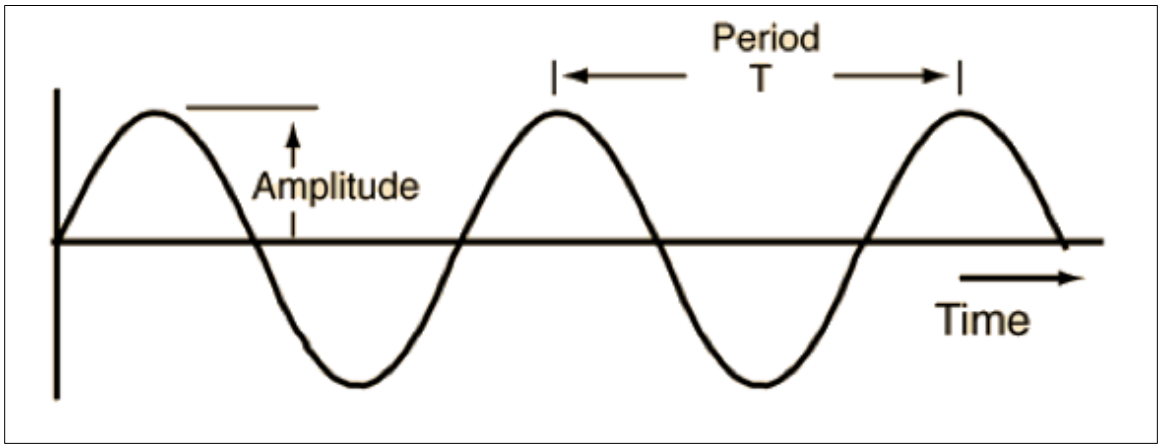

Figure 2-6: Sine wave with repetitive motion with time (Introduction to Waves, Wordpress)

The wavelength similarly, can be given in terms of the propagation velocity c and period T, as

$$u = U \sin (\text{constant} + \omega t) \tag{2.6}$$

$$v = U\,\omega \cos (\text{constant} + \omega t) \tag{2.7}$$

$$a = -U\,\omega^2 \sin (\text{constant} + \omega t) \tag{2.8}$$

So, the absolute value of the maximum motion can be given by the following when sine function is equal to 1.

$$\lambda = c/f \quad (2.9)$$

$$u = U \quad (2.10)$$

$$v = 2\pi f U \quad (2.11)$$

$$a = 4\pi^2 f^2 U \quad (2.12)$$

Thus, the maximum particle motion can be found easily from one another, in sine wave approximation of the wavelength, if frequency *f* is known.

In general, when all the three components of the particle motion are observed, i.e. the longitudinal, transverse and the vertical, none of them always dominates and peak component is different in different blasting situations. The peak value does not occur at the same time for the different components. So, for the sake of clear understanding, the peak particle motion is described as the magnitude of the highest particle motion of any of the three components. Another value, maximum vector sum is calculated by taking the square root of the summation of the squares of the maximum of each component, making it by default a larger value than any of the individual maximum value of any of the component. Thus, this value gives a safety factor giving a guidance as most of the observed empirical cracking is done by single-component peaks.

2.1.4 Vibration Frequency

The frequency of a wave as discussed before is the number of times a wave repeats itself in a second. Previous research has shown that structures respond differently when excited by vibrations, equal in all respects, but differing in principal frequency (Charles Dowding, 2000).

Vibration frequency can be calculated in a variety of ways like Fast Fourier Transformation (FFT), inversion of time periods and response spectrum techniques. The FFT as shown in Figure 2-7 is useful in understanding and processing a signal (vibration time history), which is converted into a frequency distribution to determine the dominant frequency.

Response spectrum also displays frequency distribution, and frequency and period work with function *f=1/T*.

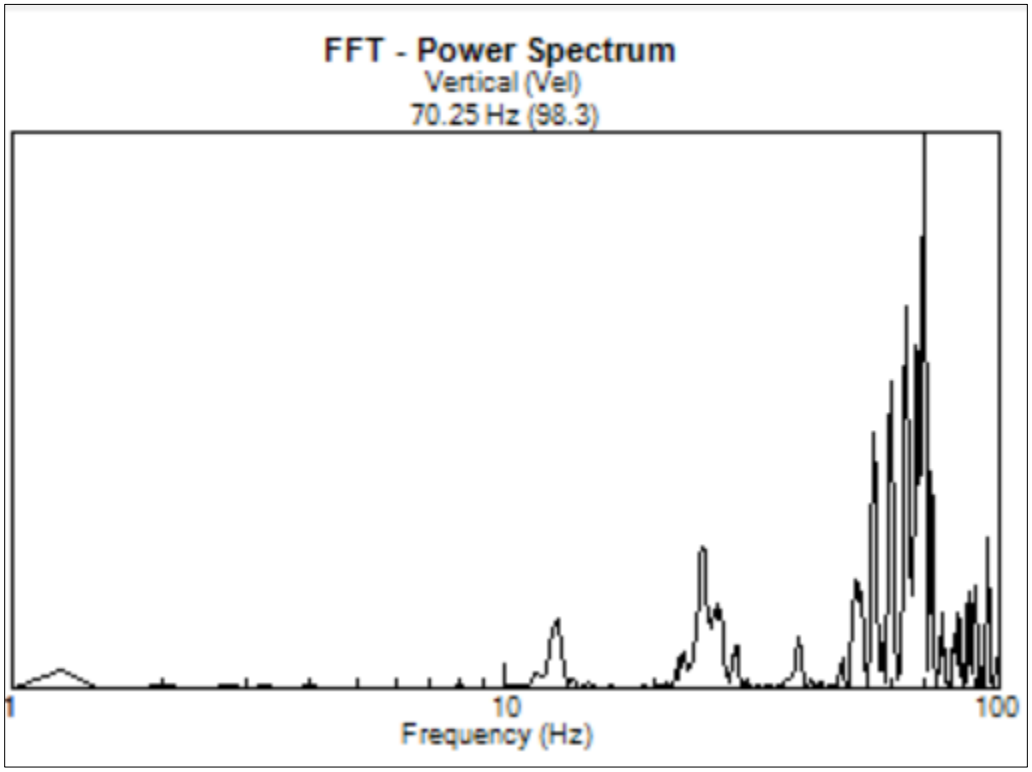

Figure 2-7: FFT of a signal giving a frequency distribution curve

The single-degrees-of-freedom (SDF) systems are the base of the frequency and the distance related blasting guides (Siskind et al. 1980b). In the well-known mug-rubber experiment, which behaves like an SDF system, it was established that the frequencies higher than the natural frequency cause less strain or displacement. This, later on, became the base for, why it is important to determine the dominant frequency of vibrations for controlling the potential to cause cracks.

Vibration frequency is sensitive to absolute distance and nature of the transmitting media. The vibrations traveling through rock retain the higher frequencies in contrast to the soil as a transmitting media. Soil layers over rock produce low-frequency vibrations through both selective attenuation and the generation of surface waves.

Vibration frequencies are possibly related to the initiation sequence intervals; however, this effect is usually masked by the scatter in the timing, but nowadays the improved initiation

systems can relate better to predicting the vibrations. RI 8507 (Siskind et al. 1980b) describes the importance of various design parameters and studies done to identify their relative importance.

2.2 Slope Stability

A slope can be defined as an inclined surface cut into the natural body, which is usually expressed as the degrees of inclination with respect to the horizontal. Slope designing in a mine is a very crucial engineering task. It is vital for the mine to have a well-planned and designed slope both from the safety and economic point of view. Slope designing in a mine is a task which is governed by the proper integration of three important divisions: Planning, Production, and Geo-mechanics.

Slope Configuration

The basic terms associated with the slope configuration are shown in Figure 2-8. The some of the important terms to be known are:

1. Crest: The top of an excavated bench

2. Face: The inclined or vertical surface of the rock exposed after excavation

3. Bench: A base that works as a single level of operations in an open-pit mining

4. Bench Angle: The angle of the bench w.r.t the horizontal

5. Toe: The bottom of the slope

6. Overall Slope Angle: The angle formed by a line joining the toe of the wall to the crest of the wall with respect to the horizontal.

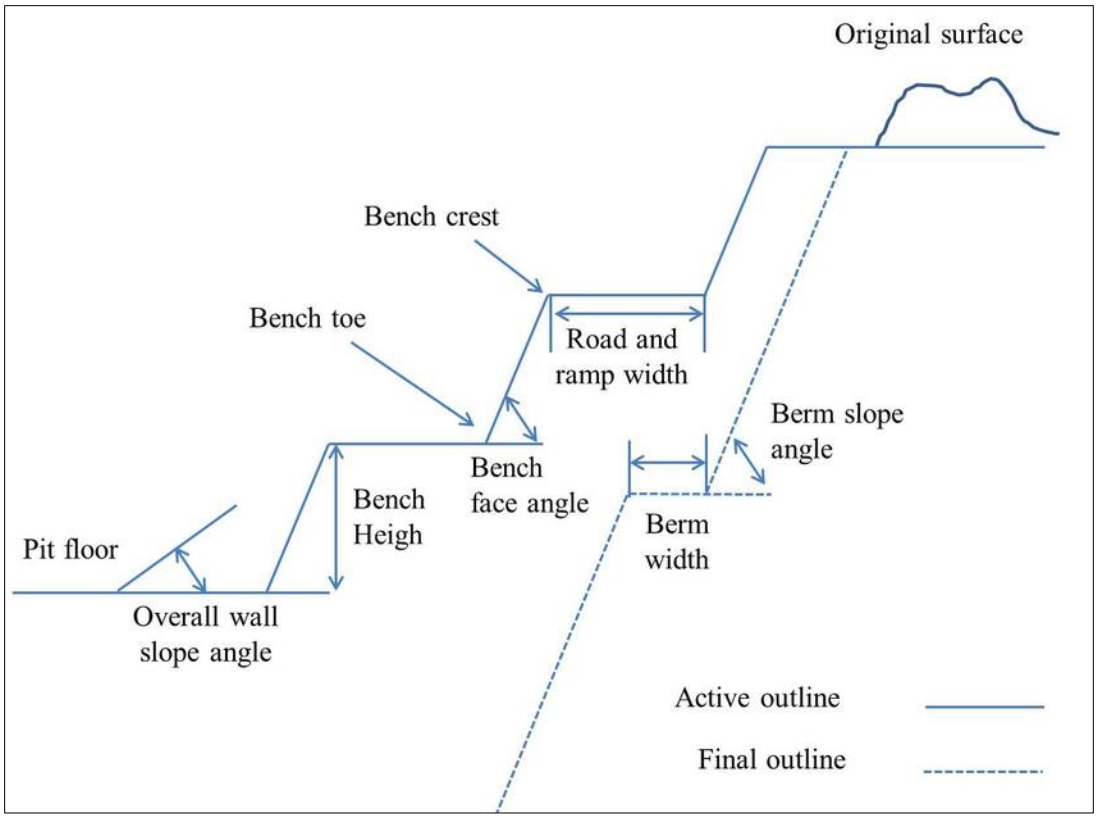

Figure 2-8: Slope Configuration (Arteaga et. al, 2014)

Slope Orientation

Orientation of a slope is defined by the following terms which are shown in the Figure 2-9

1. Dip: The angle at which a bed is inclined from the horizontal, measured normal to strike and in the vertical plane

2. Dip direction: the direction perpendicular to the strike, which is bearing of the dip

3. Strike: The outcrop of a fault plane or bed on a level surface

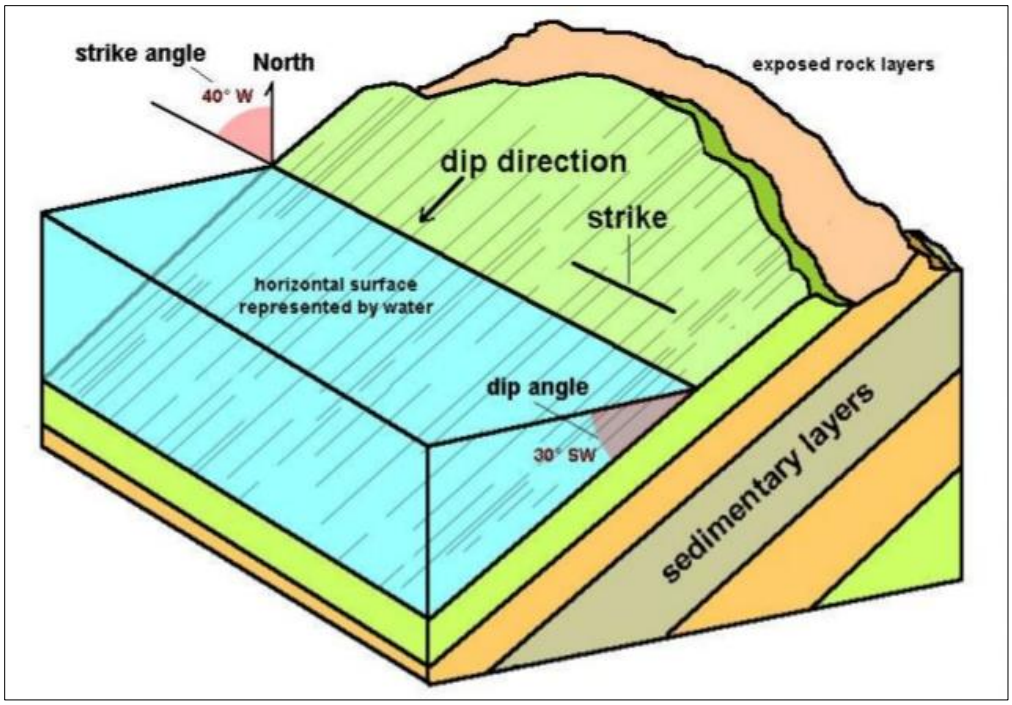

Figure 2-9: Orientation of a plane (Engineering 360, Geotechnical Services Information)

Slope Failure: Causes and Processes

Stability of a slope is dependent on several factors and it is difficult to point out any single cause for the failure of the slope. In general, it is a combination of certain factors combined at a time to cause the failure. These factors are divided into two categories:

1. Factors causing increase in Shear Stress

2. Factors reducing the Shear Strength

Increased Shear Stress

The major factors which fall into this category are:

1. The increased amount of load on a slope like that in a case of dumping excess material in an internal mine dump slope

2. Transient dynamic stresses from the blasting operations, movement of heavy mining equipment and earthquakes

3. Lateral pressure due to pore pressure, widening of cracks due to inclement weather conditions

4. Increased tectonic activities that can disrupt the stress fields

Reduced Shear Strength

The major factors which fall into this category are:

1. Inherent characteristics of the material or the geological factors such as orientation and presence of the discontinuities, the presence of the weak material.

2. The removal of the sideways support, in the case of mines it could be due to removal of the retaining structures, the soil erosion due to rainy conditions or the subsidence

3. Changes in the strength due to weathering, like the physical breakdown of the granular rocks resulting in reduced cohesion.

4. Changes in the internal forces due to discontinuities and water pore pressure

5. Weakening of the slope due to continuous creep.

2.2.1 General modes of Slope failure

The four primary modes of slope failure are:

1. Plane Failure

2. Circular Failure

3. Wedge Failure

4. Toppling Failure

The other modes of failure that are considered as slope failure include rockfalls and rock flow. All the four primary modes of failure are shown in the Figure 2-10

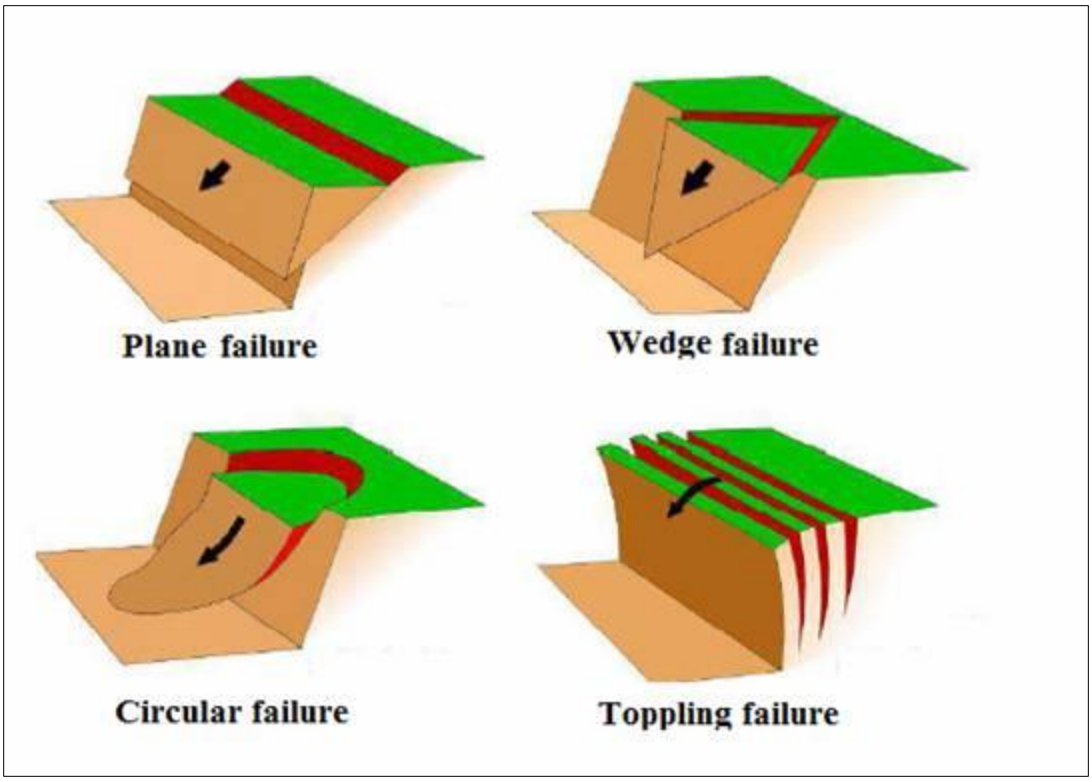

Figure 2-10: Different modes of slope failure in rock masses (R.Rai, Slope Lecture)

1. Plane Failure

Planar failure can occur where weak planes such as joints, faults, and bedding planes dip into the excavation due to unfavorable face orientation. A build-up of high water pressures may lead to sudden failure where critical planes daylight in the quarry face. Tension cracks can also be monitored for movement.

2. Circular Failure

These can occur in high faces in weak materials such as silts and clays, heavily jointed rock, tailings and spoil heaps. Loading at the crest of the slope and toe excavation combined with high water pressures may lead to failure. Tension cracks may form behind the slope and these can be monitored to give some indication of the progress of the movement.

3. Wedge Failure

Wedge sliding in mutually inclined and intersecting planes can occur where weak planes dip into the excavation due to unfavorable face orientation. The buildup of high water pressures may lead to sudden failure where critical planes daylight in the quarry face.

4. Toppling Failure

This occurs in hard rock with columnar structure and over-steep faces with closely spaced and adversely inclined steep discontinuities dipping into the face. The resulting movement is due to forces that cause an over-turning moment about a pivot point below the center of gravity of the block. If unchecked, it will result in a fall or slide of the material.

2.2.2 Mechanical approach to Stability Analysis

The stability analysis of the slope has been approached in numerous ways, including probabilistic methods, static equilibrium methods, finite difference or element methods and many more. The most common method employed is the simple limit equilibrium method to evaluate the sensitivity of possible failure conditions to slope geometry and rock mass parameters (Piteau and Martin, 1982). The other detailed methods such as finite element or probabilistic analysis are taken into consideration when the stability of the slope is sensitive to the failure mechanisms. Limit equilibrium technique is usually applied in the cases where the failure mechanism and the strength parameters can easily be defined, for the more complex issues where a large amount of discontinuities, complex geometry is involved, advanced techniques are considered.

The Limit Equilibrium Concept

The limit equilibrium concept, as the name suggests is the point in time when the driving forces are just equal to the resisting forces, which in turn means that all the points are on the verge of failure. This gives rise to the fact that, the factor of safety will be greater than unity, the i.e. slope will be considered stable, when the resisting forces are greater than the driving forces and less than unity otherwise, meaning an unstable slope.

The simplest approach to a limit equilibrium concept can be observed in the case of planar failure, where a block rests on the inclined slope as shown in the Figure 2-11.

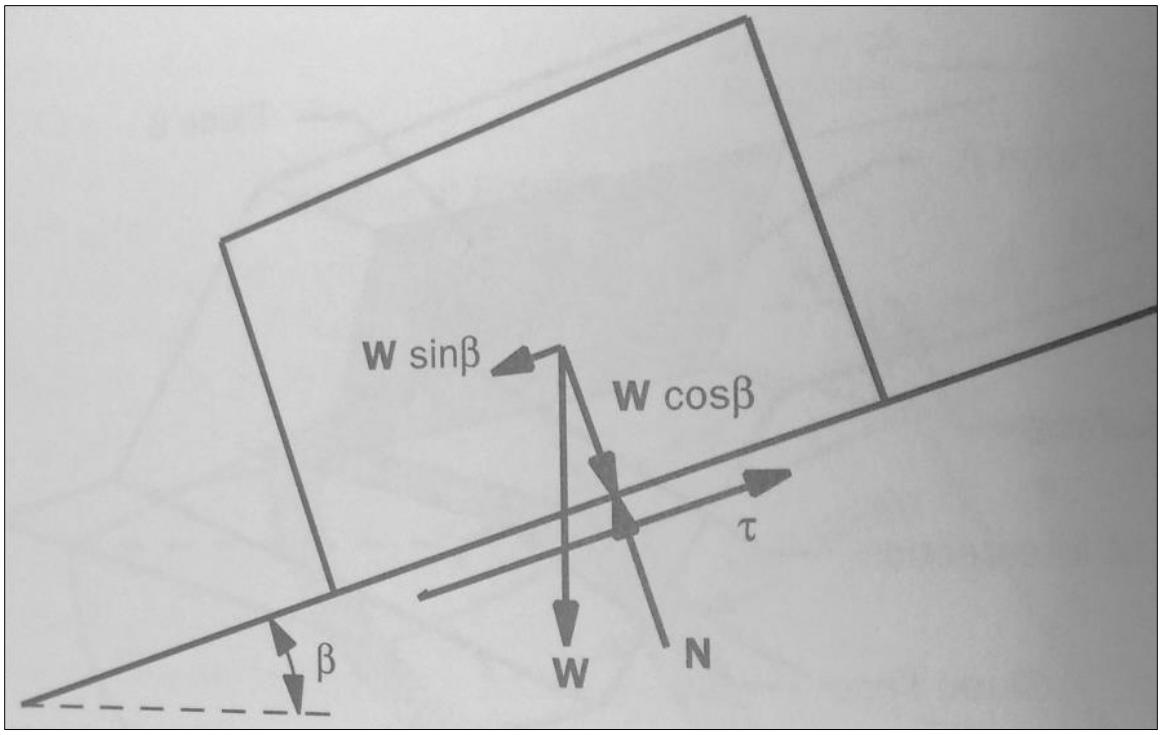

Figure 2-11: Block on an inclined plane at limiting equilibrium (Rock Slope Stability, C.A. Kliche)

The following equations describe the forces acting on the block

$$\tau = C + \sigma tan\varphi \tag{2.13}$$

$$\sigma = \frac{N}{A} = Wcos\beta/A \tag{2.14}$$

$$\tau = C + \left(\frac{Wcos\beta}{A}\right) tan\varphi \tag{2.15}$$

Shear force = τA = resisting force = $CA + Wcos\beta * tan\varphi$ (2.16)

Driving force = $Wsin\beta$ (2.17)

Equating driving and resisting forces we get equation for factor of safety (F.S.)

F.S. = Resisting Forces/Driving Forces = $(CA + Wcos\beta tan\varphi)/\ Wsin\beta$ (2.18)

here,

$\tau =$ shear stress along the failure plane

$C =$ cohesion along the failure plane

$\sigma =$ normal stress on the failure plane

$\varphi =$ angle of internal friction for the failure plane

$N =$ magnitude of the normal force across the failure plane

$A =$ area of the base of the plane

$W =$ weight of the failure mass

$\beta =$ dip angle of the failure plane

2.3 Attempts at studying and preventing effects of vibration on Slope Stability

As detailed in the previous sections, transient vibrations from the mine blasting and earthquakes are one of the driving factors in slope failures. As discussed earlier, the two important parameters when understanding vibrations are its amplitude and frequency. So, to mitigate the effects of vibrations on slope stability it has been long studied by various researchers, mines how they can control these two parameters of the vibration so that they do not affect the slope or high-wall in their mine or the subject of the study. The guidelines for controlling these parameters are introduced by the government organizations and authorities in the respective country of the study.

The common methods used by the mines or the researchers for reducing the effects of these parameters are:

1. Contour Blasting
2. Frequency Shifting

Contour Blasting:

The energy that is not used for fragmentation or displacement of the rock, sometimes 70-80% of that developed in a blast hole, is mostly responsible for the strength reduction of the rock outside the radius of excavation. New fractures and planes of weakness are created and joints and bedding planes that may have been stable before the blast but can be opened. As a result, the rock mass stability can be reduced. This can be seen as over break and the

fractured face is left with a higher likelihood of rock falls. Thus, to address such technical and economical adversities it is required to put up an appropriate level of engineering effort that can produce safe and stable high-wall. This engineering effort is termed in the mining industry as “Contour/Perimeter Blasting”.

Types of Contour Blasting

There are various types contour blasting methods, of these the most commonly used are:

1. Buffer blasting

2. Pre-splitting

3. Cushion blasting

4. Line drilling

Buffer Blasting

This is one of the simplest ways of contour blasting. Usually, the last row of production blasting is altered for the energy, by changing the blasting pattern. The explosive energy in the row is decreased so does the spacing and burden. The explosive energy is reduced by using a scaled depth of burial higher than usual or using a decoupled charge over the base of fully coupled toe charge.

Buffer blasting could be used as the sole technique of the wall control when the rock is competent. There might be some over break and fractures in the final wall, but would be much less than the production shot. Usually, buffer blasting is used in conjunction with other means of wall control, but when used alone it is very economical.

Pre-Splitting

Pre-split is a row of small diameter, blast holes with decoupled charges, which are usually fired instantly before the production blast to create a fracture plane. Creation of a pre-split fracture before the production shot considerably reduces the amount of tensile stresses damaging the high-wall.

One of the important parameters in pre-split blasting is the use of lightly loaded holes. The light powder load may be obtained by using specially designed slender cartridges, partial

or whole cartridges taped to a detonating cord downline, an explosive cut from a continuous reel, or heavy grain detonating cord. A heavier charge of tamped cartridges is used in the bottom few feet of the hole.

The depth for single pre-split is usually from limited to 45 to 60 feet due to the poor accuracy of the drill holes of the small diameters. A deviation in the range of 5-6 inch from the desired location can result in a poor pre-split outcome.

Usually, the pre-split holes are not stemmed, the decoupled charges and instantaneous firing takes care of containing the gas pressure for the wedge effect. But if the noise from the pre-splitting is a point of concern for the mining team, the holes could be stemmed but could result in the crater formation at the crest.

Pre-split charges are fired using detonating cord, electronic detonators or the instantaneous electric detonators as shown in Figure 2-12, to create the desired fracture plane. But, wherever noise is a problem a small pyrotechnic delay detonator could be used to reduce the maximum charge going off per delay. Surface lines of detonating cord should also be buried with sand or the drill chippings to reduce the noise levels.

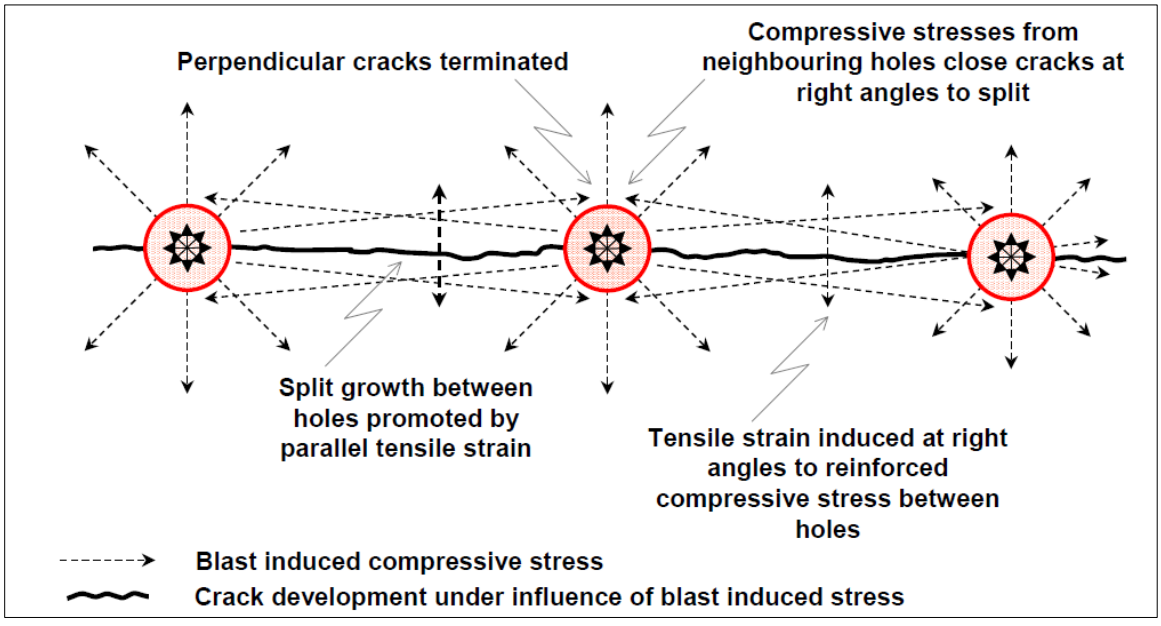

Figure 2-12: Pre-split formation through instantaneous initiation of closely spaced holes (P.Dunn, 1995)

Cushion Blasting

Cushion blasting is a common practice in the surface mines to trim or remove the excess material from the face to give a smooth wall with little over break. The blast holes for cushion blasting are drilled along the final line of excavation, the coupled toe charge is followed by a decoupled charge to reduce the damaging effect to final wall.

The common diameter for cushion blasting have varied from 4-7 inches but large holes are also used in the big surface mines. For this range of hole diameters, the common spacing used is in the range of 5-8 feet. The general thumb rule that could be useful is spacing in feet is 1.25 to 2.0 times the hole diameter in inches, higher the values correspond to the softer rock and lower to hard rock.

The trim row should be suitably decoupled, with the coupling ratio of 0.45 for clean and smooth final wall. Decoupling could be achieved using the undersized cartridges or use a suitable charge in the bottom of the hole and allow gases to move up the blast hole.

The timing consideration in case of cushion blasting is different from the pre-splitting, as in here unlike pre-split, the trim row is blasted after the main blast. The trim row needs sufficient relief to remove the excess material from the face, so it is necessary that enough time gap is provided between the production and trim row blasting. Usually the trim row detonates after one delay period after the adjacent production holes shot. Multiple trim holes can be shot per delay provided they don't fire before the production holes or they are not exceeding the vibration limits defined for the site.

Cushion blasting usually has the similar blast hole diameter as that of the production shot. The bigger diameter allows for the more accurate drilling as compared to pre-split blasting. The accurate drilling, in turn, helps to create trim holes as deep as production shot which is usually the one bench height.

Line Drilling

Line drilling is a method used seldom in surface mines as drilling closely spaced holes is expensive. They are only used when the rock is very weak and highly fractured and it is very difficult to do a pre-split or cushion blast.

The typical hole size for line drilling is from 2-3 inches. The costing is reduced if it possible to use larger holes, as spacing could also be increased with it. But in most cases, the use of small diameter blast holes due to fractured rock mass keeps the depth restricted to 30-40 feet.

Accurate drilling is the most important parameter in line drilling to be successful. The holes drilled should all lie along the plane which corresponds to the final pit wall. Unequal spacing can lead to variable results. Figure 2-13 displays initial values for the approximate hole spacing in line drilling method. The hole spacing in feet could be determined by multiplying the appropriate factor with drill diameter in use.

	Powder	Factor
Rock Strength	Lb/Ton	Kg/Tonne
High	0.30—.040	0.15—0.20
Medium	0.28—0.38	0.14—0.19
Low	0.16	0.08

Figure 2-13: Approximate Powder Factor in Cushion Blasting (C.J. Konya, 1980)

In literature, we find various (C. Brown et. al, 1972, A. Rorke et.al, 2003, G. Newman et.al, 2011) examples of contour design blasts to reduce the damage to high-wall. One of the cases discussed (K. Christopherson, 2011) in details is Morenci Mine, of Arizona, USA.

Case Study: Blast Designs in Morenci Mine

Overview

Morenci is an open-pit copper mine located in Greenlee County, Arizona. Ownership is Freeport-McMoRan Copper & Gold, Inc. (85 percent) and Sumitomo Metal Mining Arizona Inc. (15 percent). The open-pit has been in operation since 1937 producing over 7 billion tons containing over 31 billion pounds of salable copper.

Problem

The blast design for 10.625 in. holes, for the upper bench of a 100ft high-wall required a trim row at half the typical production spacing drilled 2ft off the designed toe; the 2nd row with typical production spacing drilled 18ft off the trim row; the 3rd row of the same

spacing drilled 18 ft. off the buffer row; and then standard production burden and spacing into the pit. The design for the lower bench of a 100ft high wall required same dimensions but moved 3ft in or 1ft inside of the design toe, in order to achieve the limit. This is displayed in Figure 2-14

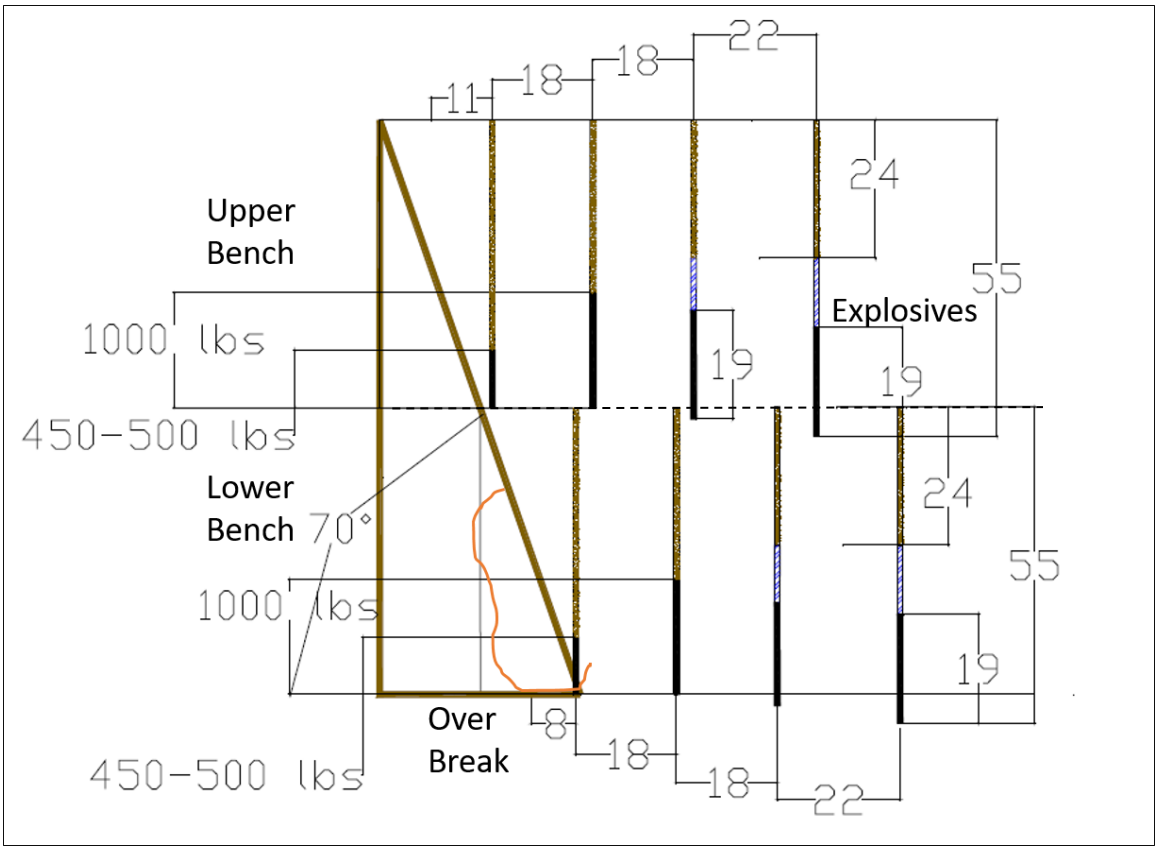

Figure 2-14: Section-view of Non-Pre-Split Final Design

It was established by the mining team that the blast achieved the designed toe but the final charge weight resulted in the over break, damaging the high wall.

Results with new blast designs

Trial 1

To resolve the issue of the over break the charge weight in the trim row was reduced and air deck was introduced in the first trial. The results were acceptable in terms of the over break but the toe of the wall measure 20 ft.-30 ft. off the designed toe.

Trial 2

To resolve the issue of designed toe the trim row was brought closer to the mid-bench and the second-row closer to the trim-row. The powder factor in buffer row was increased to 1.0 lb/yd^3. The design from the trial 1 was improved with stronger powder factor without fear of damaging the high wall. The result from the blasts were better from the trial 1, but still, the toe was off by 12 ft. to 20 ft. from the designed toe. It was concluded the buffer row could not pull the toe as much is required with this powder factor.

Trial 3

To mitigate the issue, as shown in Figure 2-15 the trim row was placed in the mid-bench and buffer row was maintained at the same spacing as in trial 2. The third trial achieved both the objectives-a sound wall and achievable toe limit.

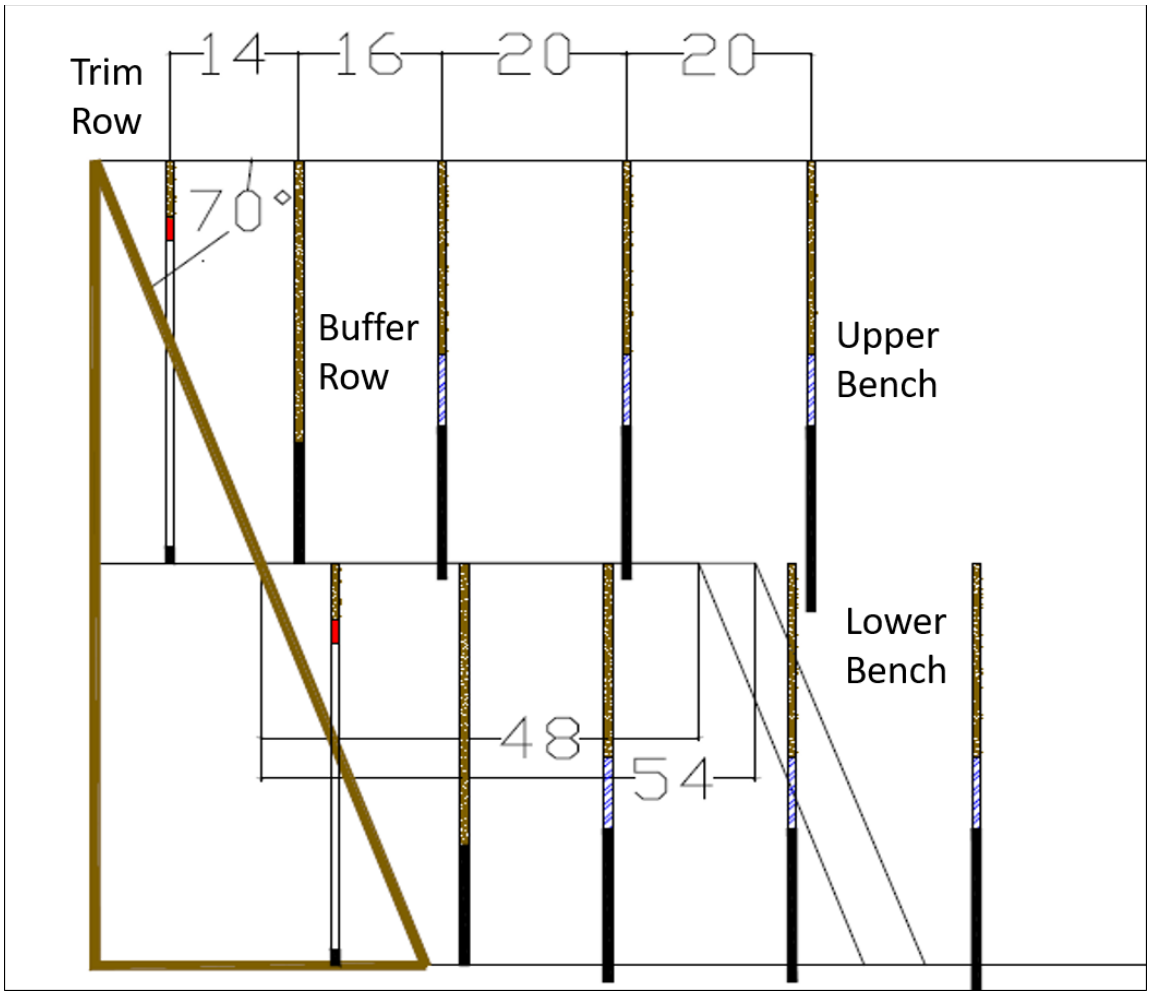

Figure 2-15: Design for the third trial

Frequency Shifting

Usually, mines or other blasting operations follow the statutory vibration standards for their blasting operations. From the previous sections, we understand that the frequency is an important parameter when defining displacement or strain at a given point or structure. For example, for the same particle velocity at a single frequency vibration of 20 Hz, the displacement will be half of the 10 Hz frequency vibration.

This concept of generating higher frequencies to stay at lower displacement levels is vital for vibration sensitive areas. But before moving from one frequency to another it is vital to understand the resonant or the natural frequency of the structure we want to protect. If in the above case, if the natural frequency of the structure under study is 20 Hz, then it coincides with the dominant frequency of the vibration, which can result in the excitation of the structure giving rise to higher displacement or strain levels. So, it is important that we find the natural frequency of the structure and then do the frequency shifting whether it is to a lower or higher frequency. This approach has been researched and practiced in many mines across the world, details of which could be found in the work of D.S.Preece (2010), A. Sharma et.al (2013). One of the most recent approach by C. Dzerzhinsky (2016) is discussed below.

Case: Shifting the blast vibration frequency to preserve high wall (Charles Dzerzhinsky, 2016)

In this case, where the name of the mine was not disclosed in the paper, the high-wall in the mine as shown in Figure 2-16, had troublesome geological conditions, which were resulting in several failures. It was a concern for the Drill and Blast team of the mine that by their actions of blasting near the wall they should not further aggravate this situation.

The most important parameter as we discussed above in shifting the frequency of vibration, it is important to determine the ground resonant frequency. This is done mostly firing single hole shots and collecting data using seismographs. As shown in the Figure 2-17, it was found that the mine had the ground resonant frequency range between 9-12 Hz and the ground was well able to support the frequencies in the range of 20-30 Hz.

Figure 2-16: East Ramp High-Wall of the mine

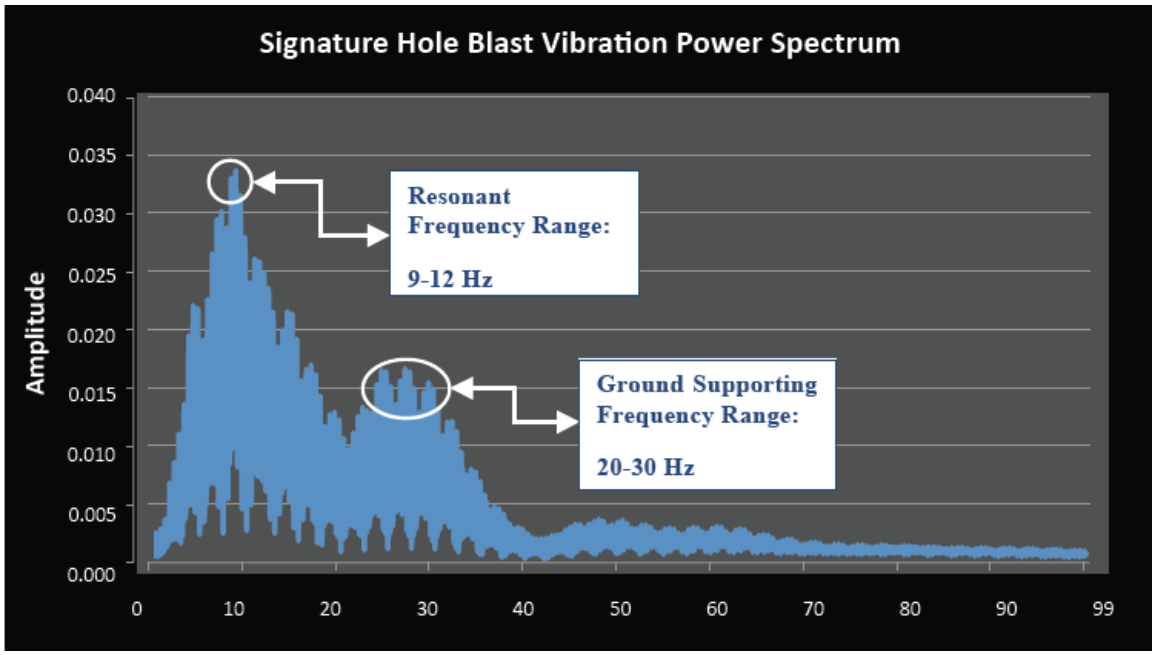

Figure 2-17: Single hole blast vibration Power Spectrum

So, it was feasible that with the correct study and use of blasting systems, the frequency could be shifted away from the dominant frequency of the ground, in case the current practices were generating vibration close to the ground dominant frequency.

Solution: The mining team did a range of study and concluded that the mine current practices are generating vibrations levels close to the dominant frequency and they need to shift away from it. The mine shifted to the blast timing regime of 40 ms between the holes which resulted in the frequency shift in the range of 28-30 Hz well away from the resonant frequency. It was observed by the geotechnical team of the mine after shifting to new practices, over the period there was a decrease in the ground movement.

There are several other practical studies (Ruling Yang et. al, 2009) that have worked in the direction of frequency shifting, which indicate that it is essential to first determine the dominant frequency of the structure to preserve and then shift away from that frequency to reduce the damage to the structure.

2.3 Numerical Modeling

The term "numerical modeling" is used for all types of calculations that are based on numerical solutions of the complex differential equations encountered in rock mechanics and engineering problems (R. Rai, 2012). Most of them apply discretization of the rock mass into a large number of individual elements and achieve an iterative solution by repetitive calculation in a computer. This technique is used mainly for the analysis of rock stresses and deformations.

The basic pre-requisites for numerical analysis are the idealization of the actual excavation within the rock mass and the division of the rock mass into different sectors, based on the results of geological investigations. Material property models are established for each of the sectors, and for the anticipated rock supports.

It is important to be aware of the restrictions and uncertainties that are inherent in such modeling, of which the most important arise from the difficulty of obtaining reliable input parameters, especially for:

- The magnitudes and directions of the in-situ stresses.

- The material model and properties of the in-situ rock mass.

- The location and extent of the various geological sectors within the rock mass.

The reliability of the analysis will never be better than the reliability of the input parameters and applied models.

Numerical modeling is widely used to resolve complex slope stability problems. These models are helpful in integrating and giving the required representation of the discontinuities such as joints, faults etc.

The numerical methods used for the analysis are divided into three approaches:

1. Continuum modeling

2. Discontinuum modeling

3. Hybrid modeling

Continuum Modeling:

Continuum modeling is used mostly in for the slopes with massive and intact rocks. The model assumes the material to be continuous throughout the body and discontinuities are introduced as an interface. The model is not very suitable for the slopes with many intersecting joints.

The finite difference, finite element, and the boundary element methods are based on the continuum modeling approach. In this approach as a basic condition, the problem is broken down into various elements by discretization and the solution is procedure is initiated based on the numerical approximations of the equations.

There are both three dimensional and two-dimensional software based on the continuum modeling, some of the examples are:

1. Fast Lagrangian Analysis of Continua (FLAC) 2D and FLAC 3D based on the finite difference methods, used to model complex behaviors, unstable systems etc.

2. Phase 2 is a two-dimensional finite element method based software used for analysis of the complex geotechnical issues.

3. PLAXIS 2D is also a two-dimensional finite element method based software widely used for the slope stability analysis.

Discontinuum Modeling:

Discontinuum modeling methods consider rock mass under study as discontinuous by treating them as a group of rigid or deformable blocks. These methods allow the slipping and movement along the discontinuities with normal and shear stiffness, which allows relative movement to one another and helps in modeling complex behavior. These methods treat the problem as a group of distinct bodies interacting with one another and the external loads. These are together termed as discrete element methods.

The variations of the discrete element methodology involve:

1. Distinct Element Method

2. Discontinuous deformation analysis

3. Particle Flow Codes

The most widely used discontinuum modeling based software used for the slope stability analysis are UDEC (Universal Distinct Element Code, Itasca Consulting Group) and 3DEC (3-Dimensional Distinct Element Code, Itasca Consulting Group).

Hybrid Modeling:

Hybrid modeling is an approach gaining popularity among the researchers as it can allow the abilities of two different methods to be combined to achieve the desired results. GEO-SLOPE could be as an example where the stress and water flow analysis is adopted using limit equilibrium stability and finite-element method. Although, the requirement of high memory for complex problems and little experience remains a challenge in the development of this modeling.

Three-Dimensional Distinct Element Code (3DEC)

As discussed in the previous section 3DEC is based on distinct element method for discontinuum modeling. 3DEC simulates the response of the media like jointed rock mass subject to either static or dynamic loading.

The salient features of the 3DEC are (User's Guide Itasca 3DEC, 5.0):

1. The rock mass is modeled as 3D assemblage of rigid or deformable blocks

2. Discontinuities are regarded as distinct boundary interactions between blocks

3. A joint structure can be built into the model from the geological mapping

4. 3DEC's in-time solution algorithm can accommodate large displacement and rotation

5. The graphics facility permits interactive manipulation of 3D objects

3DEC was initially developed to study the jointed rock mass for slope stability. But it has been used extensively in the mining engineering problems for both underground and open-pit solutions in static and dynamic conditions. The blasting effects are studied using dynamic stress or velocity waves at model boundaries. In our analysis, of the experiment, we have used the stress wave analysis approach to solve the problem.

2.3.1 Numerical Modeling application in Slope Stability Analysis

Case Study: Slope Stability at Escondida Mine

The Escondida Mine is a copper mine discovered on March 14, 1981, in Antofagasta Chile (Cristina Valdivia and Loren Lorig Slope Stability in Surface Mining, SME 2000).

Concern: The slope failure mechanism at the mine involved strong structural control with the formation of non-daylighting wedges. The mine wanted to analyze the case of mining the four benches without expanding the unstable area of the northeast corner of the mine.

Slope-Stability Analysis: The mine had been using the XSTABL a software based on the two-dimensional limit equilibrium method and FLAC 2D for the analysis of the slope stability. But they were not capable of analyzing the planar failure that allows rotation, slip or separation of the deformation blocks.

Solution: The three major stability concerns of the mine were:

- A weak rock mass
- Strong structural control resulting in non-daylighting wedges
- High pore pressures

3DEC was employed by the mine which had the capability to consider all these factors.

After numerical analysis with 3DEC, mine operations could successfully excavate the four benches without affecting the unstable area of the mine.

Other examples:

At the Barrick, Goldstrike mine, the numerical modeling (using UDEC) approach was used to interpret the failure mechanism of the slopes and complement the more traditional design assessments like limit equilibrium approach. (Nick D. Rose and Robert P. Sharon, SME 2000)

There are various other examples available where the numerical modeling has been used as a preferred approach to resolving the slope stability problems.

2.4 Vibration Standards

Vibrations from the blasting, quarrying and construction activities have been a nuisance and a hazard for a long time both for the humans and the surrounding structures. Over the decades, countries and government authorities have become more and more vigilant and rigorous in the application of the vibration standards.

In general, most of the countries developed the vibrations standards keeping the detrimental effects of the blasting operations on the concerned man-made structures and human beings. But still, most of these standards are utilized for the estimating the limits of construction blasting, pile driving and for the structures which are not directly concerned with the stipulated standards.

In the first chapter, the vibration standards established by the USBM for blasting, quarrying, and construction activities were seen. Below are the standards established by some of the other countries.

1. British Standards

The British standards provide guidance on the possibility of the damage due to the blast vibrations and the guide values are set at the lowest vibrations levels above which credible proof of damage has been established in their studies. The source of vibration considered

in establishing the standards are blasting, demolition, tunneling etc. The values in the Figure 2-15, are vibration limits for the cosmetic damage which is the maximum value of any of the three perpendicular components at any given time of the duration of the study.

Further, the figure details the transient vibration standards, if the case is of the continuous vibrations which can give rise to resonant responses at lower frequencies, the velocity levels are reduced by 50% than as shown in the Figure 2-18

Type of building	Peak component velocity in frequency range of predominant pulse	
	4 to 15 Hz	15 Hz and above
Reinforced or framed structures Industrial and heavy commercial buildings	50 mm/s at 4 Hz and above	50 mm/s at 4 Hz and above
Unreinforced or light framed structures Residential or light commercial type buildings	15 mm/s at 4 Hz increasing to 20 mm/s at 15 Hz	20 mm/s at 15 Hz increasing to 50 mm/s at 40 Hz and above

Figure 2-18: Transient vibration guide values for the cosmetic damage BS 5228-2:2009

2. German Standards

The German Standards DIN 4150, Part 3, talks about the effects of construction vibrations of both transient and continuous types. The different types of the vibrations are measured at the different locations. The Figure 2-19, shows that long-term vibrations are independent of the frequency. This is a frequency dependent guidance of the values of the velocity based on the different types of buildings.

Structure/Object Type	Frequency Hz	Peak Velocity mm/s Short-term:	mm/s Long-term	Location of measurement
Offices and industrial premises	1	20	-	
	10	20	-	
	10	20		
	50	40	-	Foundation
	50	40	-	
	100	50		
	1	-	10	Top floor,
	100	-	10	horizontal
Domestic houses and similar construction	1	5	-	
	10	5	-	
	10	5		
	50	15		Foundation
	50	15	-	
	100	20		
	1	-	5	Top floor,
	100	-	5	horizontal
Other buildings sensitive to vibrations	1	3	-	
	10	3	-	
	10	3		
	50	8		Foundation
	50	8	-	
	100	10		
	1	-	2,5	Top floor,
	100	-	2,5	horizontal

Figure 2-19: DIN-4150 (3) Vibration velocity levels for the evaluation of the short term and long-term impact

3. Swiss Standards

Swiss standard SN 640312 was introduced in 1979 and takes continuous and transient vibrations. The buildings are divided into various categories as shown in Figure 2-20.

Building Category	Building Type
I	Reinforced concrete structures for industrial purposes, bridges, towers etc.
	Subsurface structures such as caverns, tunnels with or without concrete lining
II	ildings with concrete foundations and concrete floors, buildings made of stone a concrete masonry/blocks
	Subsurface structures, water mains, tubes and caverns in soft rock
III	lings with concrete foundations and concrete basement, timber floors, masonry
IV	Especially vibration-sensitive structures and buildings requiring protection

Figure 2-20: Building categories, SN 640312

The two frequency ranges are fixed for the various recommended vibration velocities.

Building Category	Frequency Range Hz	Recommended vibration velocity mm/s
I	10 – 30	12
I	30 - 60	12 – 18
II	10 – 30	8
II	30 - 60	8 – 12
III	10 – 30	5
III	30 - 60	5 – 8
IV	10 – 30	3
IV	30 - 60	3 - 5

Figure 2-21: Frequency range for the various building types

4. Indian Standards

The Directorate General of Mines Safety (DGMS) has set the permissible limits of vibrations, as detailed in the Table 2-2 that must be complied by the mines in India, to continue their license to operate

Table 2-2: DGMS prescribed permissible limits for ground vibration in India

Type of Structures	Dominant Frequency		
	<8 Hz	8-25 Hz	>25 Hz
1. Building/structures not belongings to owner			
1.1 Domestic houses/ structures	5 mm/s	10 mm/s	15 mm/s
1.2 Industrial building	10 mm/s	20 mm/s	25 mm/s
1.3 Objects of historical importance & sensitive structures	2 mm/s	5 mm/s	10 mm/s
2. Buildings belonging to the owner with limited span of life			
2.1 Domestic houses/structures	10 mm/s	15 mm/s	20 mm/s
2.2 Industrial Buildings	15 mm/s	25 mm/s	50 mm/s

The various vibrations standards set up by the countries across the world are widely spread and have a large range of frequency for the similar velocity levels, which is difficult to understand. Further, it can be observed the standards are for the structures and buildings inhibited by the human beings and cannot be generalized for any structure like high-wall. So, it appears that each structure under consideration and those which can be affected by the vibrations causing a safety concern should be studied independently to estimate the impact of vibrations.

3 Experiment

As discussed in the first chapter, high-wall related incidents are still prevalent and there is no significant guideline directly stating this problem. To better understand these high-wall behaviors under dynamic inputs, an experiment was designed. The aim of the experiment was to observe the effects of blast vibrations and observe the safe levels of vibrations and frequency to operate under given conditions.

3.1 Experiment Stages

The project was broadly divided into two stages, with each stage having different steps. The first stage consists of collecting the field data and second stage comprised of assessing that field data and develop working numerical models after calibrating them by simulating the field conditions. The various steps of the experiment are as shown in the Figure 3-1.

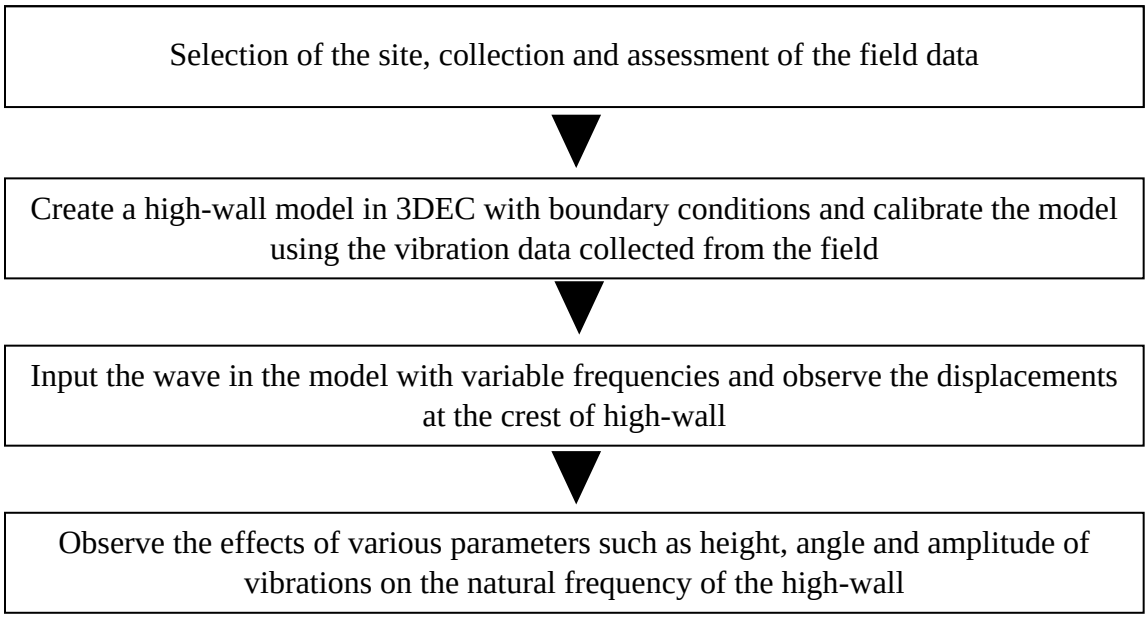

Figure 3-1: Experimental setup process of the research

Once the calibrated numerical model is created in 3DEC, a parametric study is done in an attempt to understand the effects of various parameters such as the height of the high-wall, the angle of the slope and the amplitude of the vibrations and the natural frequency of the high-wall.

3.1.1 Field data collection

The site understudy was Nally and Gibson, Georgetown Limestone Quarry located in Georgetown Kentucky, where the underground excavation of limestone is done using drill and blast. The high-wall, as shown in the Figure 3-2, along the ramp connecting the open pit with the underground entry is studied as any adverse effect on the wall would be damaging to the operations and safety of the mine.

Figure 3-2: High-wall under study at Nally & Gibson, Limestone Quarry, Georgetown, Kentucky

The field data collection aims to gather day to day vibrations generated from underground blasting operations and capture the locations of the points on high-wall at various time during the period of study.

The field data collection was divided into two stages:

1. Setup seismographs in the field

2. Scan high-wall using Maptek I-Site 8800

3.1.1.1 Seismograph Setup

To monitor the vibrations affecting the high-wall, seismographs as shown in Figure 3-3, were set up. The seismographs were set up to collect the vibration, frequency, amplitude of the blast vibrations. The data collected by the seismographs is accessed remotely using a modem used to transmit data.

Figure 3-3: Setting up seismograph in field for data collection

3.1.1.2 Site Scanning

The high-wall under study was scanned using Maptek I-Site 8800, as shown in Figure 3-4. The scanner collects the current location of the points on the high-wall. The data collected at multiple times can help to identify the points, if any, which have moved from there baseline position. The scanner is set up in the field at multiple locations, usually three, to cover the high-wall from all the angles. The scanner takes a 360° picture of the area and then the picture is divided into multiple sections to scan as per instructed by the user. Sections expected to be most affected due to blasting vibrations and sections far away are scanned with high density, implying that more data points are collected by reflection for the given area of the wall. The scanned data is stored in a portable hand handled controller, which can be later exported for further processing using I-Site Studio.

Figure 3-4: Maptek I-Site 8800 Scanner used to scan high-wall in field

3.1.2 Data Processing

The data collected from the field is processed at the lab and is used to develop numerical models for the predictions of movement of the high-wall from blasting vibrations. The data collected is processed in three stages:

1. Generate a digitized scan of high-wall from the acquired scanner data using I-Site Studio software

2. Import and assess the vibration data collected by seismograph using Seismograph Data Analysis

3. Develop a numerical model in 3DEC

3.1.2.1 Scanner Data Processing

The data collected by scanning the high-wall in the field is imported from the hand-held controller. The different scans which are represented by different colors are stitched together to generate a model as shown in Figure 3-5, comprised of all the points collected in the field. The stitched model can be used to generate surfaces which further could be used as an input for further numerical modeling using 3DEC. In the present research, due to time constraint, this was not utilized, but it can be a further course of the study for the future work.

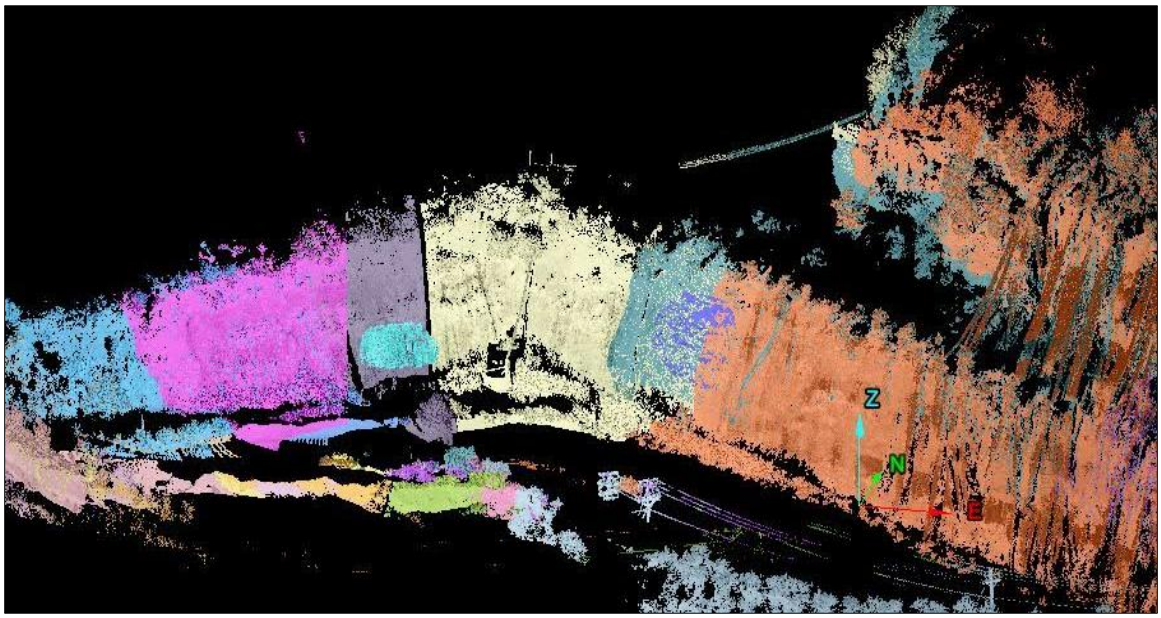

Figure 3-5: Model generated by I-Site software from scan data collected in field

3.1.2.2 Vibration Data assessment

The vibration data from the underground blasting operations is stored in the seismographs installed at the site. The data is accessed using Seismograph Data Analysis software as shown in Figure 3-6, the data collected is used as an input for the simulating a dynamic model in 3DEC.

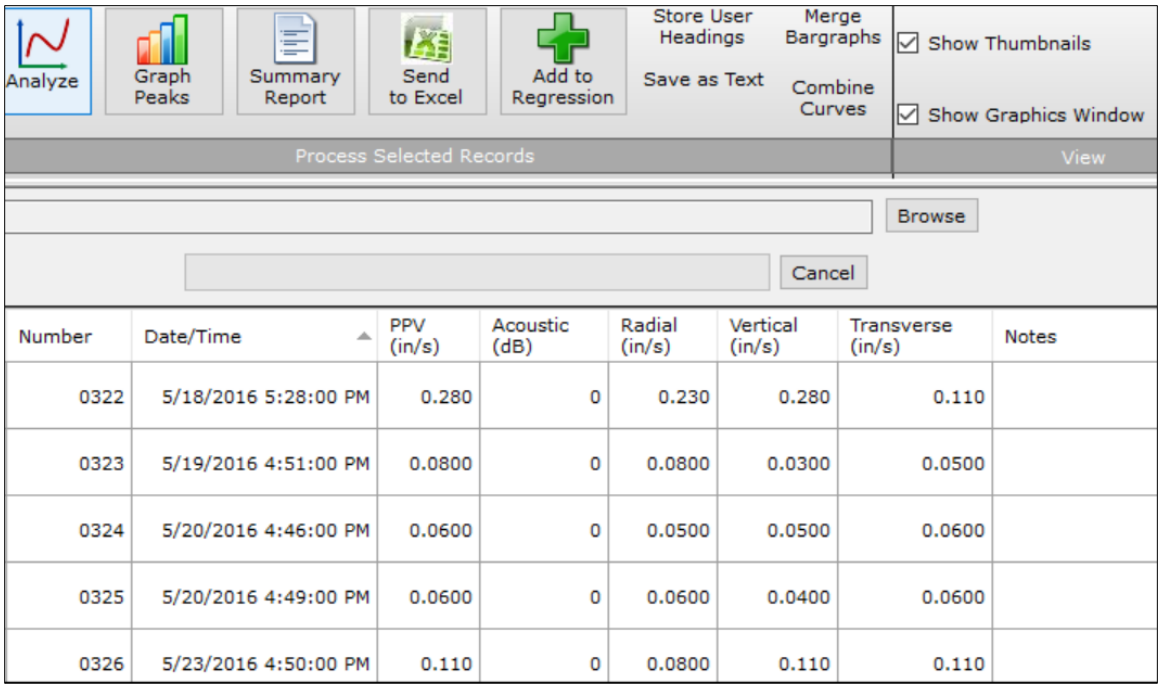

Number	Date/Time	PPV (in/s)	Acoustic (dB)	Radial (in/s)	Vertical (in/s)	Transverse (in/s)	Notes
0322	5/18/2016 5:28:00 PM	0.280	0	0.230	0.280	0.110	
0323	5/19/2016 4:51:00 PM	0.0800	0	0.0800	0.0300	0.0500	
0324	5/20/2016 4:46:00 PM	0.0600	0	0.0500	0.0500	0.0600	
0325	5/20/2016 4:49:00 PM	0.0600	0	0.0600	0.0400	0.0600	
0326	5/23/2016 4:50:00 PM	0.110	0	0.0800	0.110	0.110	

Figure 3-6: Vibration data accessed using Seismograph Data Analysis

3.1.3 Numerical Modeling

A numerical model was implemented in 3DEC, and for design, simplicity and considering the blast vibration amplitudes, the model was assumed to be made of a single material with elastic properties. Table 3-1, details the properties of limestone that were assigned to the model after the calibration of the model.

Table 3-1: Properties of Limestone assigned in model

Properties of Limestone	Values
Density	5.5 slugs/ft^3
Bulk Modulus	6e8 lbf/ft^2
Shear Modulus	2.4e8 lbf/ft^2

Initially, for the numerical simulation, a 100ft model was implemented, Figure 3-7 shows the boundary conditions of the model and Figure 3-8 details a schematic diagram of the model. For, the dynamic input, the velocity recorded from the field was converted to a stress history using equation 3.1 and a viscous boundary at the bottom of the model was used to avoid reflection of the outgoing stress wave back into the model.

$$\sigma = 2(\rho C)V \quad (3.1)$$

here,

σ = applied shear stress

ρ = mass density

C = speed of s-wave propagation through medium

V = shear velocity

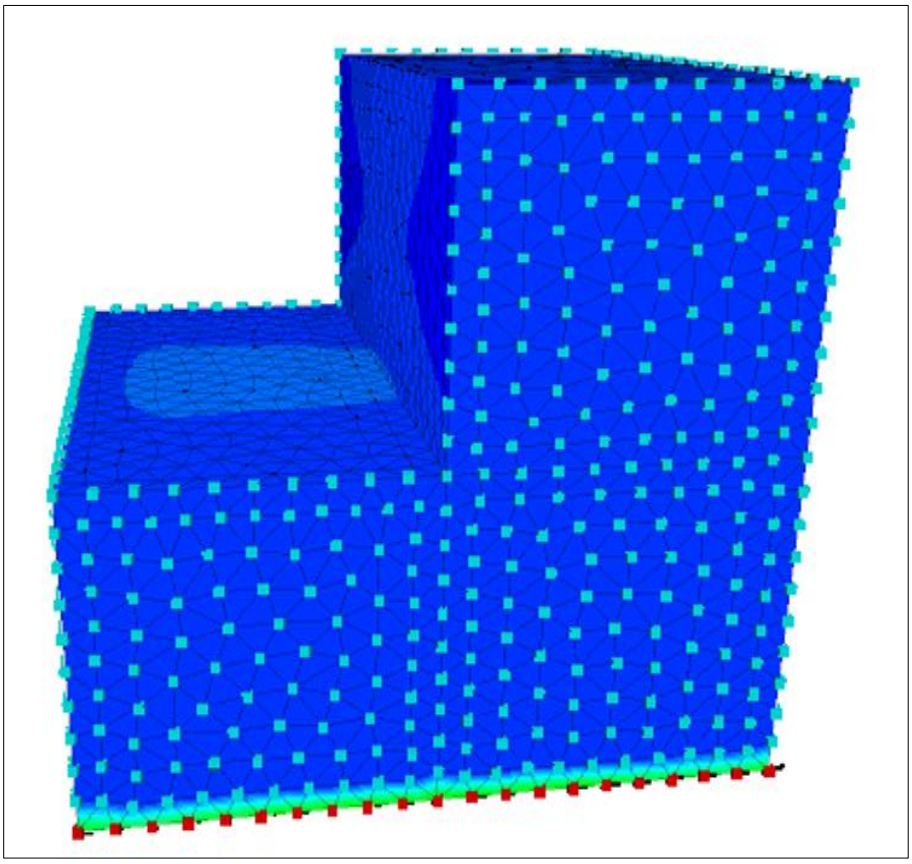

Figure 3-7: 3D model with boundary conditions for the numerical model in 3DEC

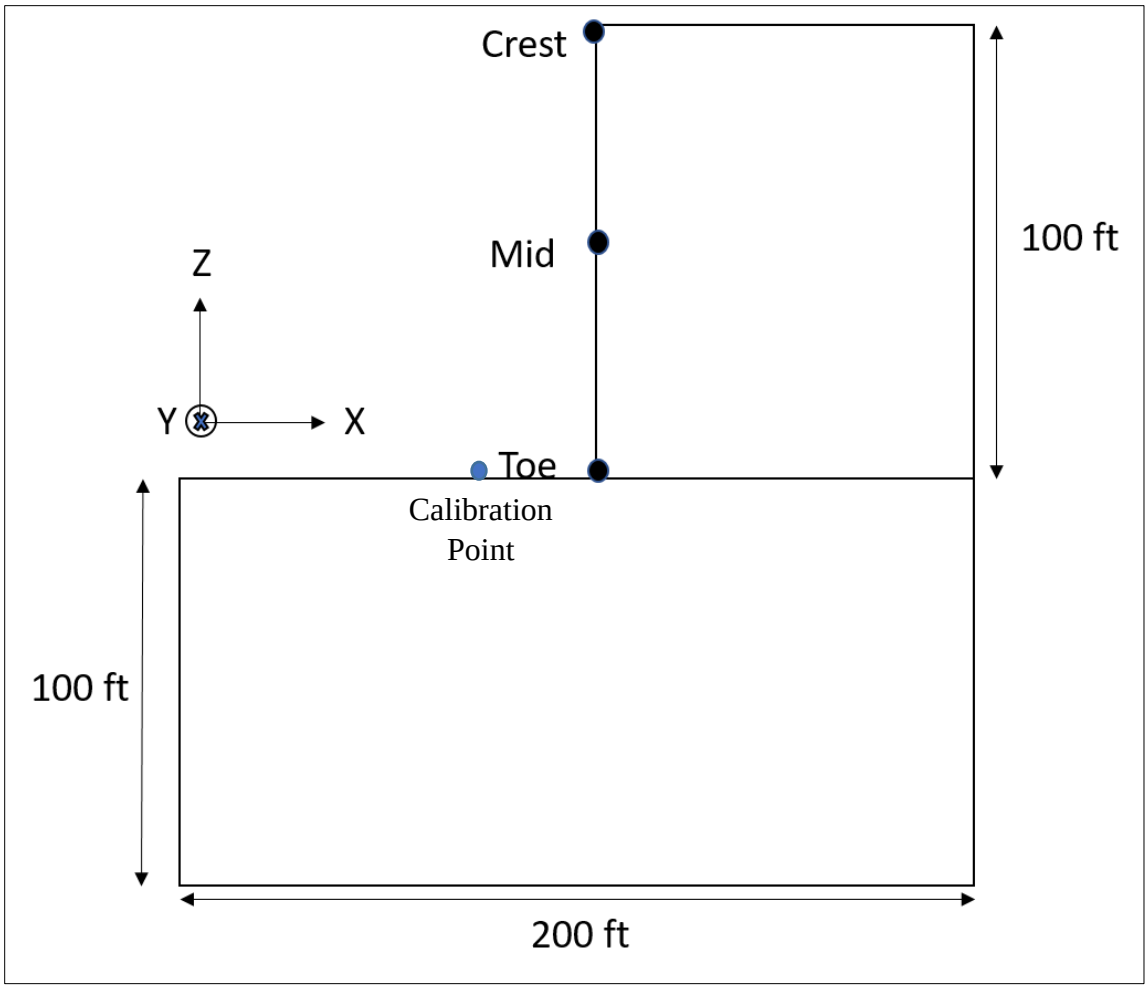

Figure 3-8: Schematic 2D diagram of a 100ft model for the analysis

3.2 Calibration of the Model

Before the use of 3DEC model for parametric studies, the model was calibrated using the vibration data collected from the field in a surface mine operation. Figure 3-9, shows one of the velocity record collected from the field. The properties of the rock material were adjusted as detailed in Table 3-1, and as shown in Figure 3-10, the resulting Fast Fourier Transformation (FFT) comparison between numerical output and field data gives a reasonable correlation. The calibration was done taking a numerical simulation output on the base of the floor across the toe of the high-wall as the real-time data was collected on the floor of the wall around 20 feet away from the toe as shown in Figure 3-8.

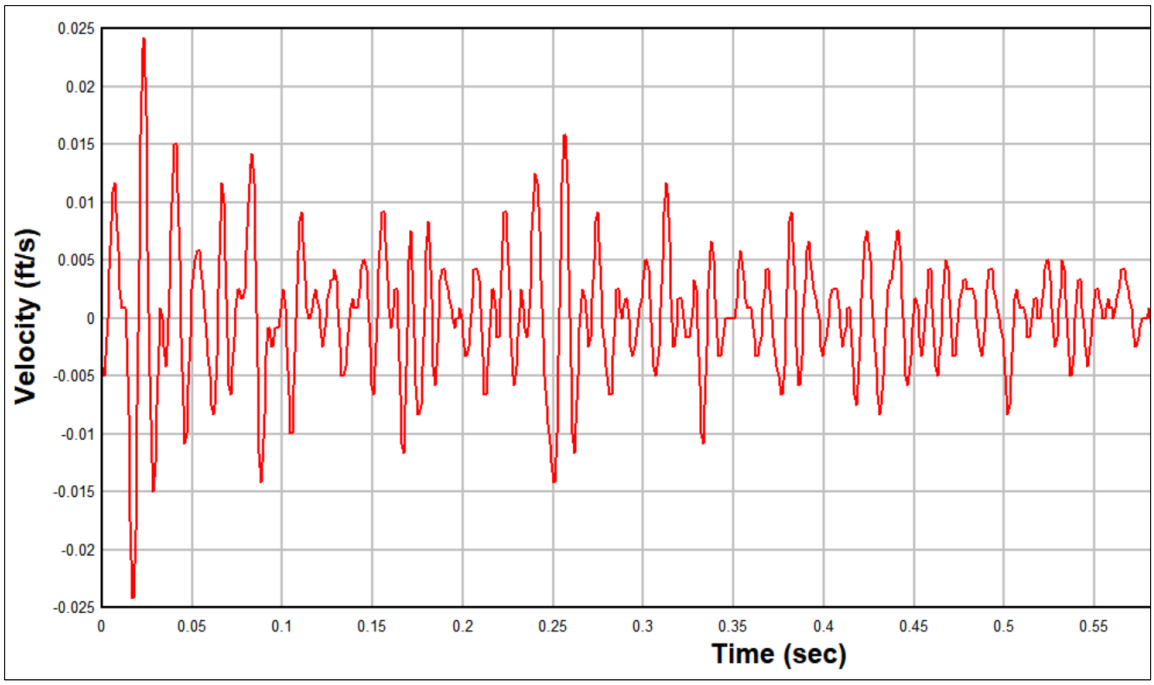

Figure 3-9: Velocity record data collected in the field

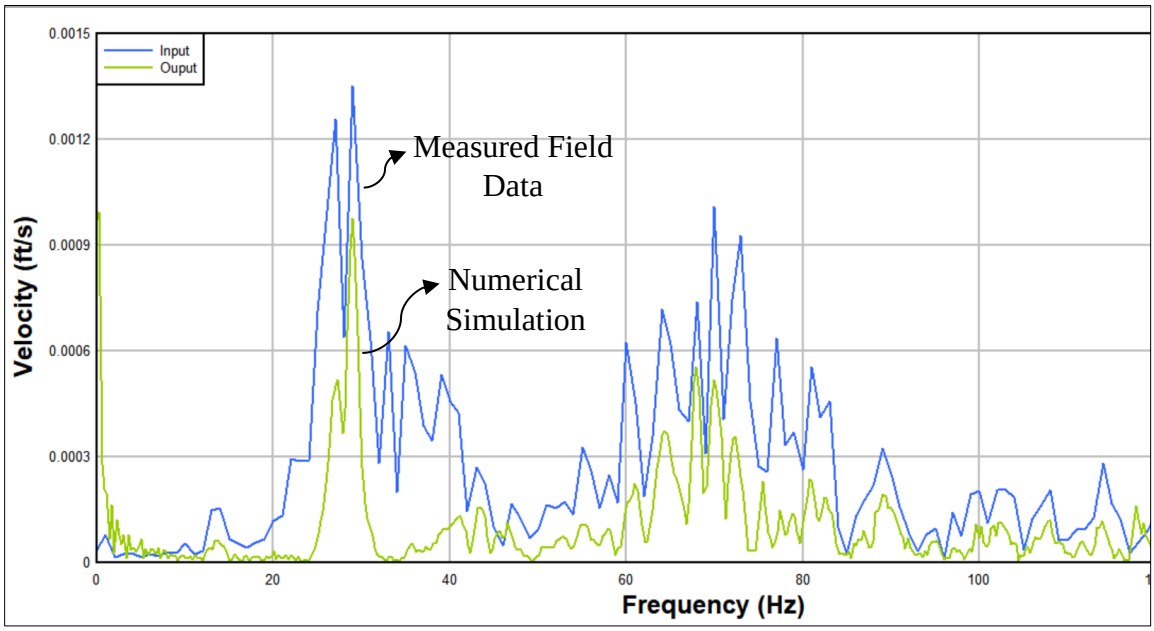

Figure 3-10: Calibration of the model by using the field vibration data

3.3 Parametric Study

The parametric study was focused on the determining the effects of variations in geometric parameters as detailed in Table 3-2, of high-wall and vibration parameters of a blast on the

frequencies affecting the strain rate in the high-wall. The parameters considered for this study were:

1. High-wall height
2. Slope angle of the high-wall
3. Amplitude of vibration on the high-wall

Table 3-2: Various parameters considered for the study and their variations

High-Wall Height	Slope Angle	Amplitude
100ft	90 degrees	1 in/s
200ft	65 degrees	3 in/s
300ft	45 degrees	5 in/s
400ft	30 degrees	
500ft		

For the parametric study, initially, the natural frequency of the calibrated 100ft 3DEC high-wall model was established. To determine the natural frequency of the model, it was decided to shake the model with a constant amplitude velocity vibration. For this purpose, an artificial input sinusoidal wave was created as shown in Figure 3-11, where the shear stress histories were generated using the Equation 3.1 and they were applied at the base of the model. The model was shaken with a wide range of the frequencies from 5 Hz to 60 Hz for the fixed velocity amplitude of 1 in/s. The boundary conditions and the properties of the model were not changed and were kept the same as when the calibration of the model was done.

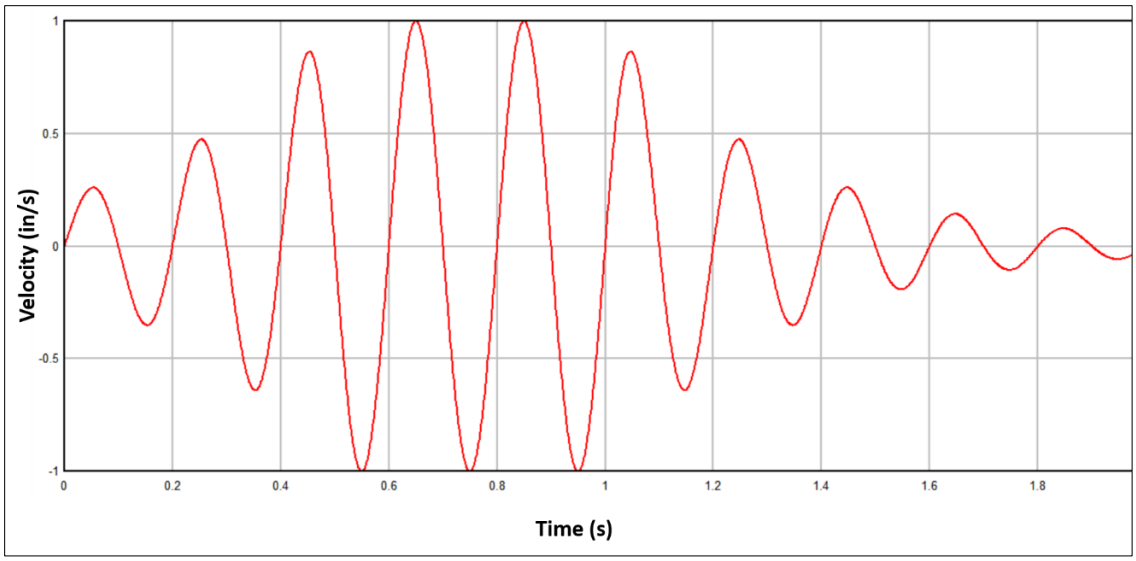

Figure 3-11: An artificial ground vibration sine wave with a frequency of 5 Hz

3.3.1 Establishing the natural frequency of the 100ft model

The 100ft calibrated 3DEC model was shaken with a range of shear wave frequencies and the x-displacement of the mid-point of the crest line was recorded against the applied stress wave as shown in the Figure 3-12. The figure displays that the displacement

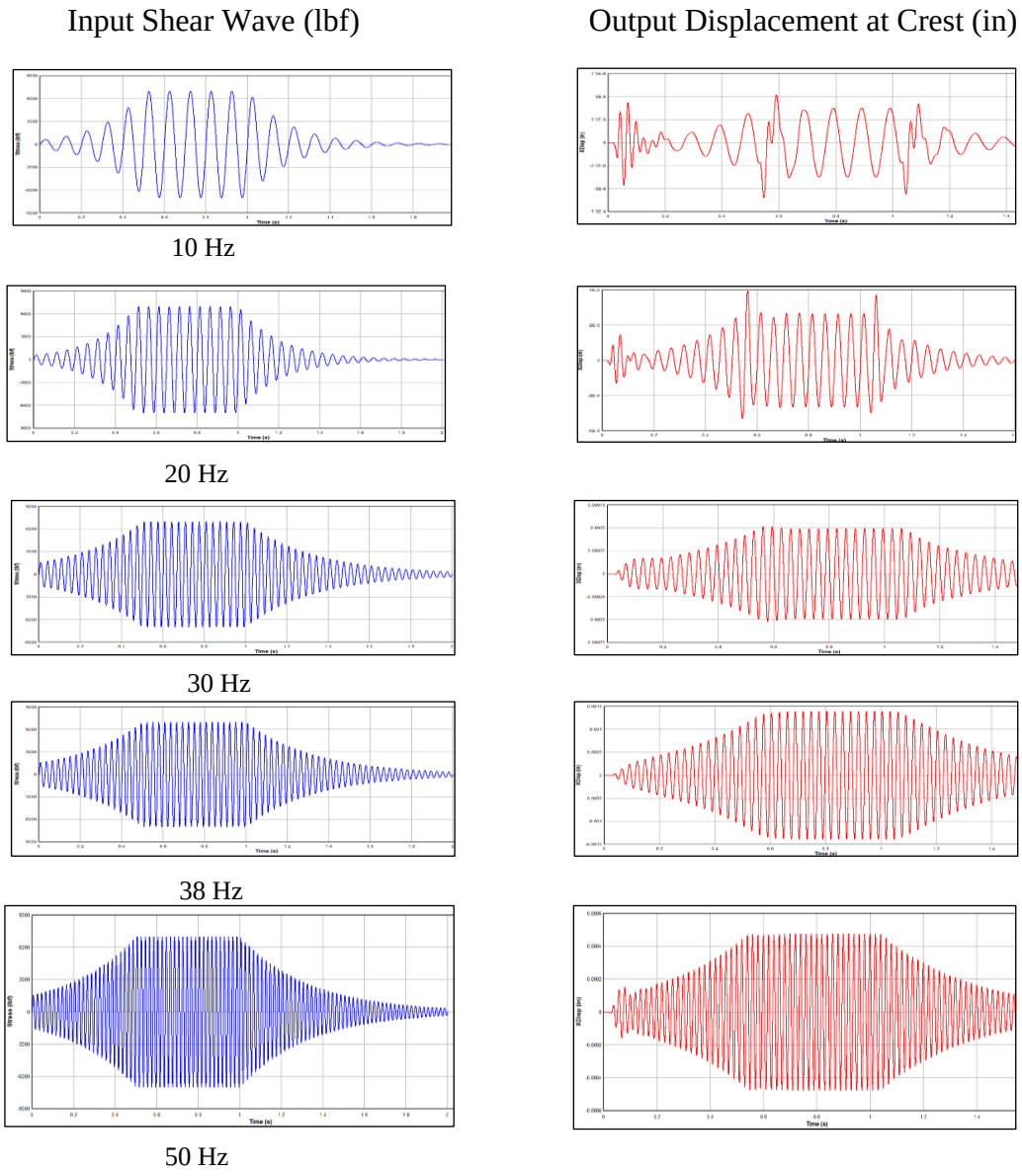

Figure 3-12: Output Displacement at the crest on various Input Shear Wave Frequencies

Further, the following figures explain the behavior of the model at various input frequencies. The points 4,5,6 in the figure refers to the point on the toe, mid and crest of the high-wall.

1. Frequency 5 Hz

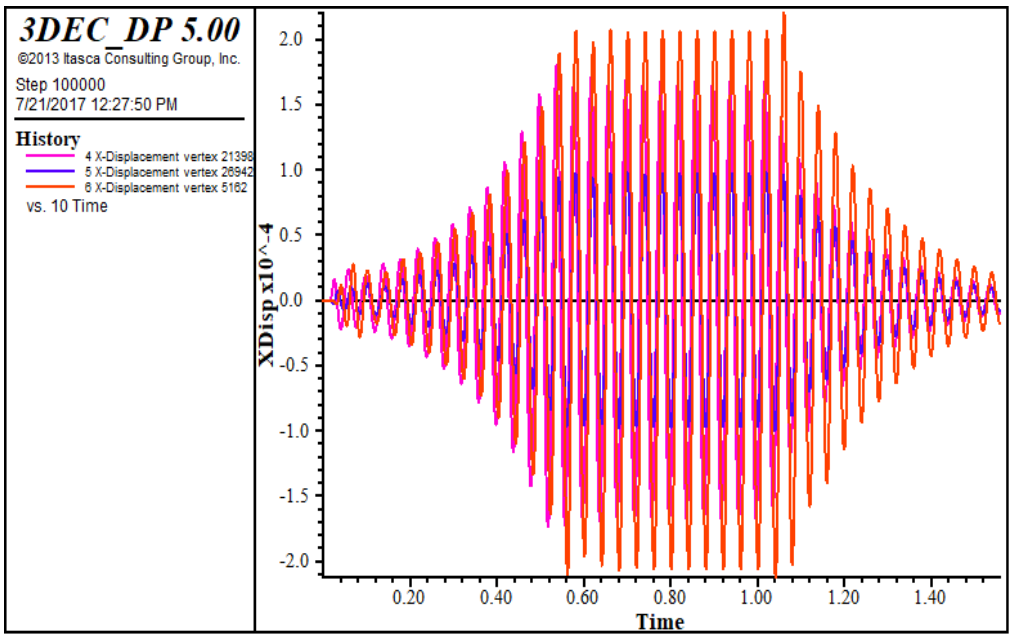

Figure 3-13: The X-displacement time history for the 5 Hz stress wave on 100ft model

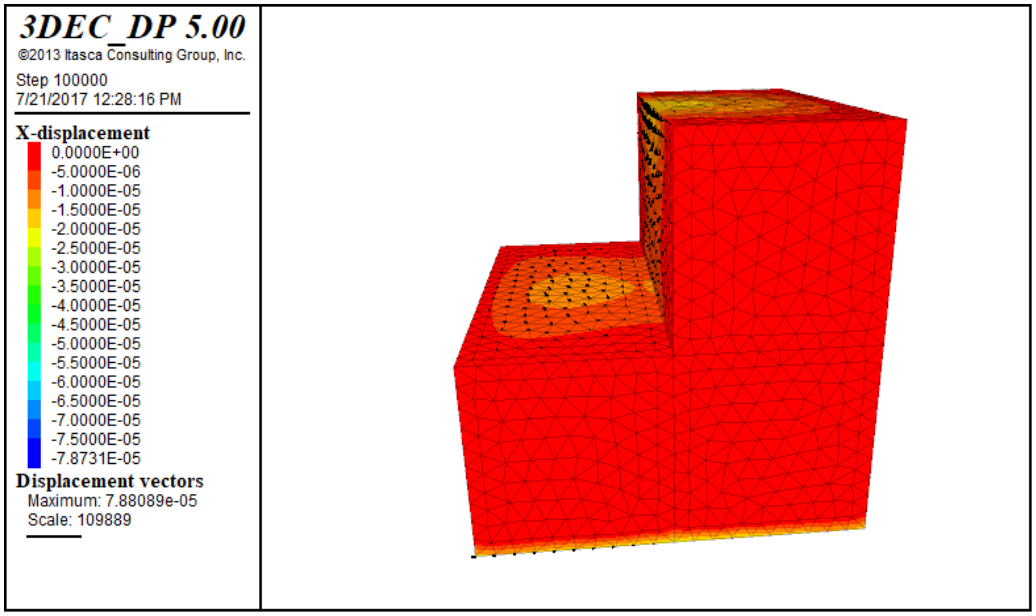

Figure 3-14: The X-displacement contour for the 5 Hz stress wave on 100ft model

2. Frequency 20 Hz

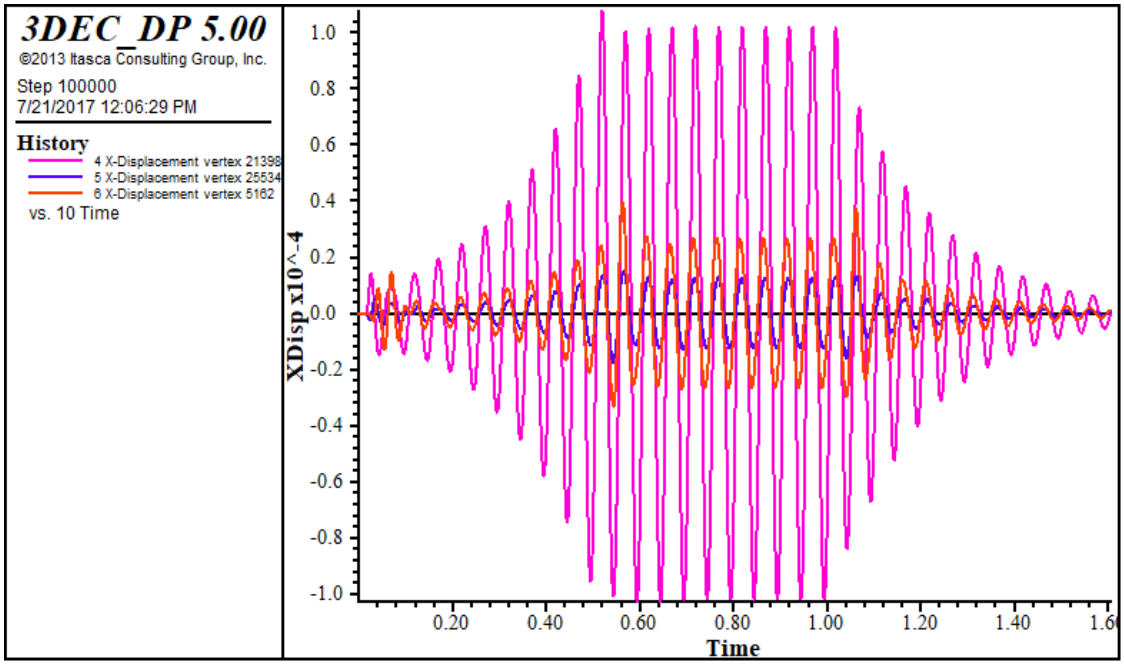

Figure 3-15: The X-displacement time history for the 20 Hz stress wave on 100ft model

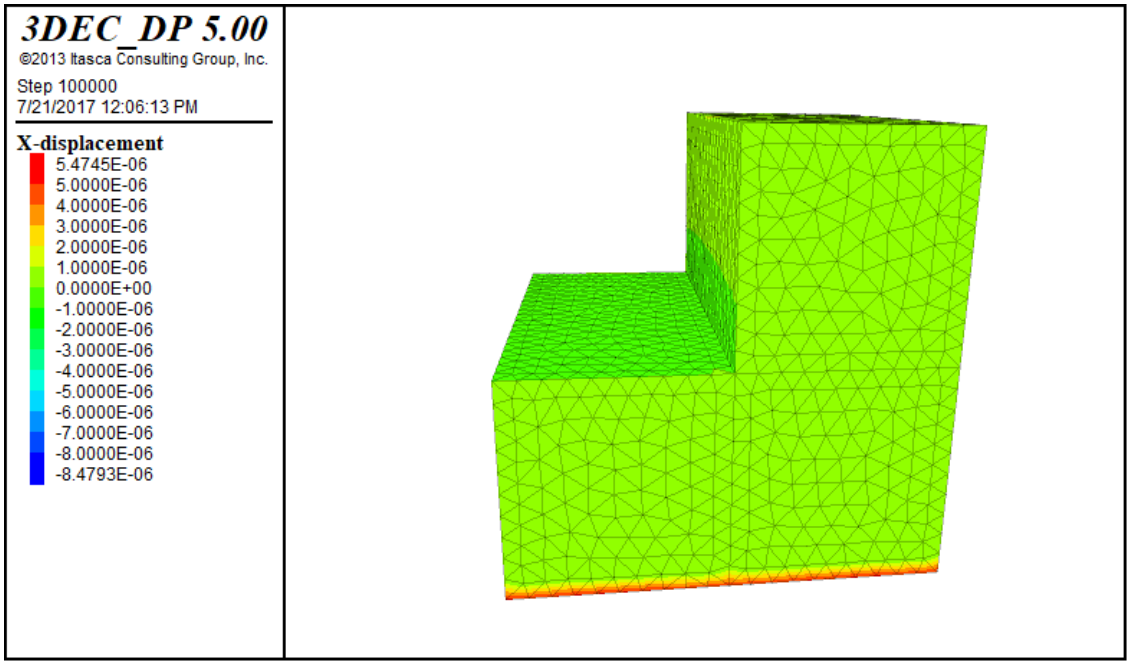

Figure 3-16: The X-displacement contour for the 20 Hz stress wave on 100ft model

3. Frequency 30 Hz

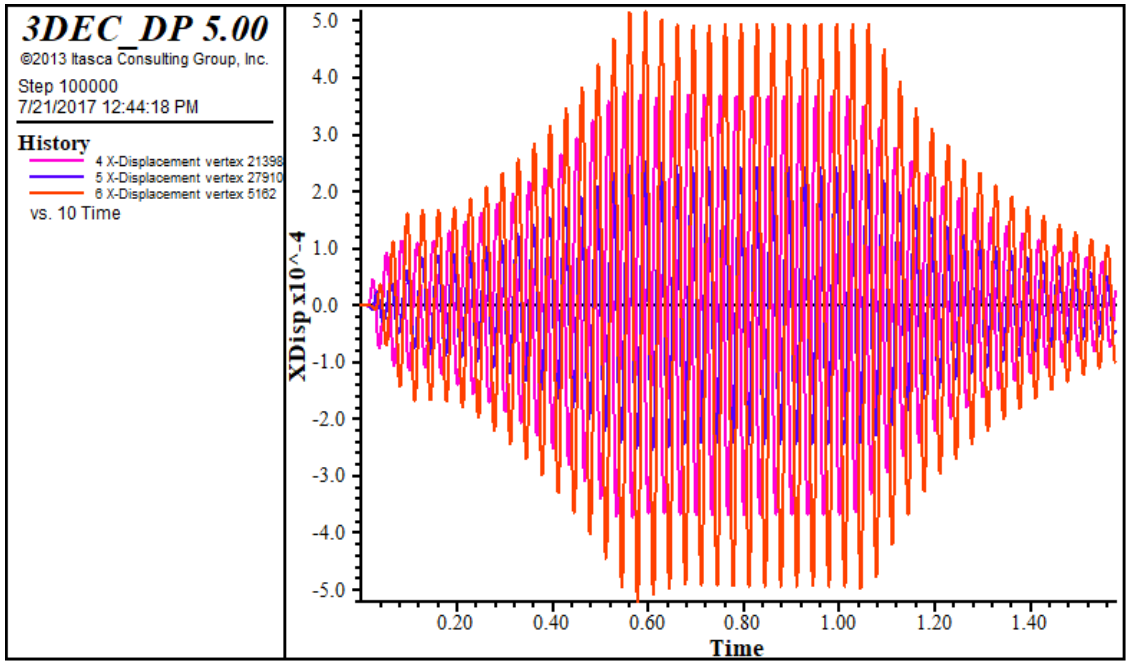

Figure 3-17: The X-displacement time history for the 30 Hz stress wave on 100ft model

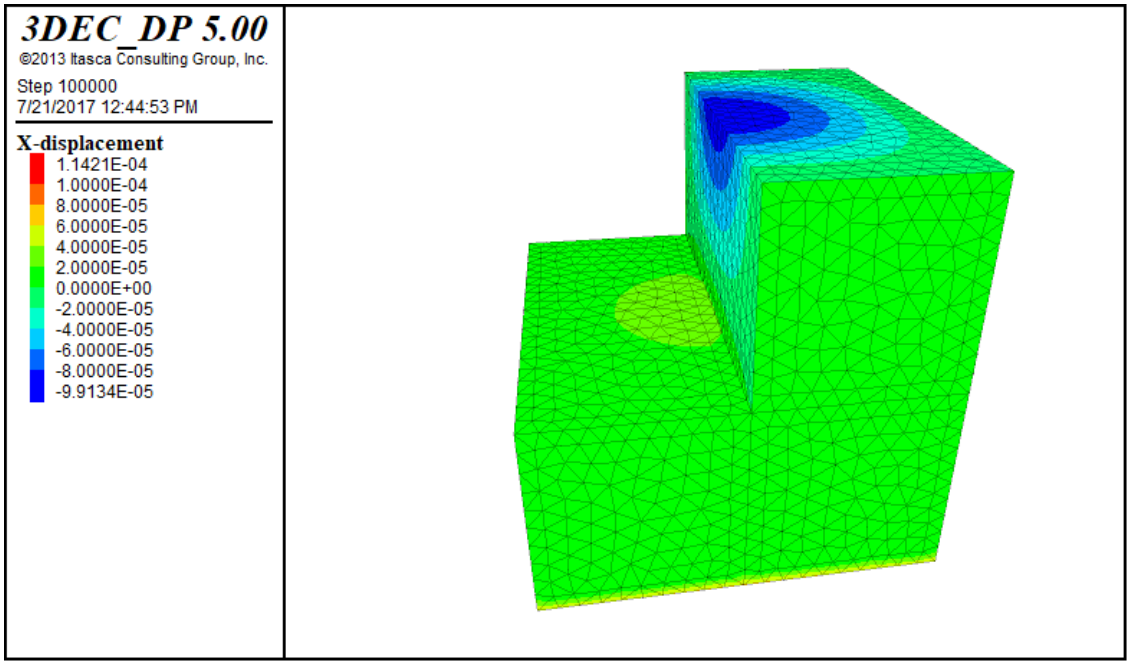

Figure 3-18: The X-displacement contour for the 30 Hz stress wave on 100ft model

4. Frequency of 38 Hz

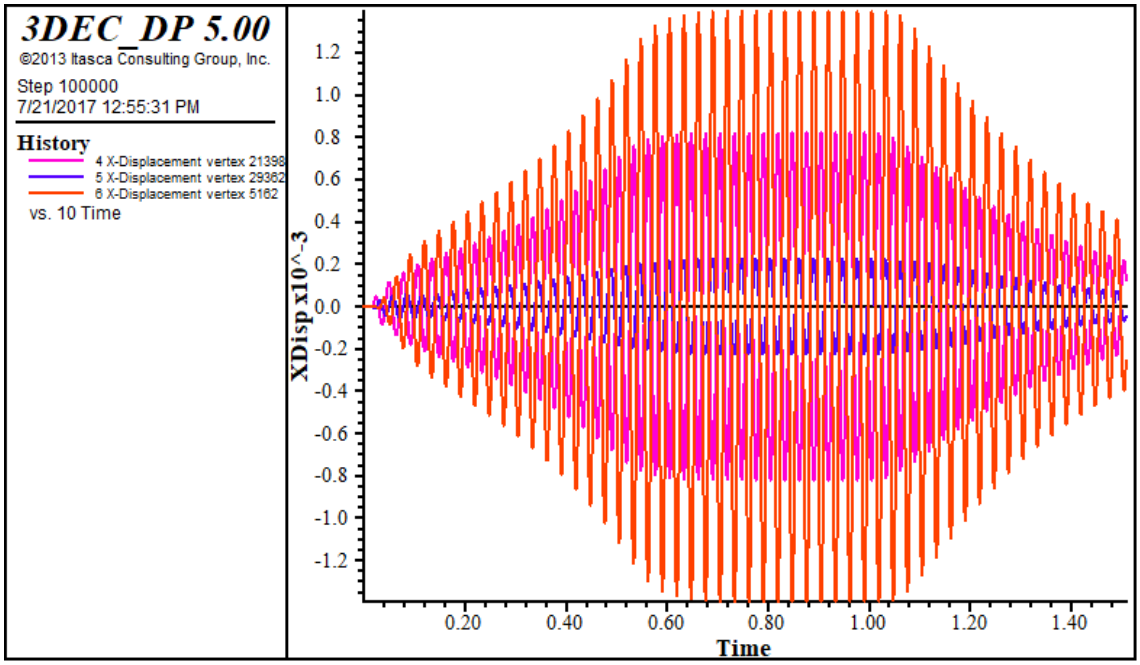

Figure 3-19: The X-displacement time history for the 30 Hz stress wave on 100ft model

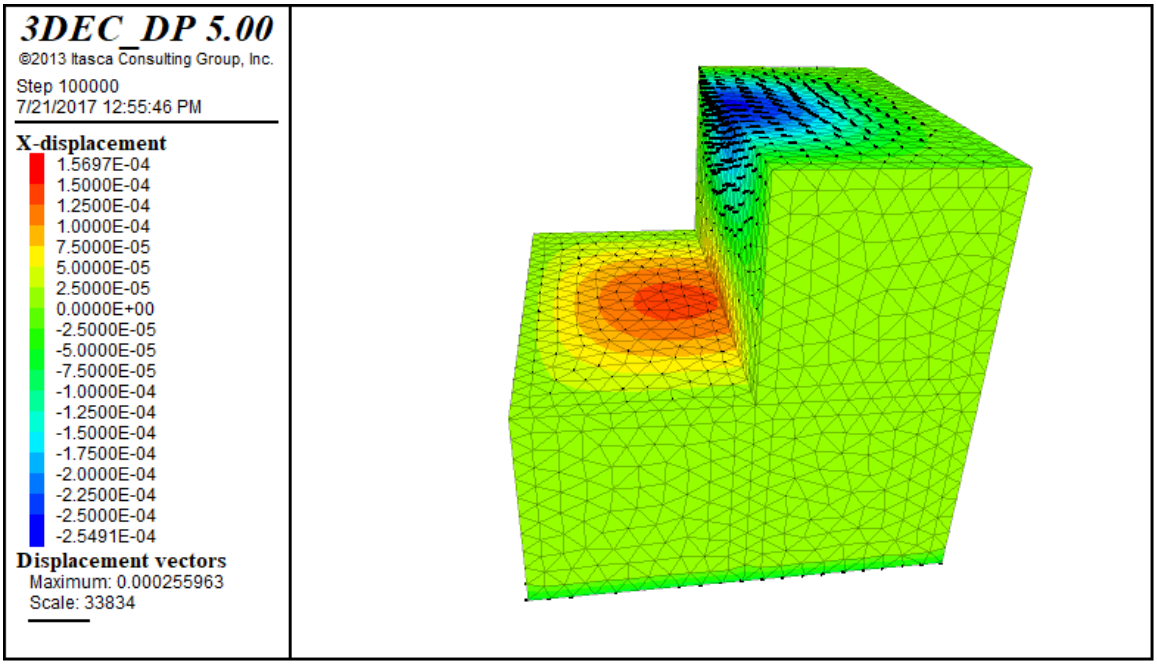

Figure 3-20: The X-displacement contour for the 38 Hz stress wave on 100ft model

5. Frequency 50 Hz

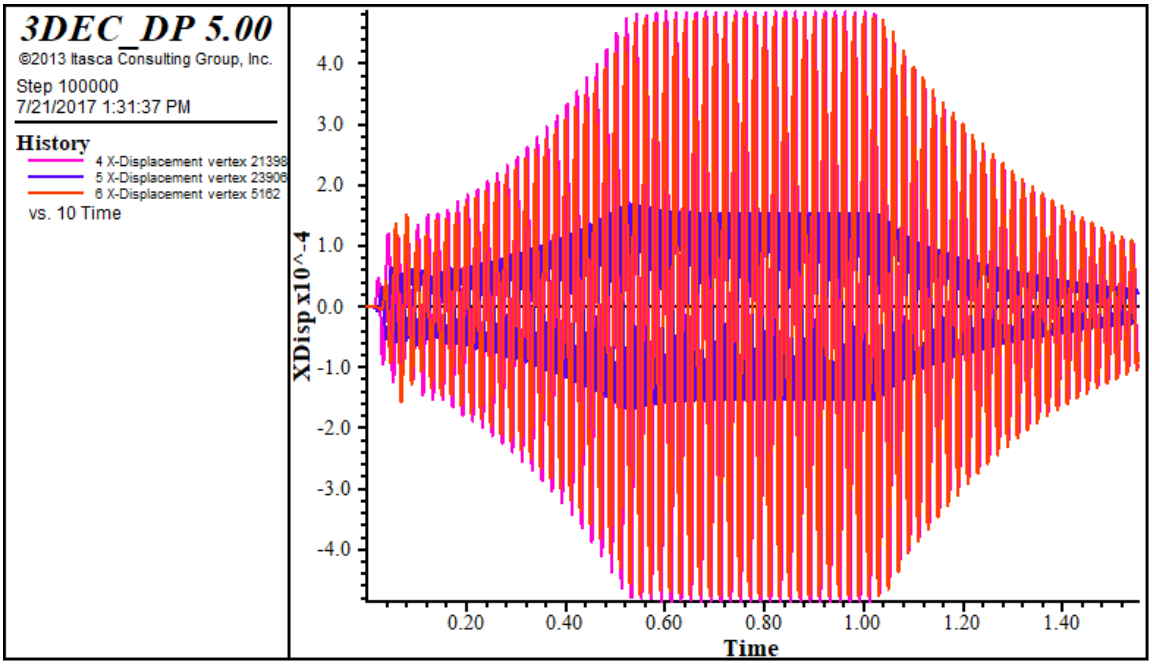

Figure 3-21: The X-displacement time history for the 50 Hz stress wave on 100ft model

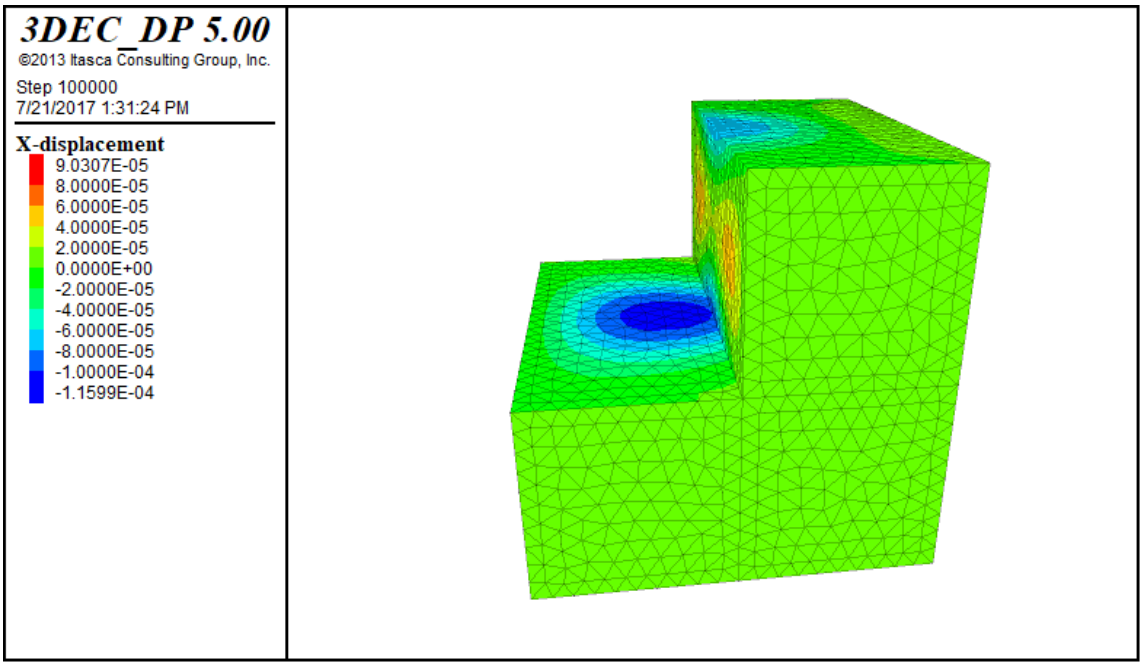

Figure 3-22: The X-displacement contour for the 50 Hz stress wave on 100ft model

6. Frequency 60 Hz

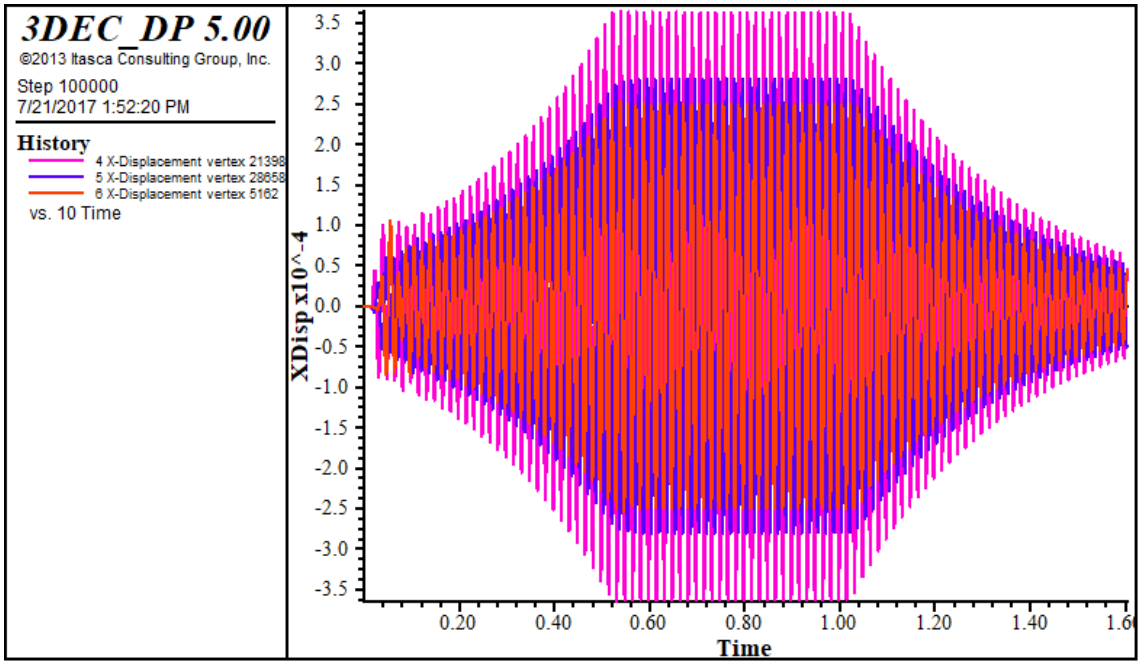

Figure 3-23: The X-displacement time history for the 60 Hz stress wave on 100ft model

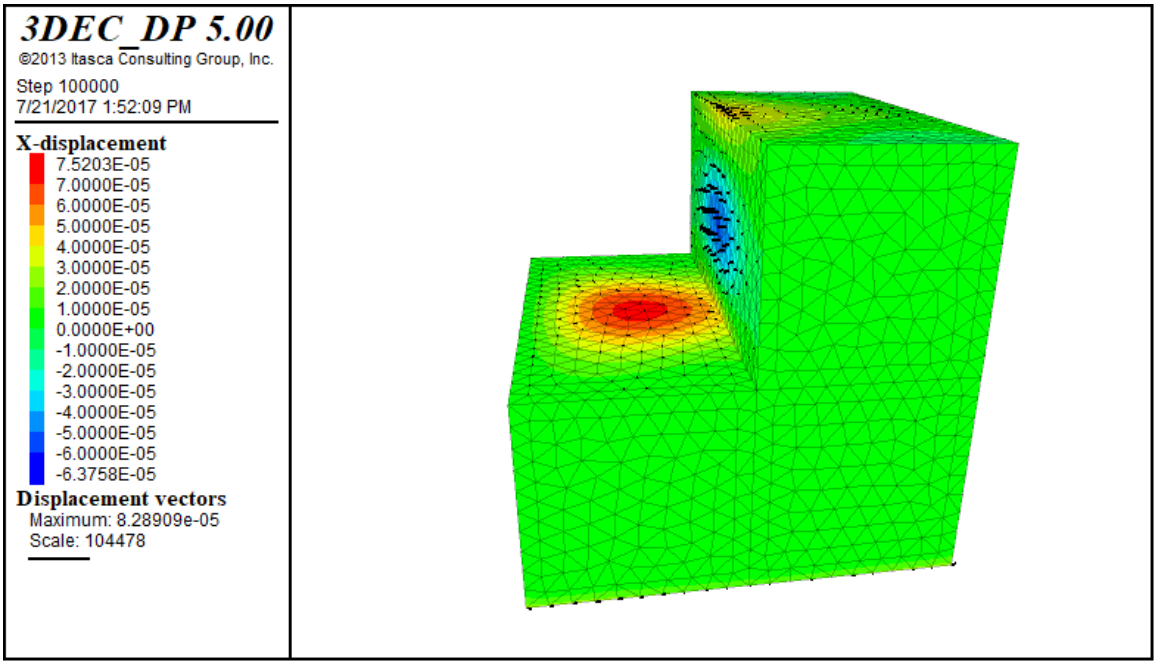

Figure 3-24: The X-displacement contour for the 60 Hz stress wave on 100ft model

It was observed as shown in Figure 3-25 that for up to a certain frequency of 38 Hz the displacement of the particle at the mid-point of the crest line kept on increasing but after that on increasing the frequency of the input wave, the displacement declined steadily. This nature of any structure is observed at the natural frequency, where the maximum displacement is observed and displacement on both sides of that frequency is smaller than the displacement at that natural frequency.

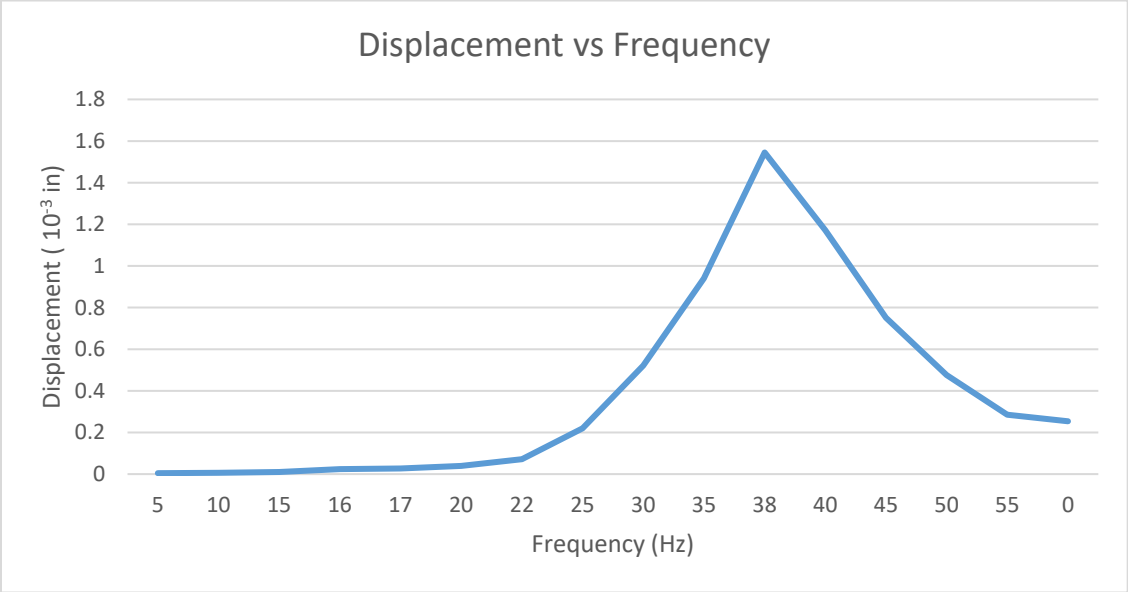

Figure 3-25: Displacement vs Frequency, with 38 Hz natural frequency of the 100ft high-wall

3.3.2 Effect of height of the high-wall on natural frequency

Once the natural frequency of the 100ft model was established, the height of the high-wall was varied from 100ft to 500ft, keeping all the other parameters and properties the same. The modeling was done to determine the effect of height on the natural frequency of the different models. The models were shaken with the same stress history as was in the previous case of the 100ft model. The results of the variation are detailed in Table 3-3 below.

Table 3-3: Variation in Natural Frequency with Height of the High-wall

Height of the High-wall	Natural Frequency
100ft	38 Hz
200ft	35 Hz
300ft	32 Hz
400ft	30 Hz
500ft	29 Hz

3.3.3 Effect of slope of the high-wall on natural frequency

Once the effect of variation of the height of the model was established the next parameter that was considered for the study was the slope of the wall. In the case of variation in height the slope of the wall was kept constant at 90 degrees. In this case, the height of the wall was kept at 100ft and slope of the wall varied from practical values in the range of 90 degrees to 30 degrees. The data for the natural frequency for the slope of 90 degrees was captured in the previous section, so the other data points were captured during this study. The frequency of the stress wave for the study was varied from the range of 5 Hz to 60 Hz. The sampling rate was increased in some cases to collect close in data figures.

1. Slope Angle 45 degrees

1. Frequency 20 Hz

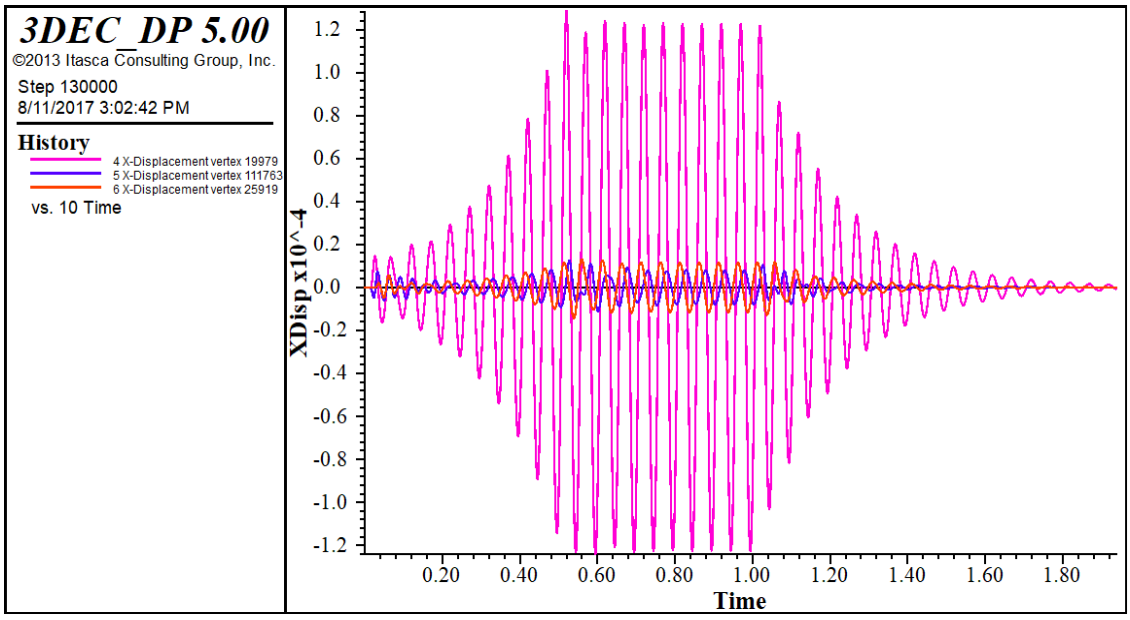

Figure 3-26: The X-displacement time history for the 20 Hz stress wave on 100ft model

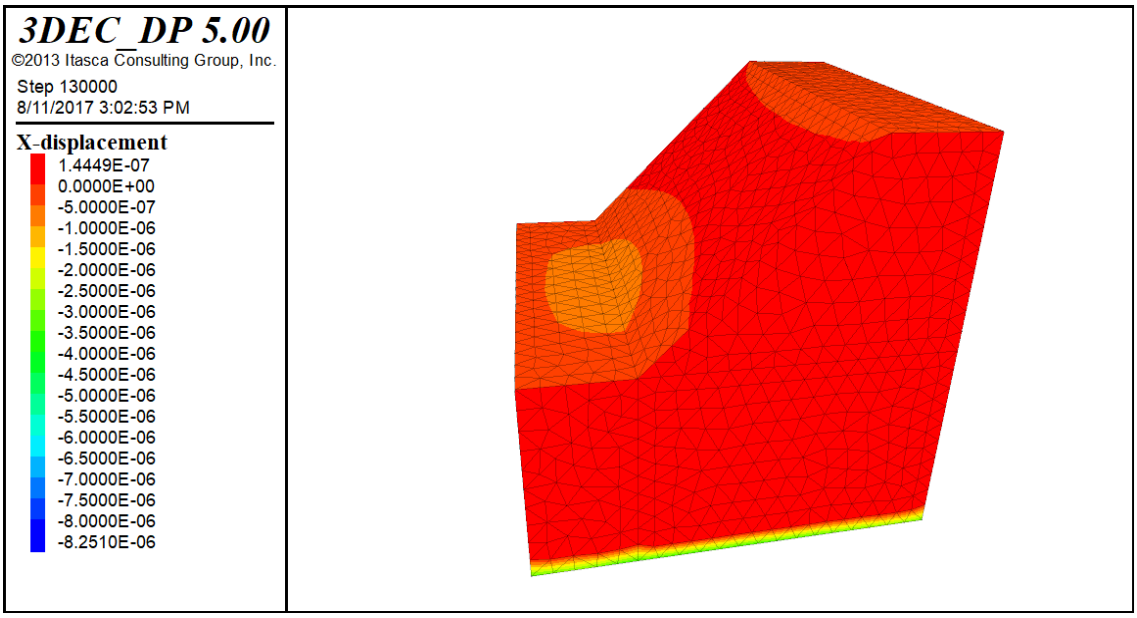

Figure 3-27: The X-displacement contour for the 20 Hz stress wave on 100ft model

2. Frequency 28

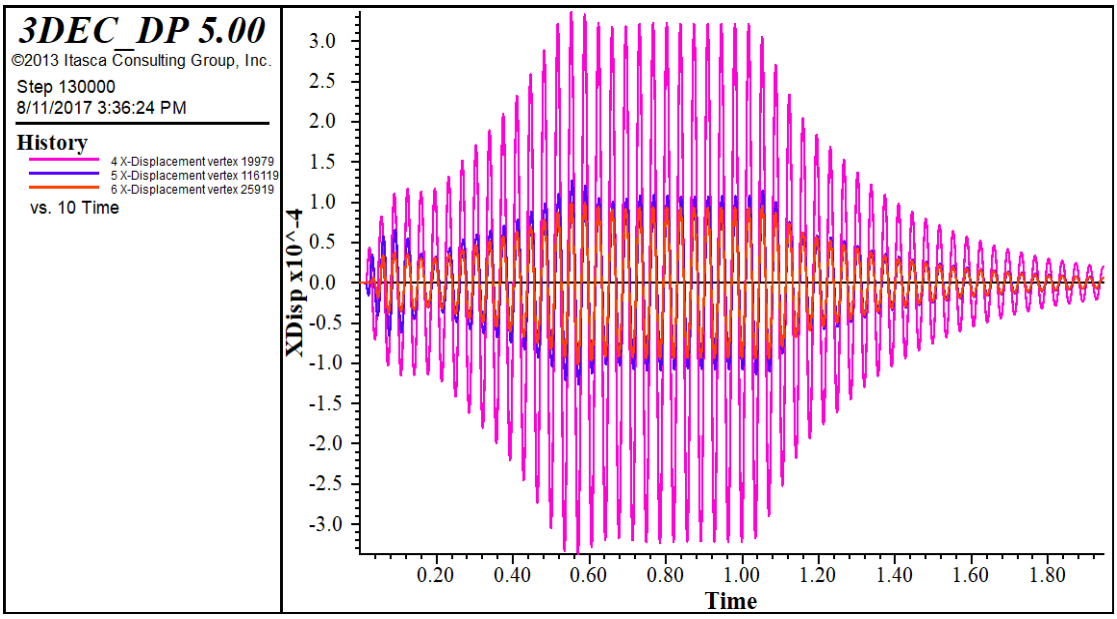

Figure 3-28: The X-displacement time history for the 28 Hz stress wave on 100ft model

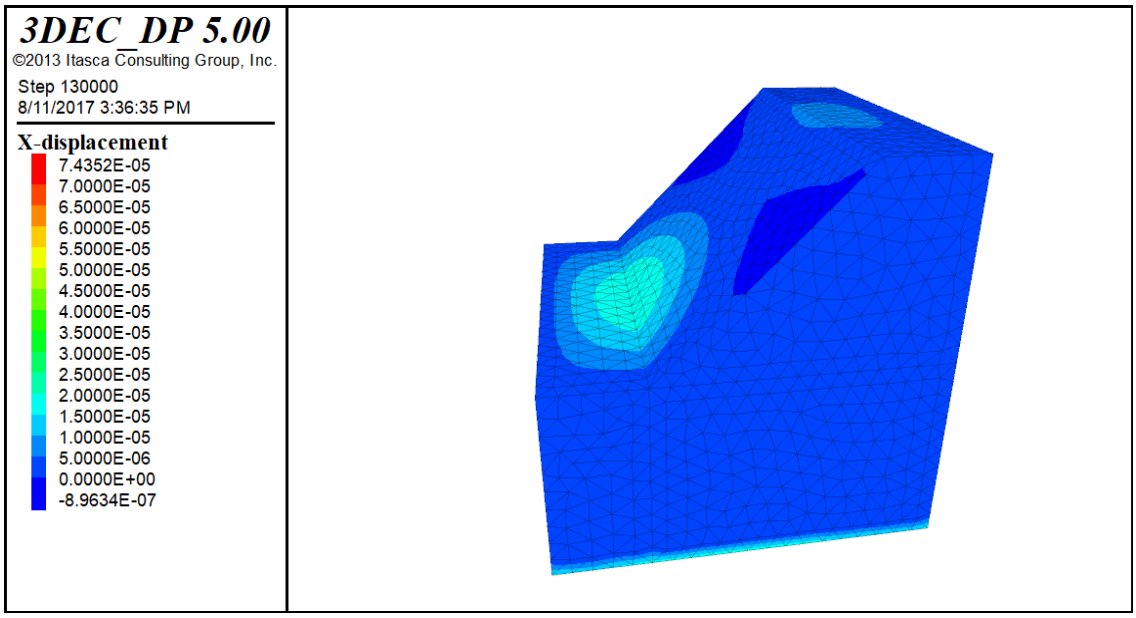

Figure 3-29: The X-displacement contour for the 28 Hz stress wave on 100ft model

3. Frequency 44

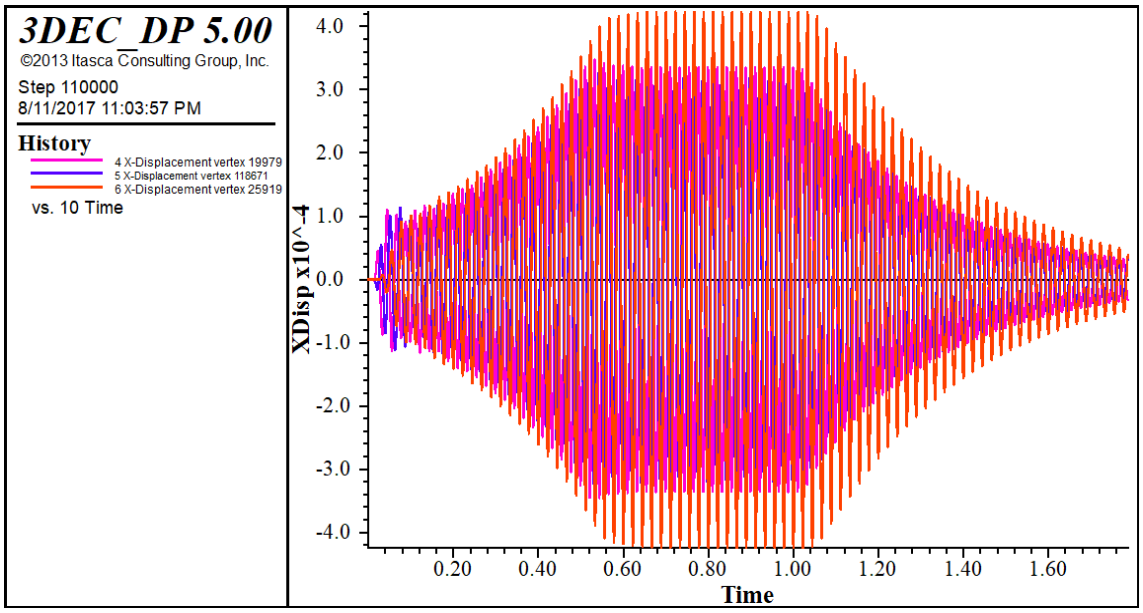

Figure 3-30: The X-displacement time history for the 44 Hz stress wave on 100ft model

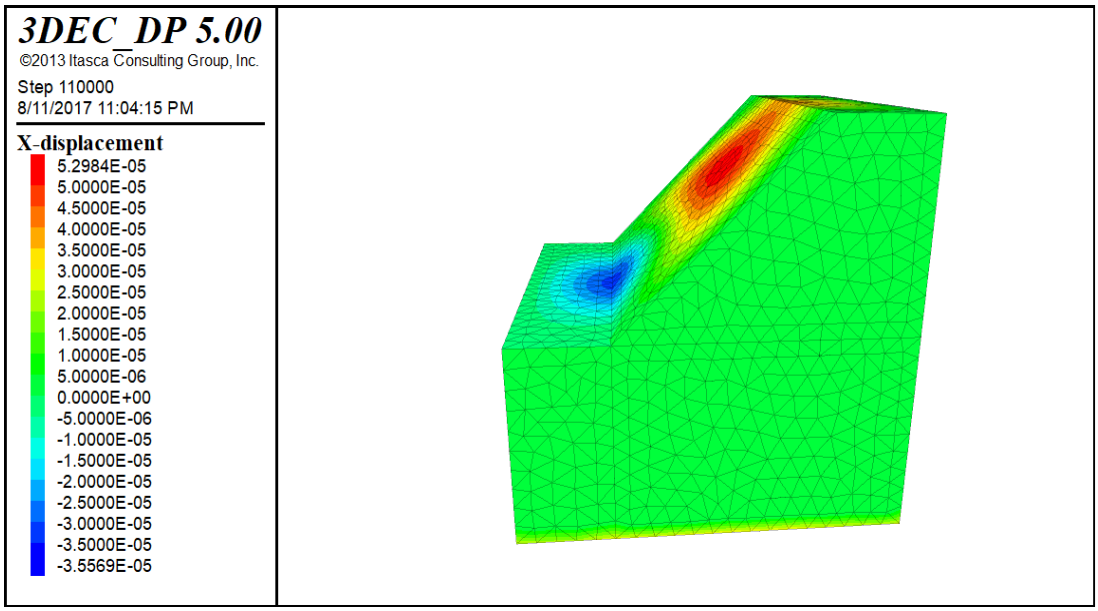

Figure 3-31: The X-displacement contour for the 44 Hz stress wave on 100ft model

4. Frequency 55

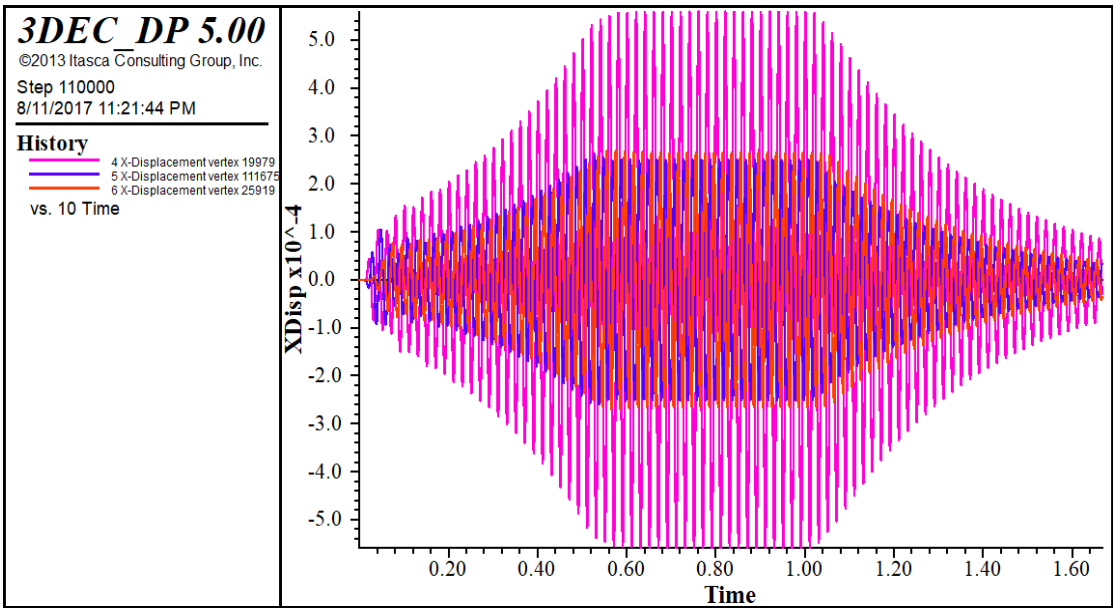

Figure 3-32: The X-displacement time history for the 55 Hz stress wave on 100ft model

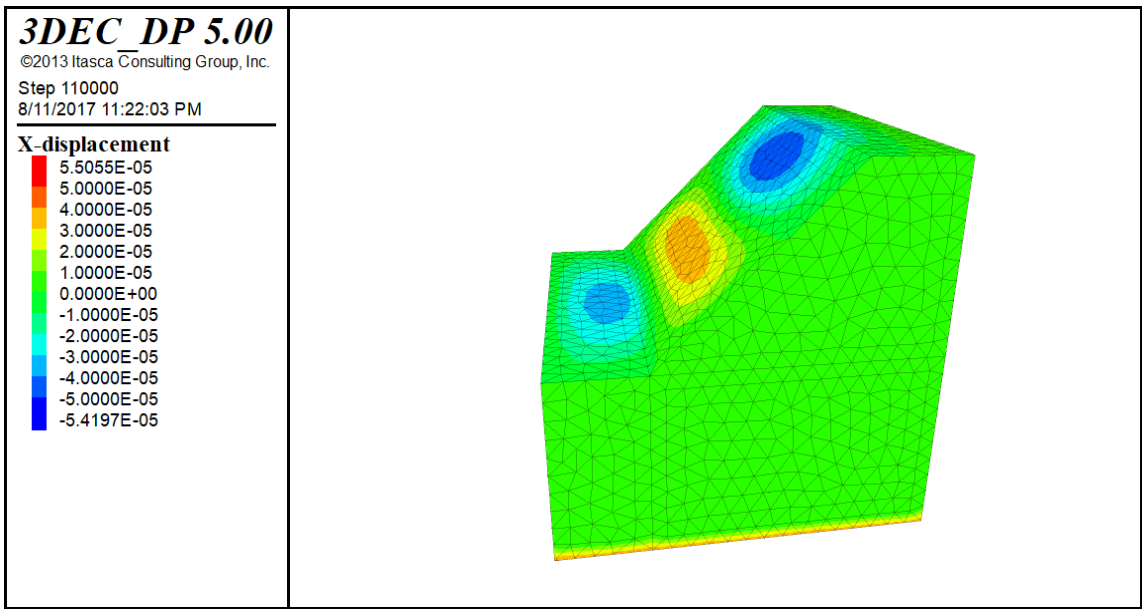

Figure 3-33: The X-displacement contour for the 55 Hz stress wave on 100ft model

Similar data was collected for the slopes with 65 degrees and 30 degrees. In the variation in the natural frequency of the high-wall with the slope as detailed in Table 3-4, it was observed that the natural frequency shifts slightly towards the higher side as the slope becomes flatter.

Table 3-4: Variation of the Natural Frequency of the high-wall with Slope angle

Slope of the 100ft High-wall	Natural Frequency
90 degrees	38 Hz
65 degrees	42 Hz
45 degrees	44 Hz
30 degrees	46 Hz

3.3.4 Effect of the amplitude of the vibration on natural frequency of high-wall

The amplitude of the artificial wave used for the simulation of the models at various frequency was kept at 1 in/s for the sake of simplifying the calculation process. But to see if there is any effect on the natural frequency of a high-wall due to change in the amplitude of the input stress wave. The calibrated models of the 100ft and 300ft while keeping all the other parameters same were shaken with the increased amplitude of the 3 in/s and 5 in/s.

It was found that the displacement measured at all the three concerned points at the different frequencies was increased by the similar factor as the increase in the amplitude of the input stress wave. The results of the study are detailed in Table 3-5 below.

Table 3-5: Effect of change in amplitude on Natural Frequency of High-wall

Height of the High-wall	Peak Amplitude of Velocity	Natural Frequency
100ft	1 in/s	38 Hz
	3 in/s	
	5 in/s	
300ft	1 in/s	32 Hz
	3 in/s	
	5 in/s	

4 Results

The parametric study concentrated on the effects of the following factors on the natural frequency of the high-wall:

1. High-wall height
2. Slope angle of the high-wall
3. Amplitude of vibration on the high-wall

1. Effect of Height on Natural Frequency

Based on the results of the 100ft model, the study was extended to understand and observe the effect of changing heights on the behavior of the high-wall. As shown in the Figure 4-1 it is observed that for the similar properties and the vibrations levels, the natural frequency starts to shift gradually to lower frequency levels with the increase of the high of the high-wall.

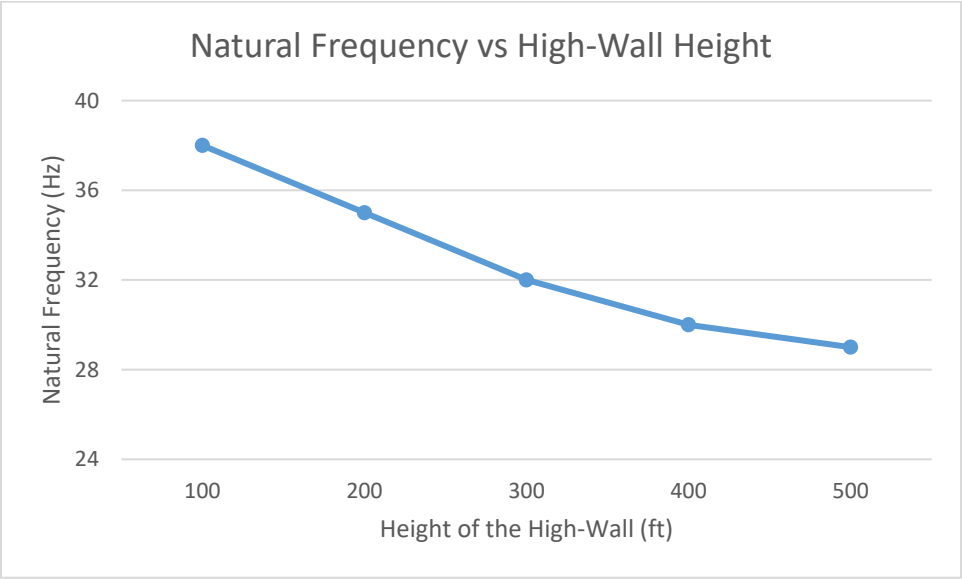

Figure 4-1: Line Graph between Natural Frequency and High-Wall Height

2. Effect of Slope of the wall on Natural Frequency

The slope of the high-wall left in the mine depends on the various parameters, like economic viability, the stability of the overall pit-slope angle and others. As the part of the parametric study, as shown in Figure 4-2, the slope of the 100ft, 300ft, 500ft models were

varied to various angles to see the effect of changing slope on the natural frequency of the high-wall. Table 4-1, details the results of this study on the 100ft high-wall. It was observed, as the slope of the high-wall moved towards more flatter angles, the natural frequency of the wall shifted to higher frequencies. Further, Figure 4-2 shows the variations of the natural frequency with the slope of the high-wall for various heights under study.

Table 4-1: Effect of Slope angle on the Natural Frequency of the 100ft High-wall

Slope of the 100ft High-wall	Natural Frequency
90 degrees	38 Hz
65 degrees	42 Hz
45 degrees	44 Hz
30 degrees	46 Hz

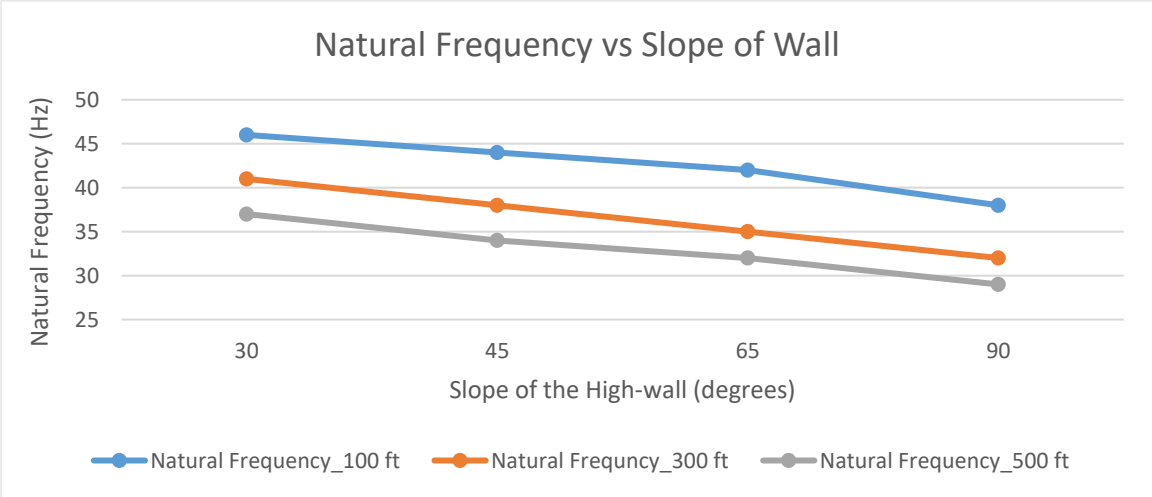

Figure 4-2: Variation of Natural Frequency with Slope of High-Wall for various heights

3. Effect of Increase in Amplitude of Vibration on Natural Frequency

All the vibrations standards across the countries include the amplitude of the vibration, as one of the key parameters. As the part of this parametric study, the effects on the natural frequency of the high-wall was observed due to the change in amplitude of the blast vibration shaking the high-wall.

Table 4-3, below shows that the changing amplitude of the vibration does not have any effect on the natural frequency of a high-wall. However, it was noted that the amplitude of the displacement of the particle for varying frequencies increased by the similar factor as the vibration levels.

Table 4-3: Effect of change in amplitude on Natural Frequency of High-wall

Height of the High-wall	Peak Amplitude of Velocity	Natural Frequency
100ft	1 in/s	38 Hz
	3 in/s	
	5 in/s	
300ft	1 in/s	32 Hz
	3 in/s	
	5 in/s	

Figure 4-3, shows the effect change in displacement by corresponding factor of three but no change in natural frequency.

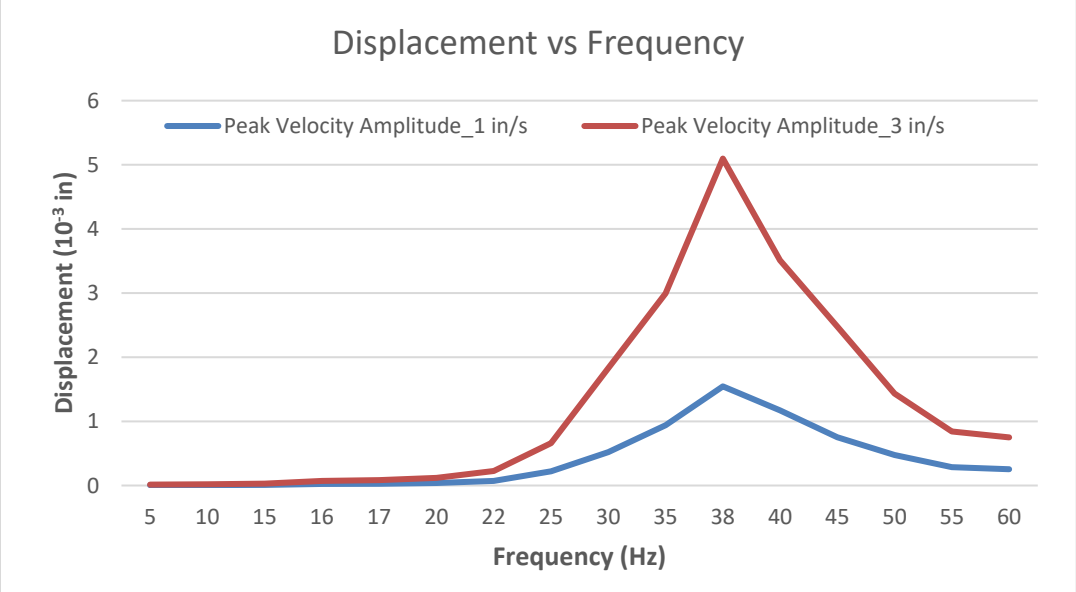

Figure 4-3: Comparison of Displacement and Frequency with Amplitude of 1 in/s & 3 in/s

5 Conclusions and Recommendations

Based on the outcomes of the parametric study done, it can be observed that the natural frequency of the high-wall, varies with the geometry, more specifically with the height and slope angle of the high-wall. It was observed that, while keeping all the properties same, with the increase in the height, the natural frequency of the high-wall shifts gradually to relatively lower frequencies. A trend of lower natural frequencies was noted for more vertical slopes as compared to the higher once with flatter slopes. Another important observation was that there is no effect of the change in amplitude of the blasting vibrations on the natural frequency of the high-wall. However, a corresponding increase in the displacement of the particles was noted.

The Z-curve given by USBM gives safe limits of peak particle velocity and frequency from blasting vibrations for buildings. It shows that blasting vibrations at low frequency could be more damaging than those at the higher frequency. However, unfortunately, they are restricted to specific cases of household structures and do not throw light on the limits for the high-walls, a permanent and crucial structure to the safety of a mine.

As the perception of the moving away from lower frequencies to higher frequencies goes stronger for buildings of one story and houses. It is required that other types of structures be considered like high-walls.

It can be understood that most of the mines cannot afford to take the time and resources out to do the numerical modeling of their structures and design their blasts accordingly. One of the most useful methods to estimate the ground resonant frequency is the use of single blast hole detonation as an input and measure the frequency of the ground. This can be a good starting point for the blasting engineers.

A fundamental step in the analysis of ground vibrations produced by blasting and its effects on the stability of high-walls is first to determine the natural frequency of the high-wall and make sure that, in the process of shifting to different frequencies, either higher or lower,

the shift should be away from the natural frequency so that safety of high-wall and miners is not compromised.

5.1 Future Course of Action

The natural frequencies observed during this study were on the higher side as compared to what is usually monitored or discovered in the field. One of the reasons for this observation could be the use of intact rock for the modeling. In the future course of study, it would be interesting to see what are the effects on the natural frequency, when the joints and other discontinuities are introduced in the numerical model. The use of scanners like the Maptek I-Site 8800 in conjunction with numerical modeling, could also be useful for understanding the movement of the wall and monitor the changes during the lifetime of high-wall.

Appendix

A. Variation in the natural frequency with the height of high-wall

A1. Model: 300ft and 90 degrees

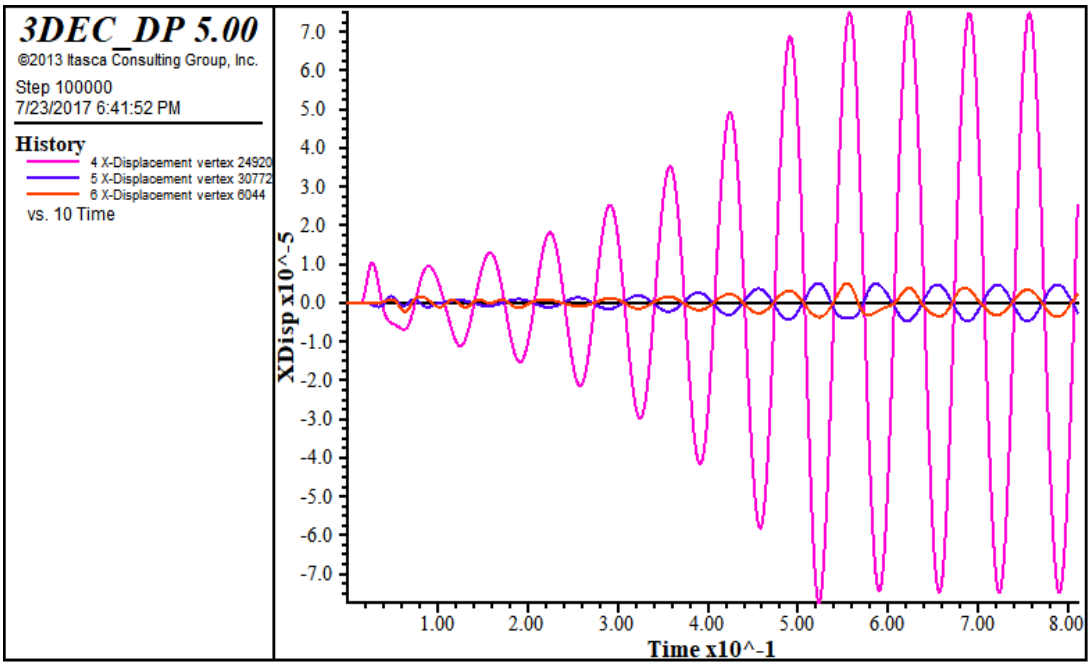

Figure A 1:The X-displacement time history for the 15 Hz stress wave on 300ft model

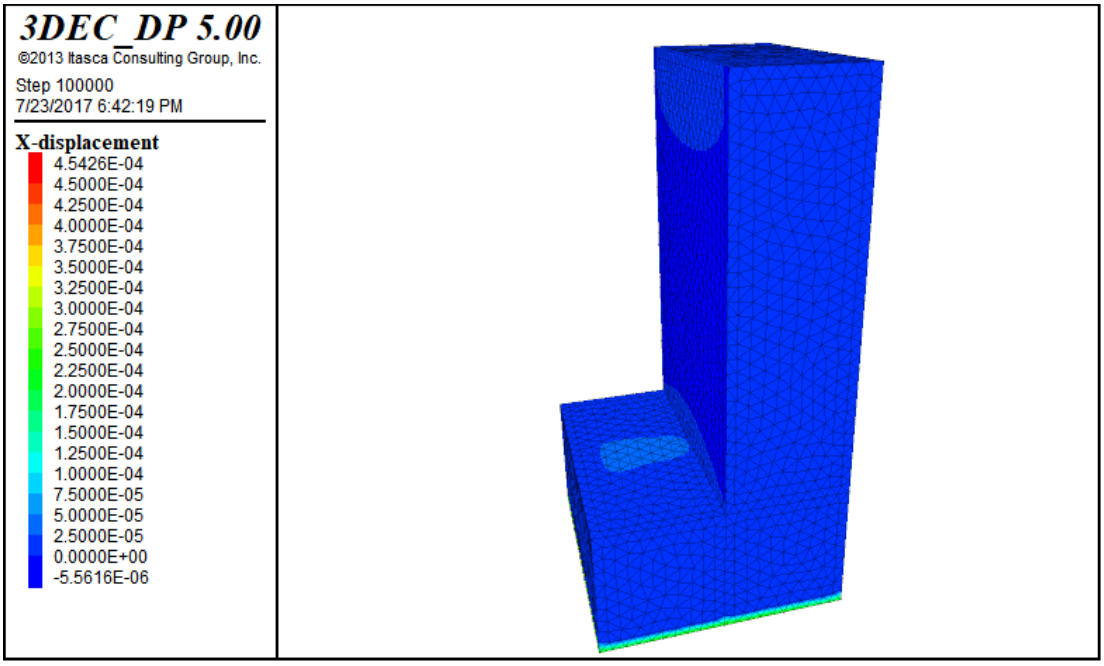

Figure A 2: The X-displacement contour for the 15 Hz stress wave on 300ft model

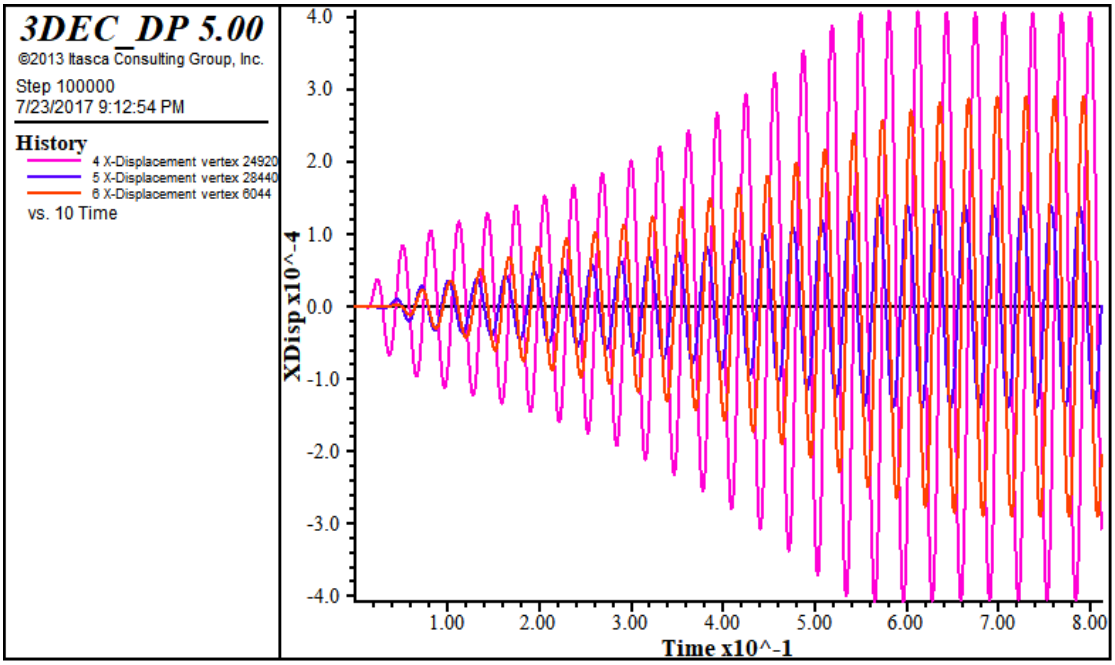

Figure A 3: The X-displacement time history for the 32 Hz stress wave on 300ft model

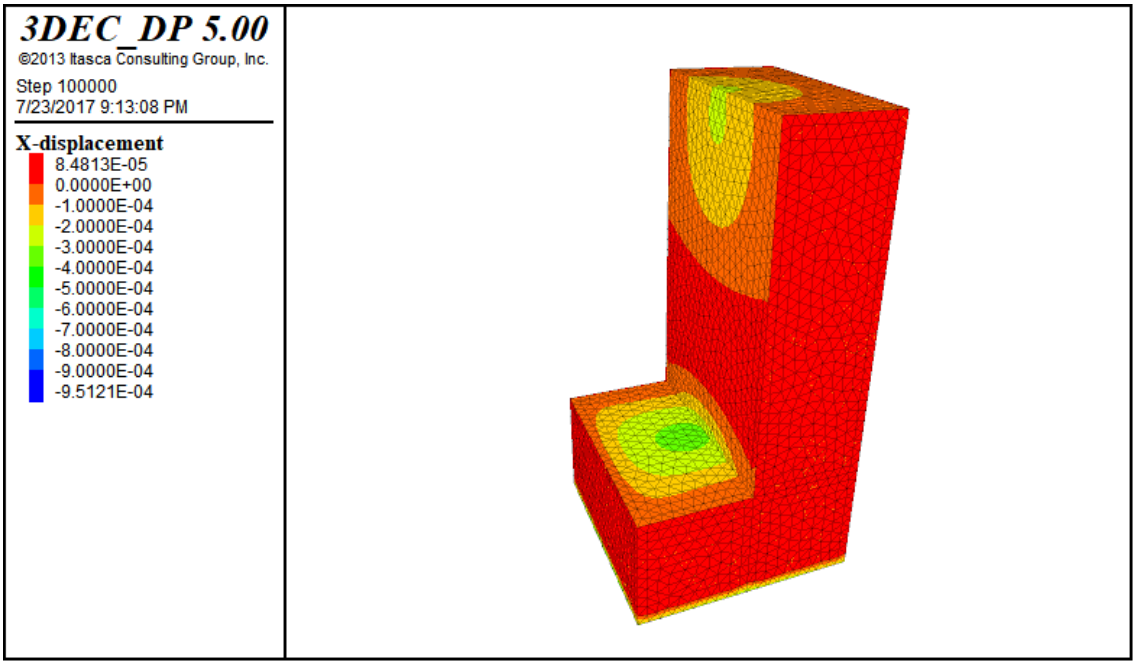

Figure A 4: The X-displacement contour for the 32 Hz stress wave on 300ft model

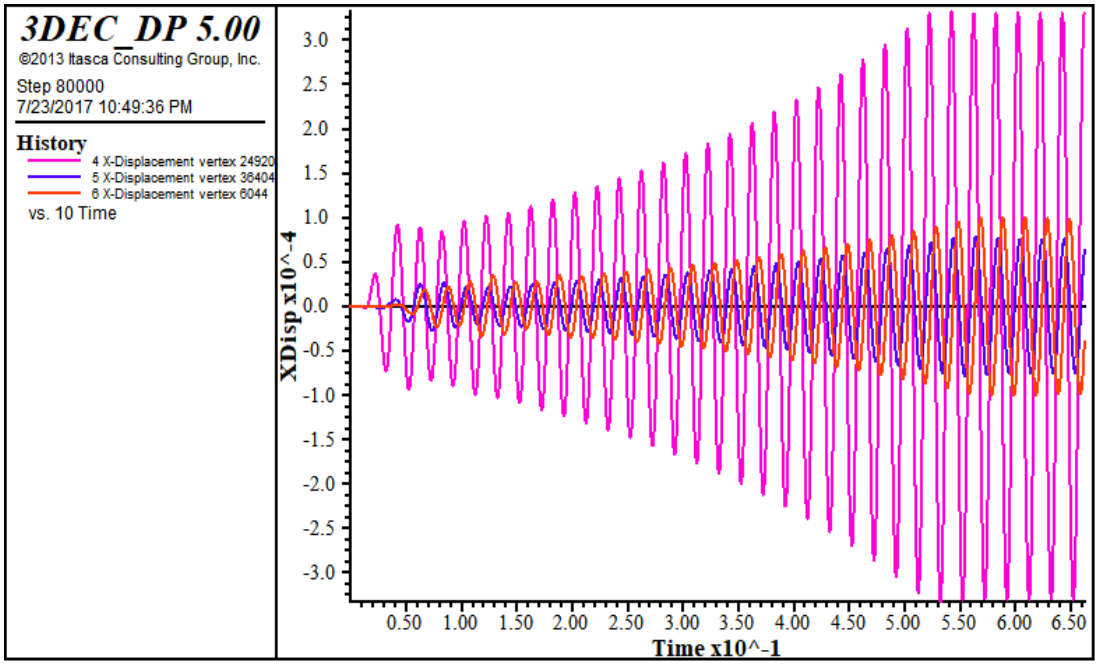

Figure A 5: The X-displacement time history for the 50 Hz stress wave on 300ft model

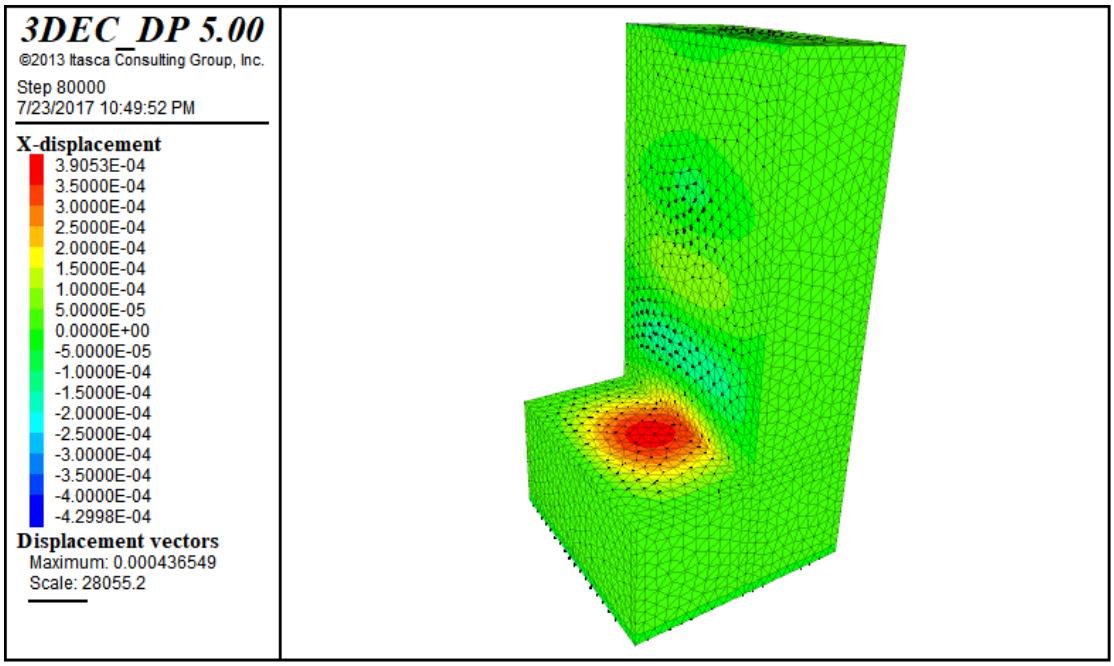

Figure A 6: The X-displacement contour for the 50 Hz stress wave on 300ft model

A2. Model: 500ft and 90 degrees

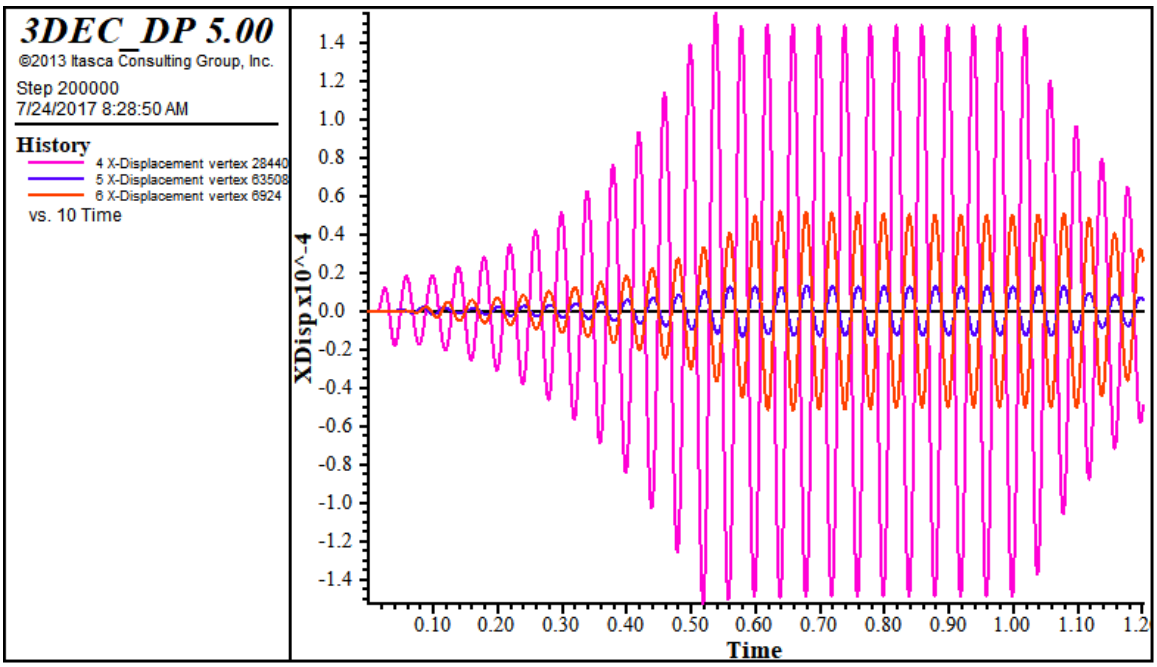

Figure A 7: The X-displacement time history for the 25 Hz stress wave on 500ft model

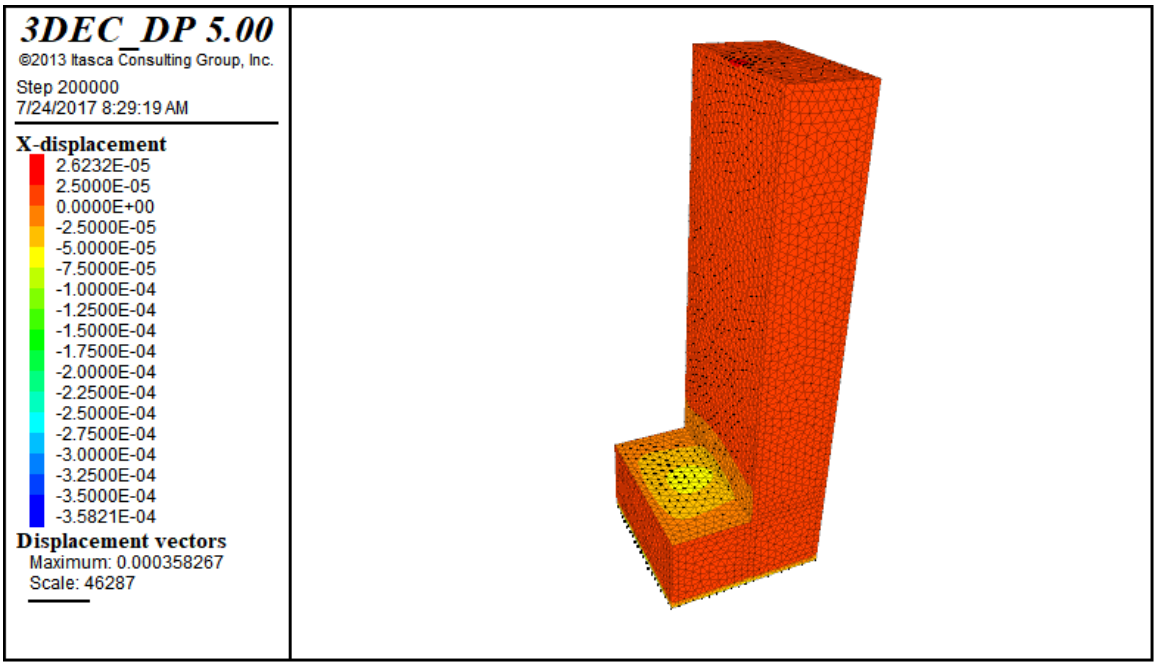

Figure A 8: The X-displacement contour for the 25 Hz stress wave on 500ft model

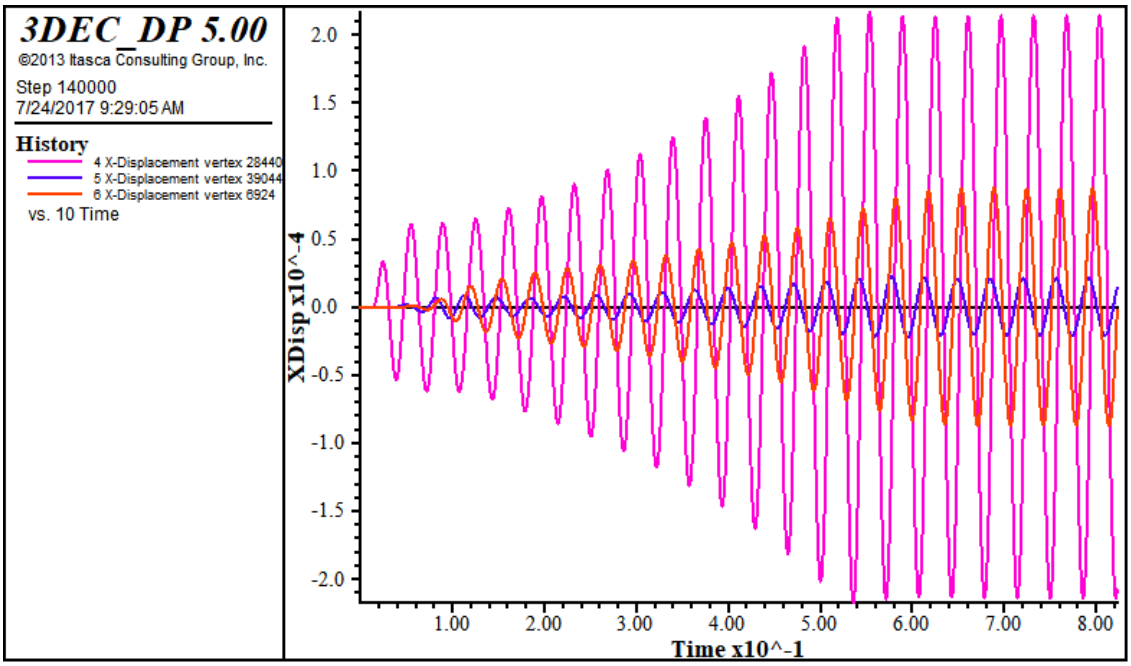

Figure A 9: The X-displacement time history for the 28 Hz stress wave on 500ft model

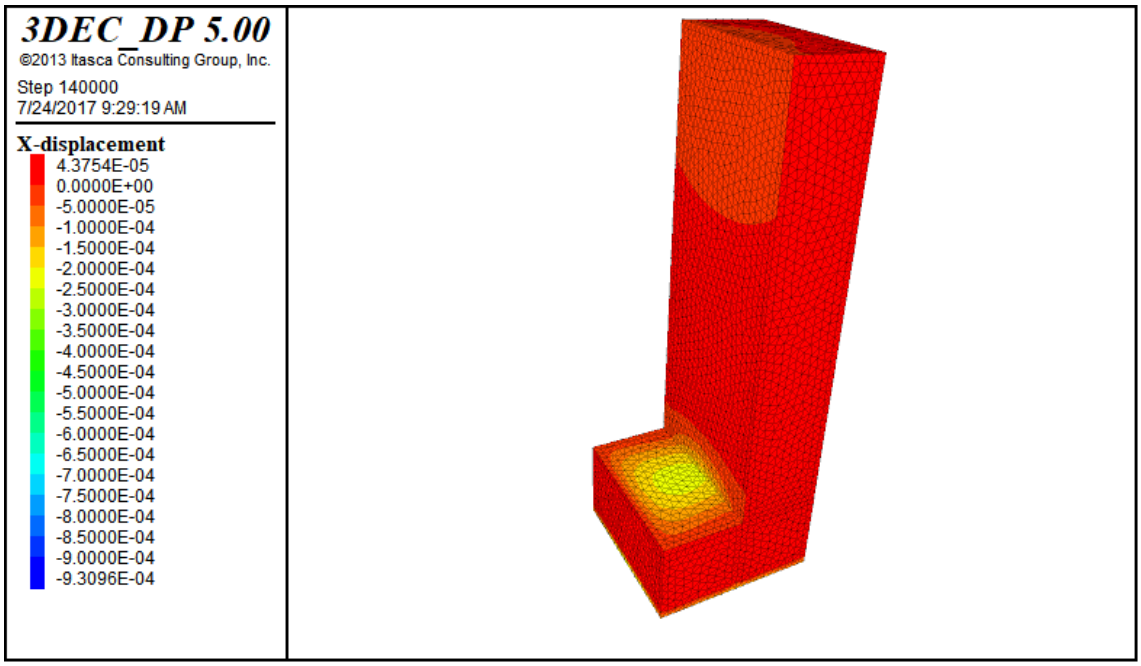

Figure A 10: The X-displacement contour for the 28 Hz stress wave on 500ft model

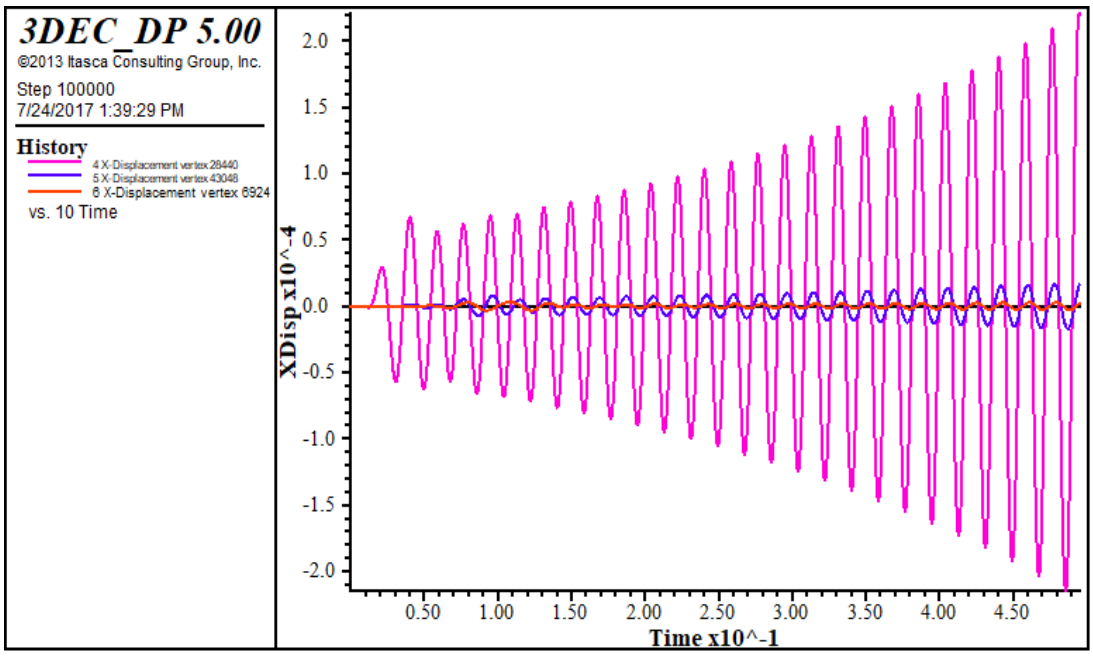

Figure A 11: The X-displacement time history for the 55 Hz stress wave on 500ft model

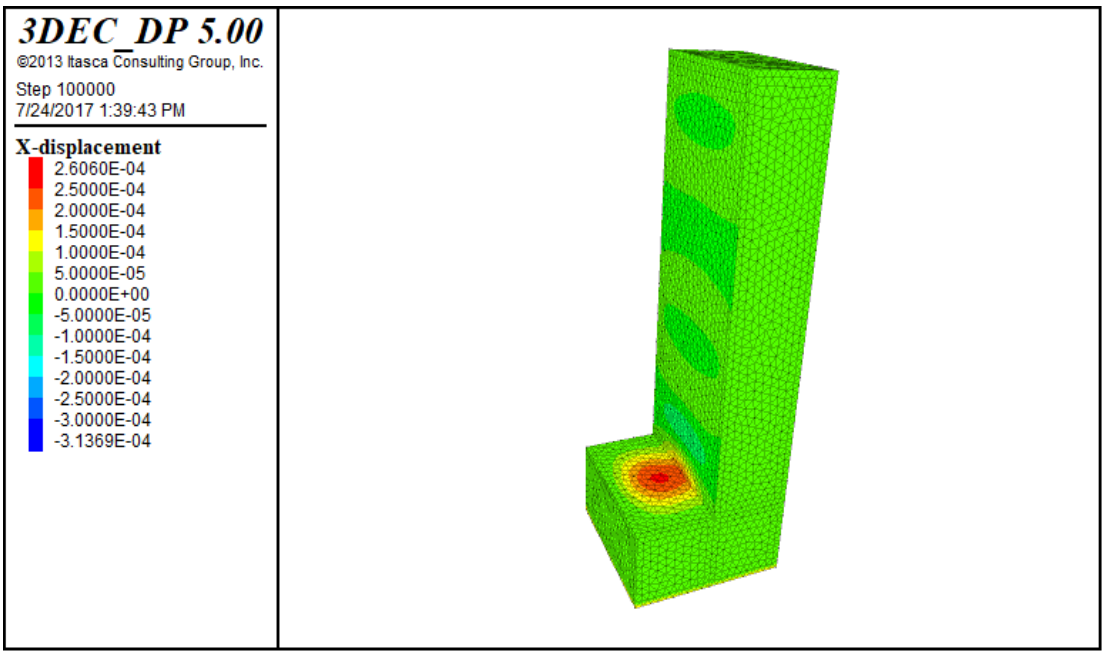

Figure A 12: The X-displacement contour for the 55 Hz stress wave on 500ft model

B. Variation in the natural frequency with the slope of high-wall

B1. Model: 100ft and 65 degrees

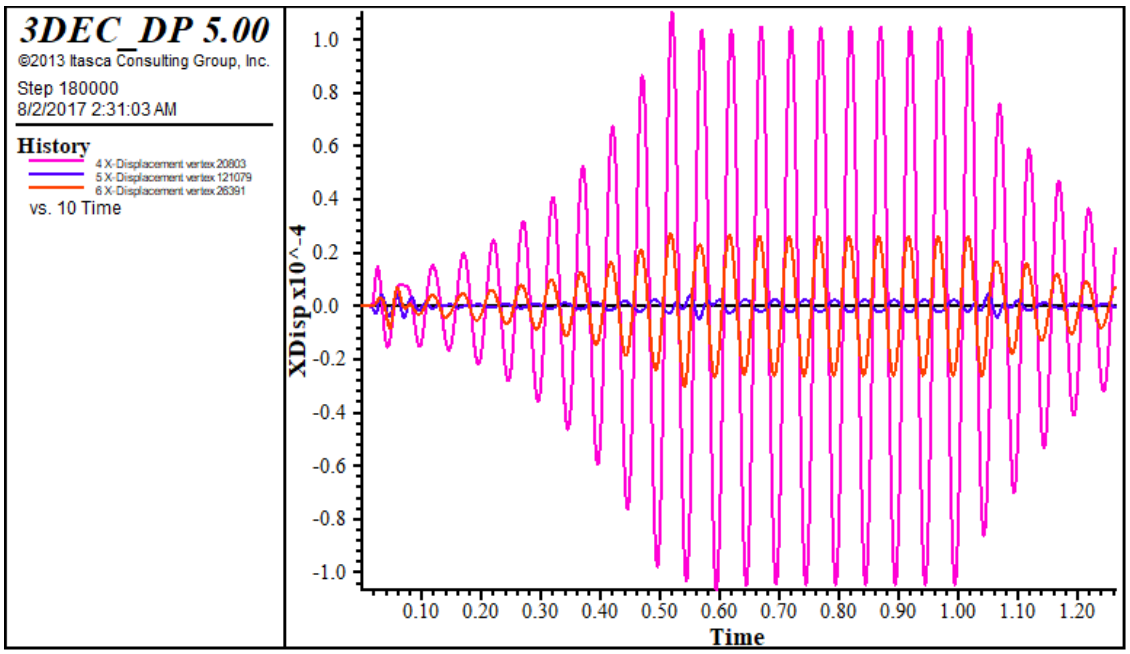

Figure B 1: The X-displacement time history for the 20 Hz stress wave on 100ft model

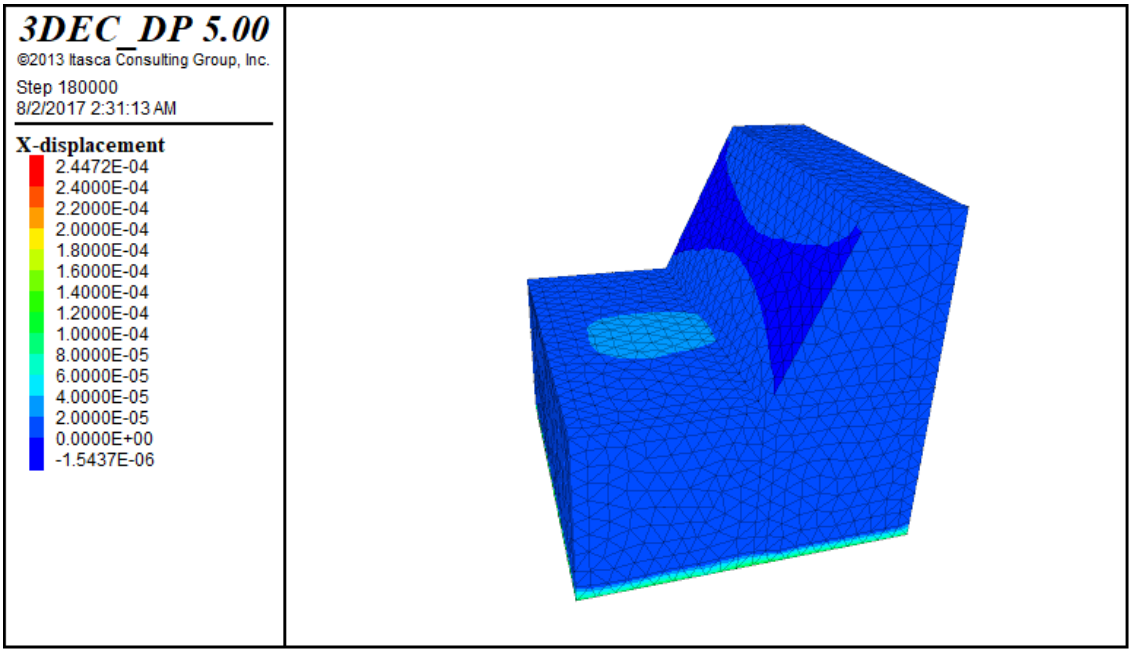

Figure B 2: The X-displacement contour for the 20 Hz stress wave on 100ft model

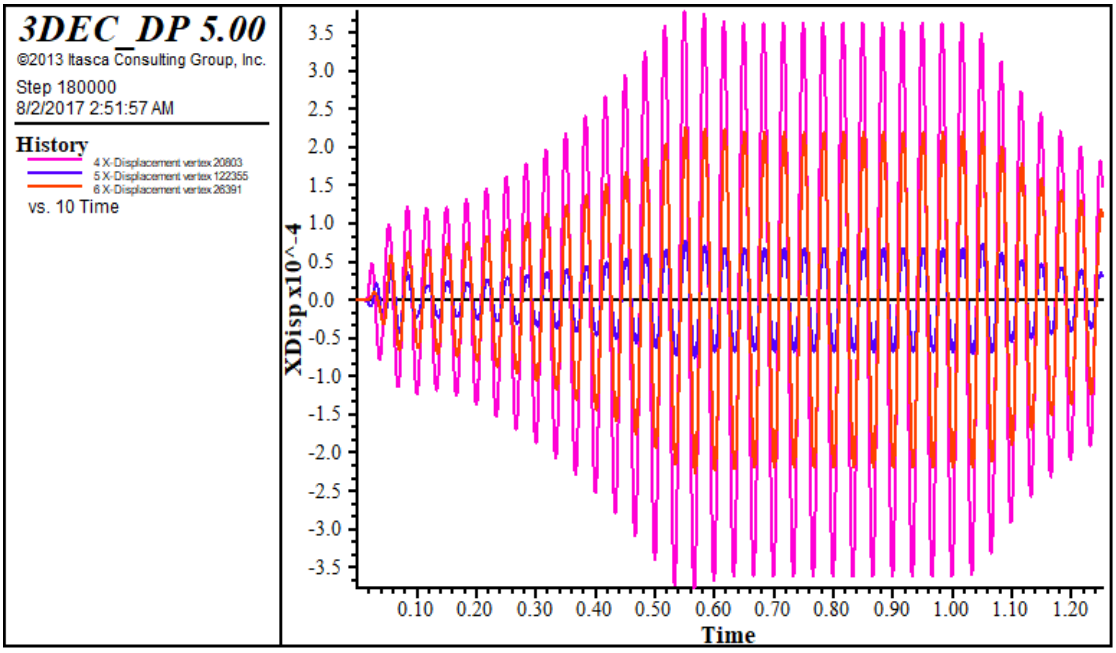

Figure B 3: The X-displacement time history for the 30 Hz stress wave on 100ft model

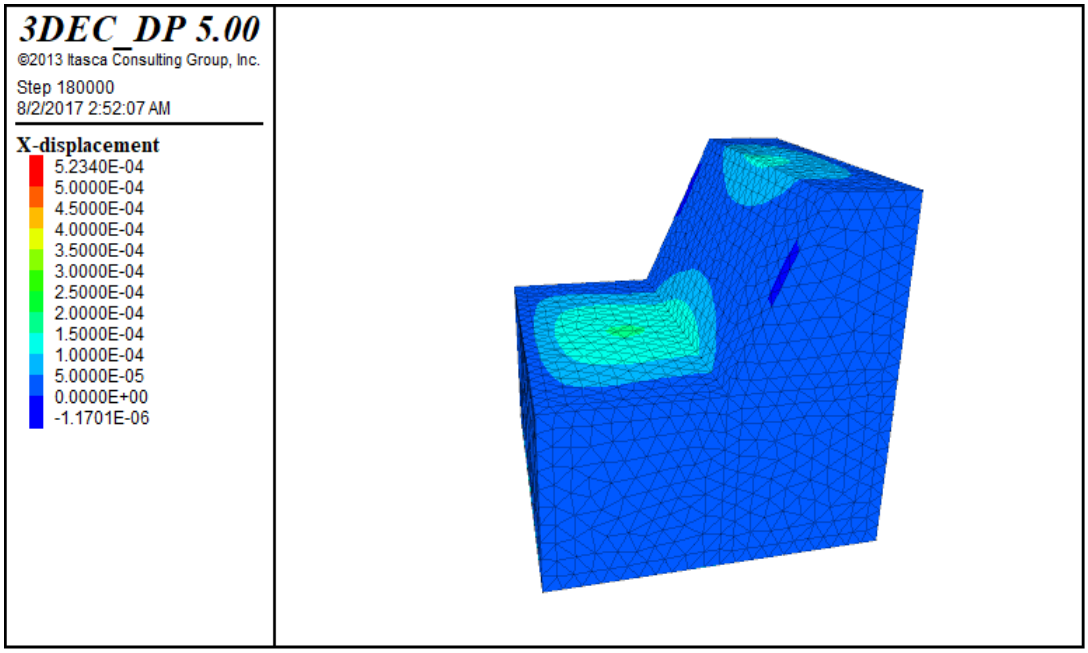

Figure B 4: The X-displacement contour for the 30 Hz stress wave on 100ft model

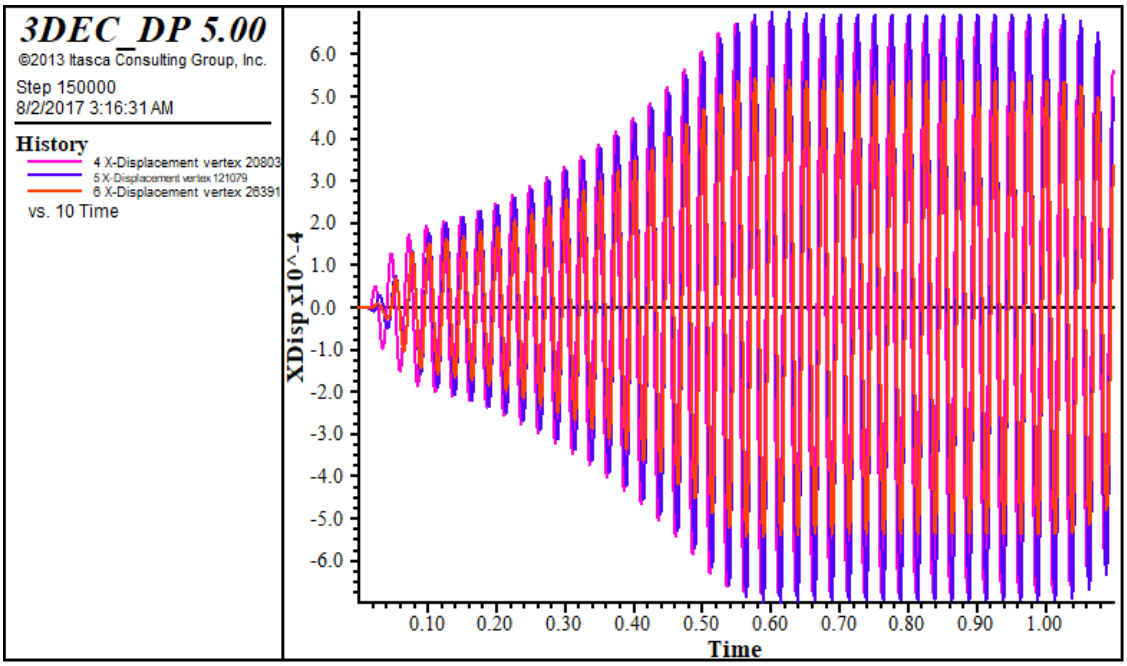

Figure B 5: The X-displacement time history for the 42 Hz stress wave on 100ft model

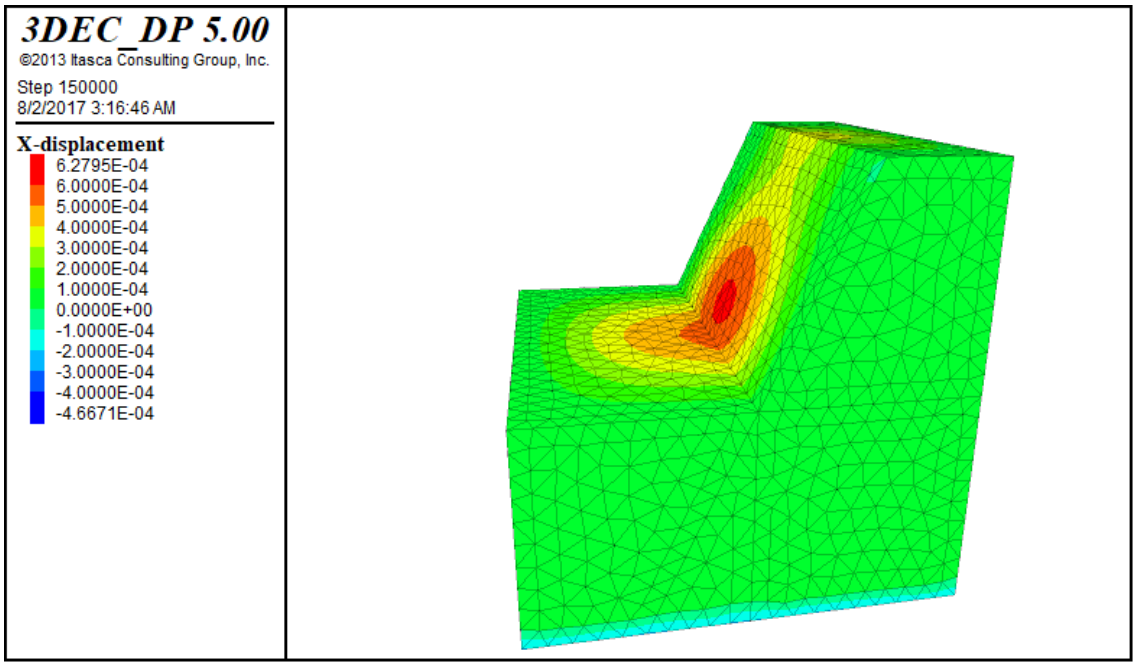

Figure B 6: The X-displacement contour for the 42 Hz stress wave on 100ft model

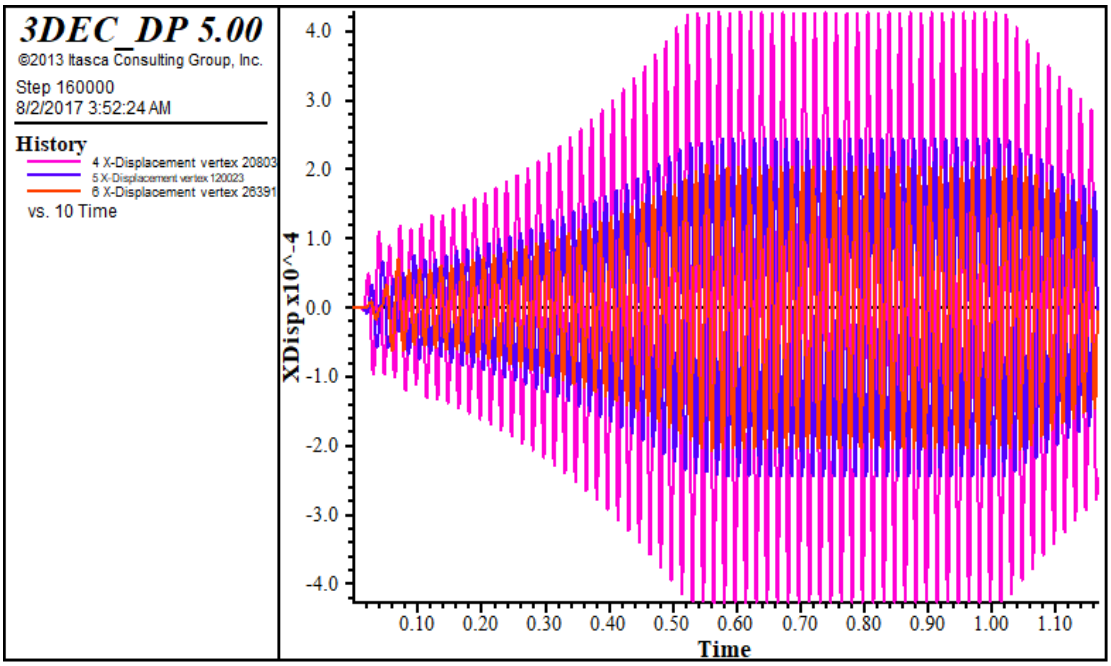

Figure B 7: The X-displacement time history for the 60 Hz stress wave on 100ft model

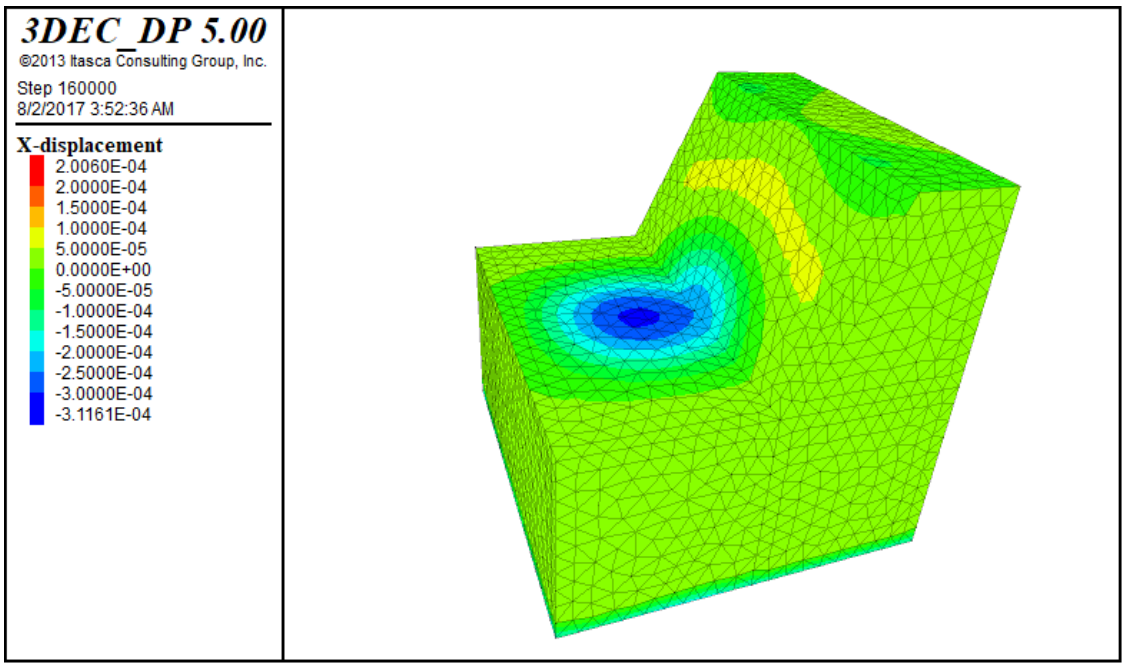

Figure B 8: The X-displacement contour for the 60 Hz stress wave on 100ft model

B2. Model: 100ft and 30 degrees

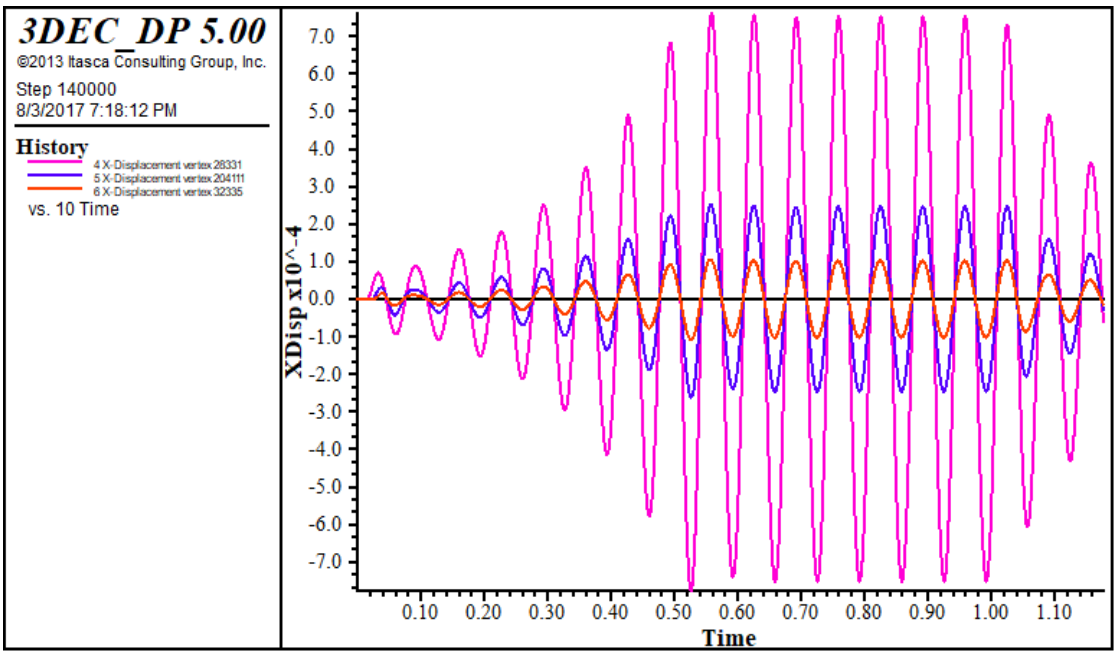

Figure B 9: The X-displacement time history for the 15 Hz stress wave on 100ft model

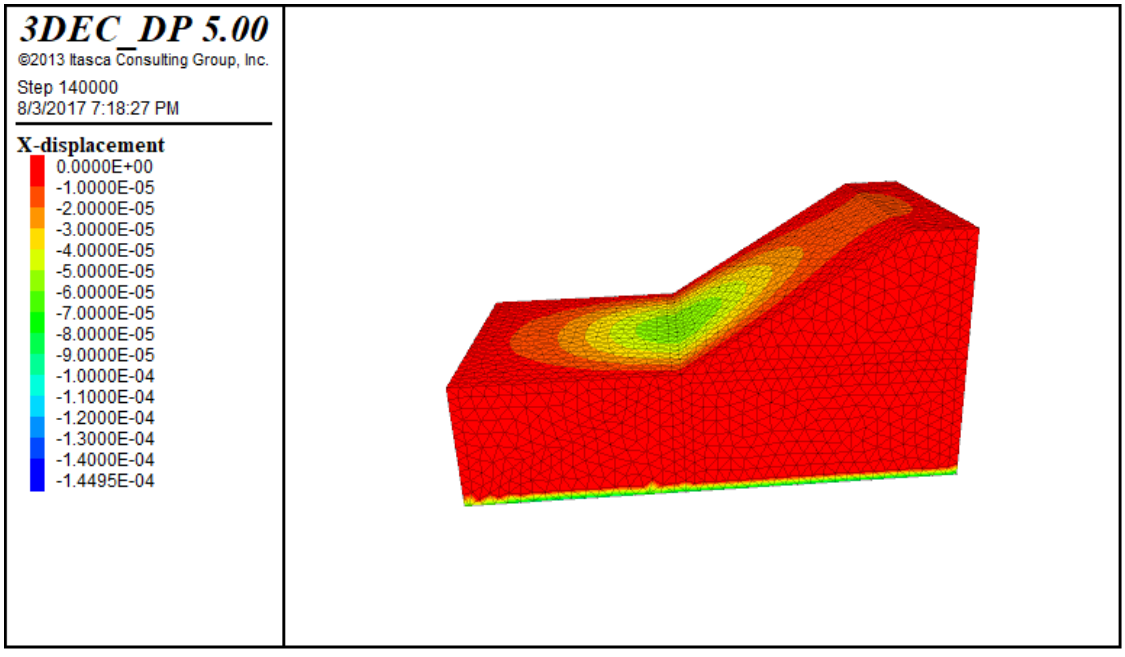

Figure B 10: The X-displacement contour for the 15 Hz stress wave on 100ft model

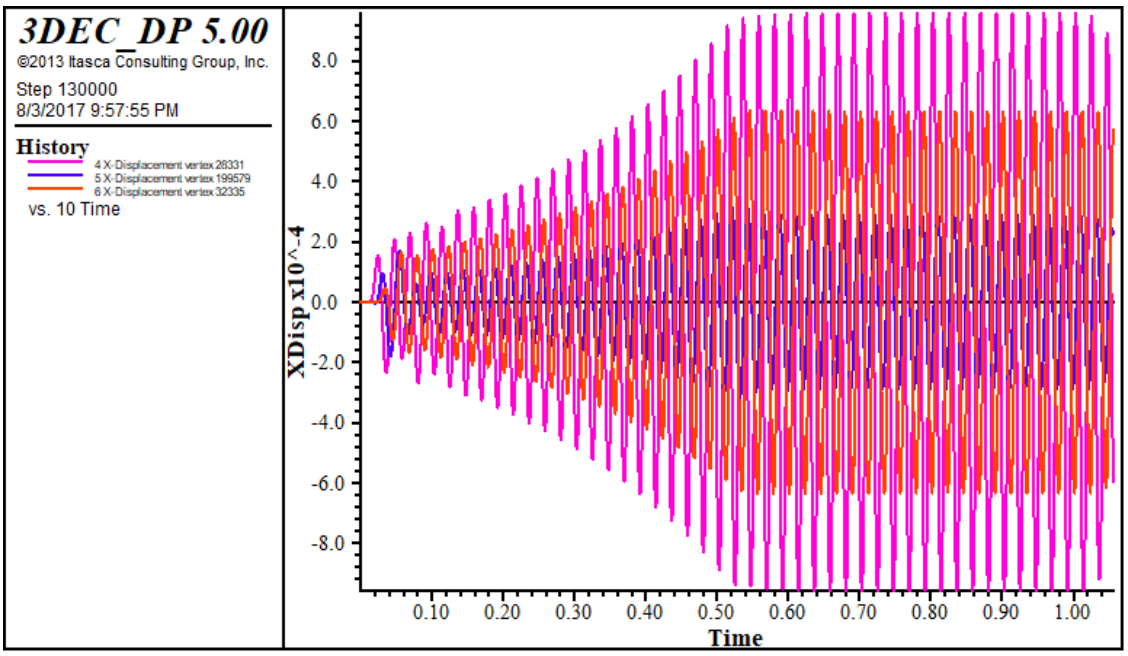

Figure B 11: The X-displacement time history for the 46 Hz stress wave on 100ft model

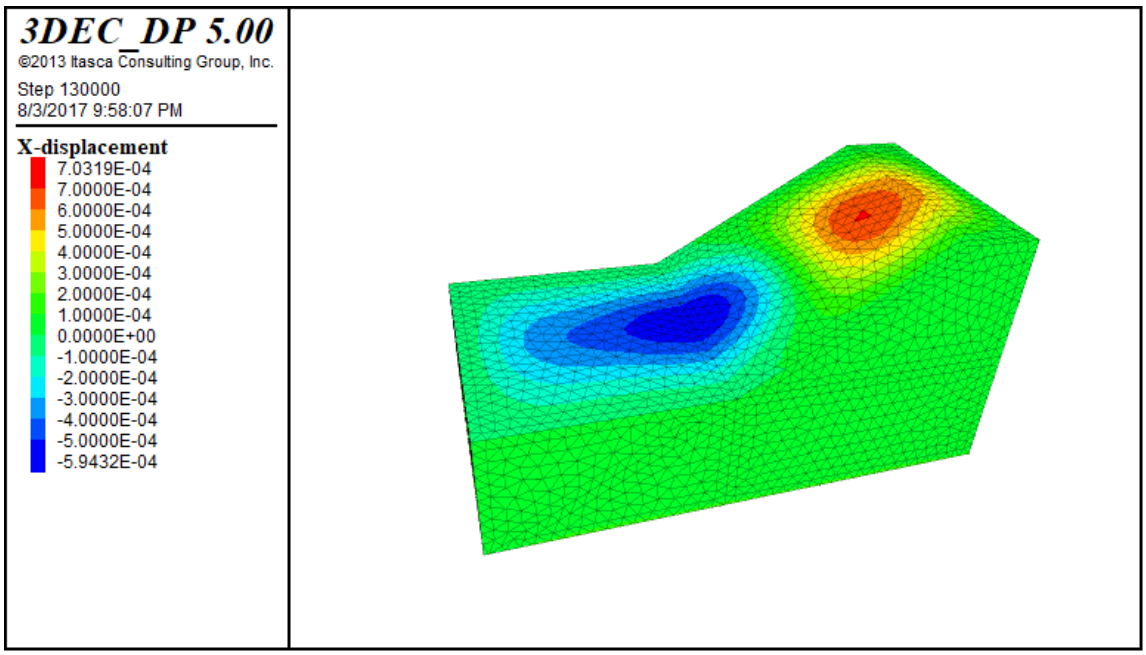

Figure B 12: The X-displacement contour for the 46 Hz stress wave on 100ft model

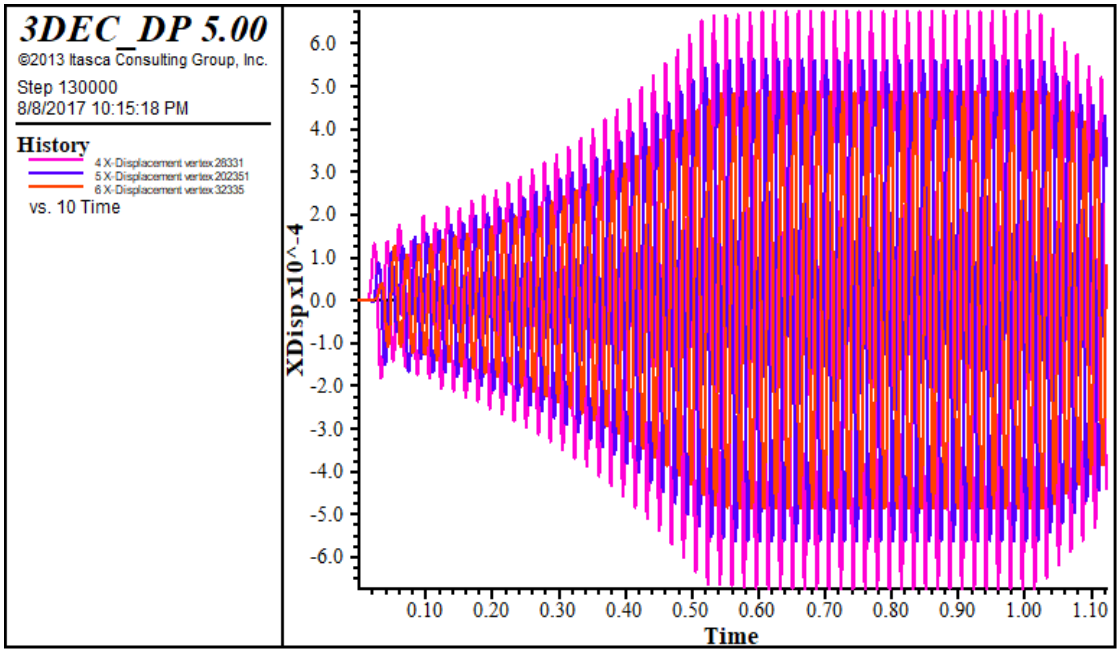

Figure B 13: The X-displacement time history for the 55 Hz stress wave on 100ft model

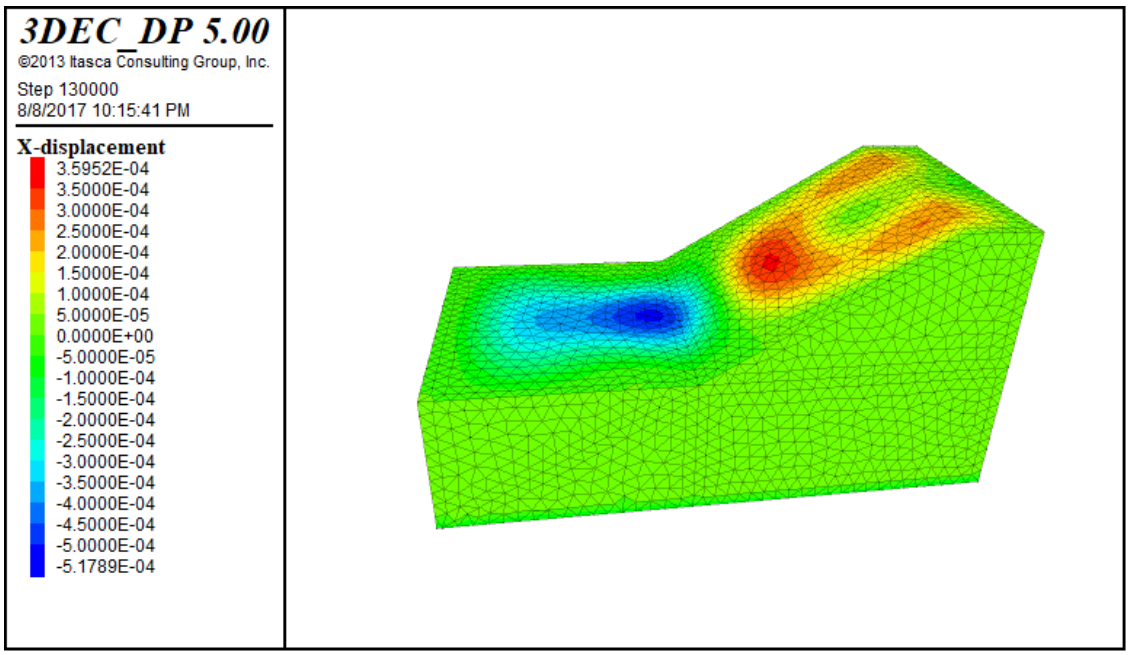

Figure B 14: The X-displacement contour for the 55 Hz stress wave on 100ft model

C. Variation in high-wall natural frequency with the amplitude of vibration

C1. Model: 100ft and 3 in/s Amplitude

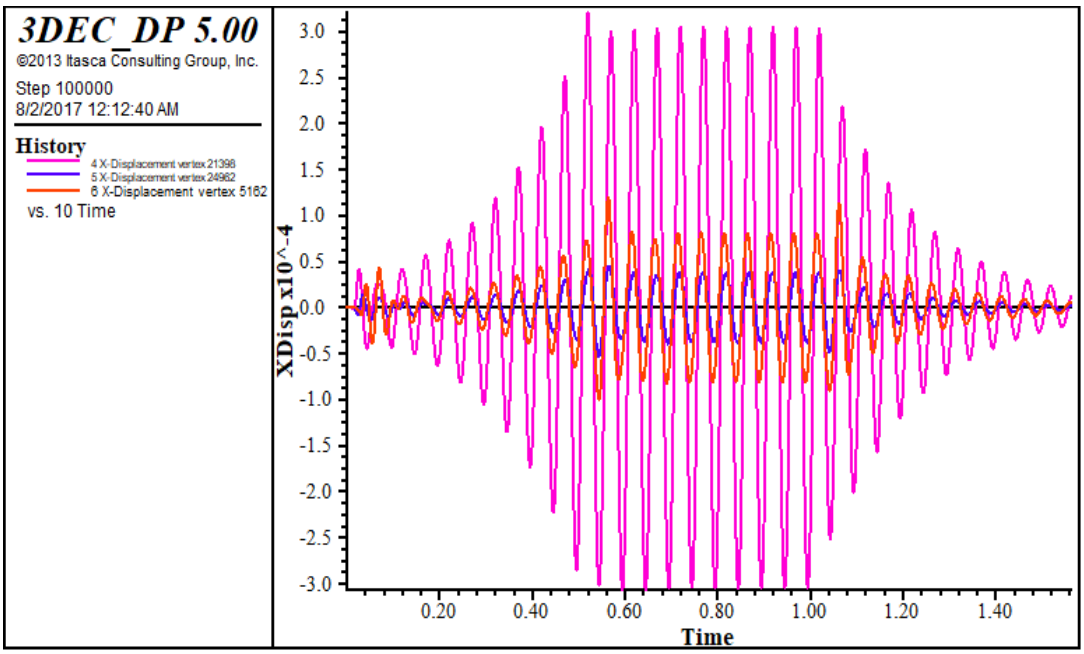

Figure C 1: The X-displacement time history for the 20 Hz stress wave on 100ft model

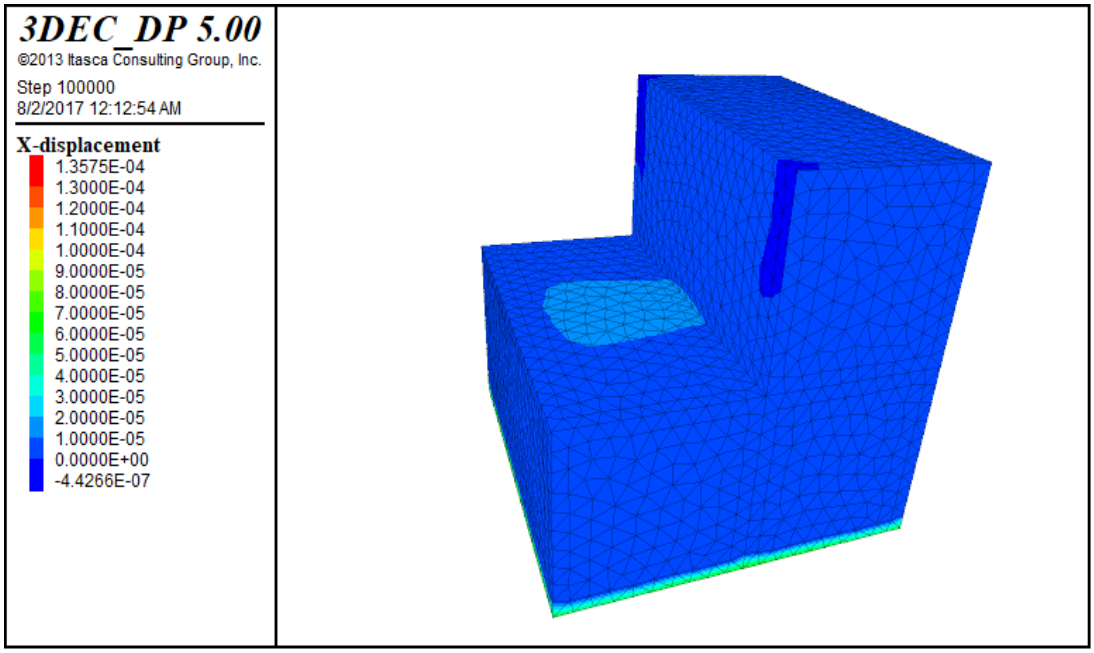

Figure C 2: The X-displacement contour for the 20 Hz stress wave on 100ft model

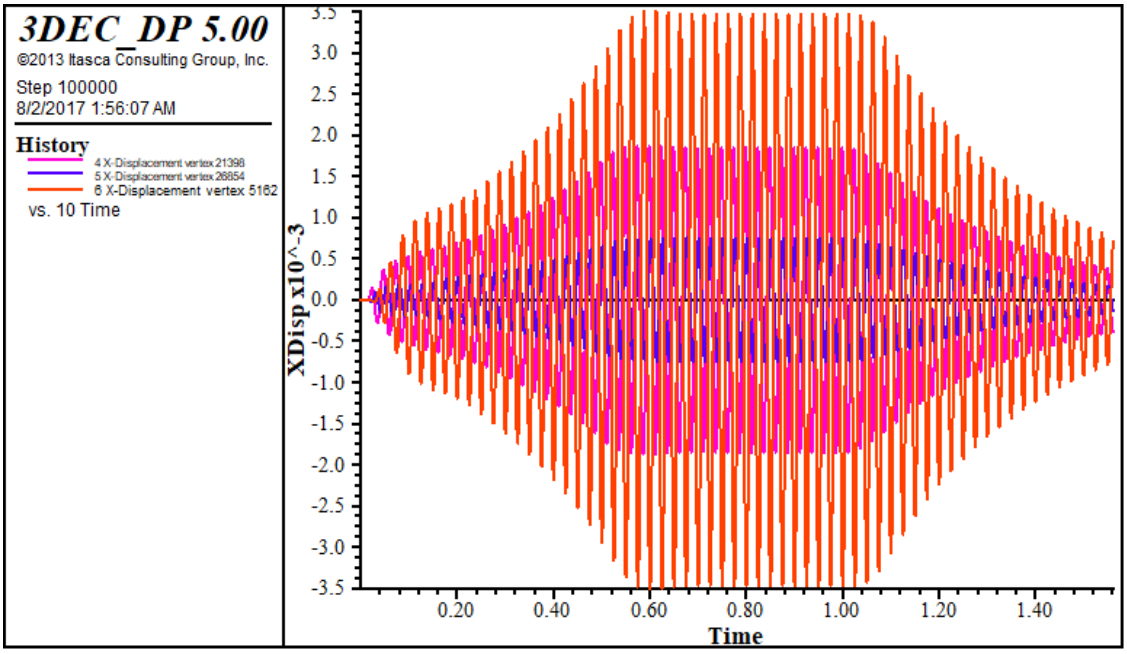

Figure C 3: The X-displacement time history for the 40 Hz stress wave on 100ft model

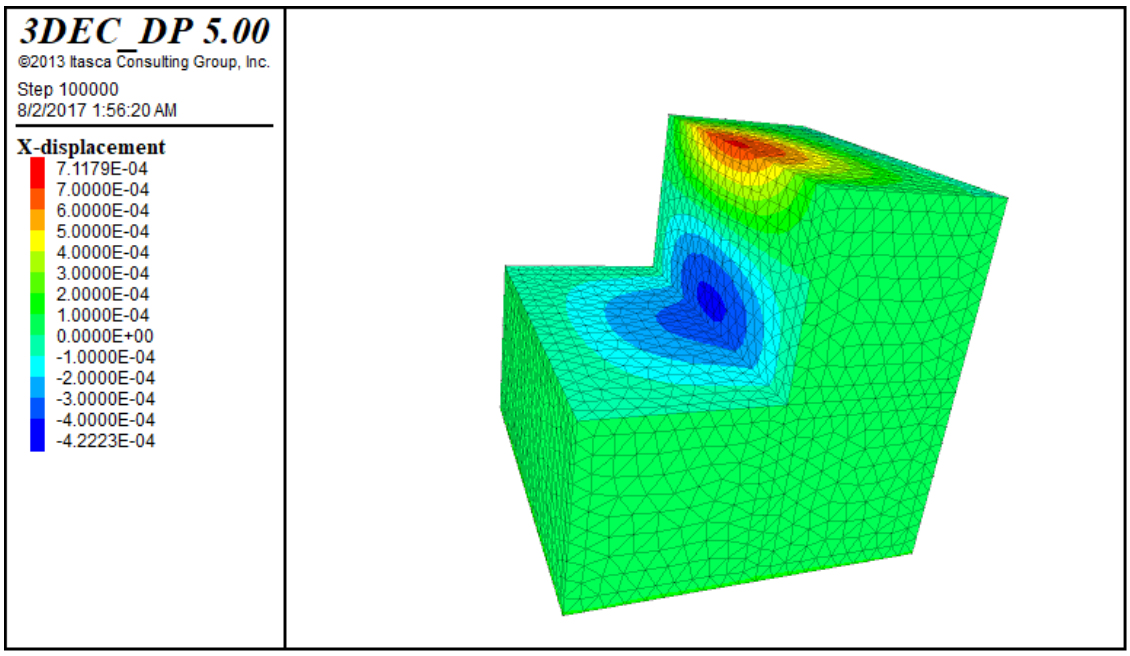

Figure C 4: The X-displacement contour for the 40 Hz stress wave on 100ft model

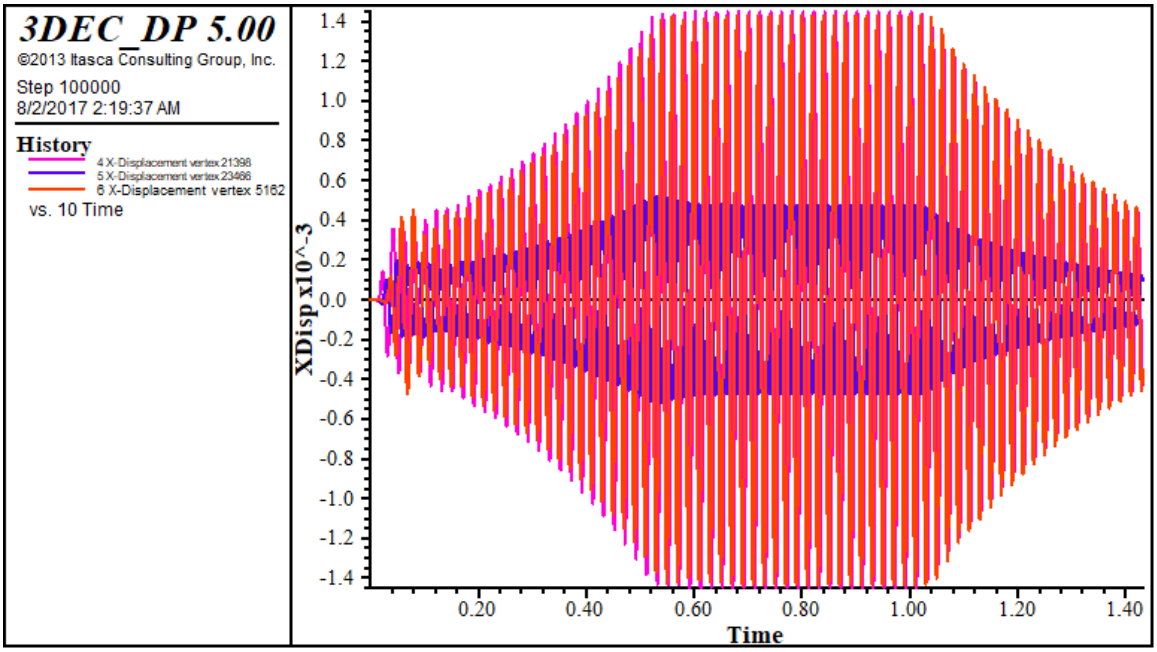

Figure C 5: The X-displacement time history for the 50 Hz stress wave on 100ft model

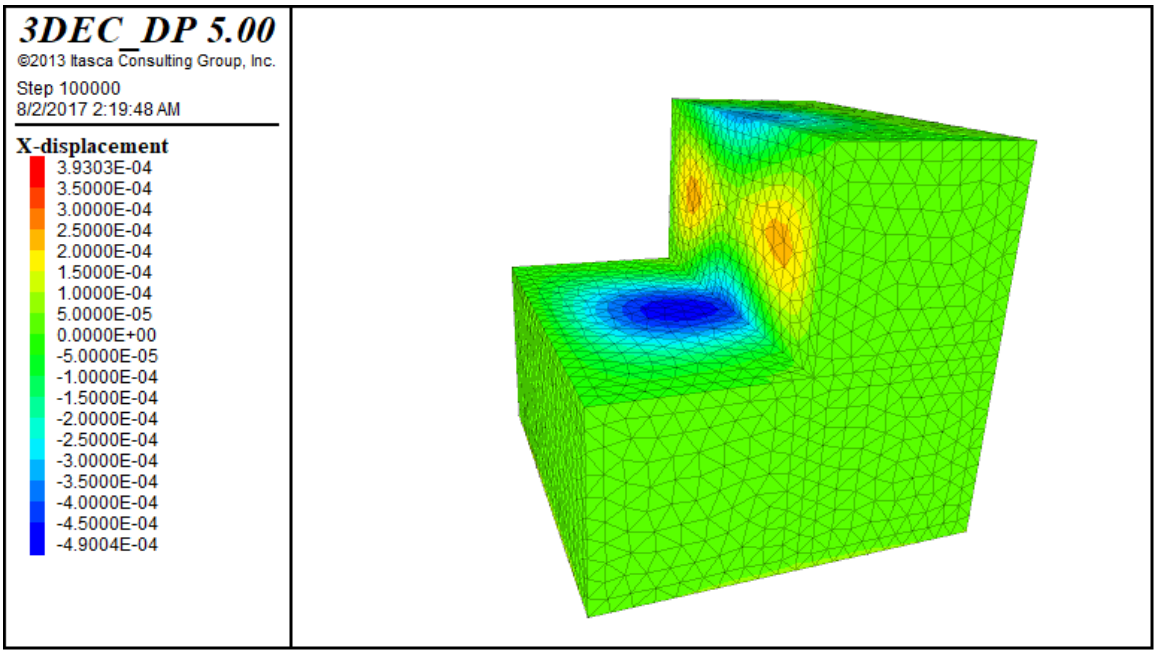

Figure C 6: The X-displacement contour for the 50 Hz stress wave on 100ft model

C2. Model: 100ft and 5 in/s Amplitude

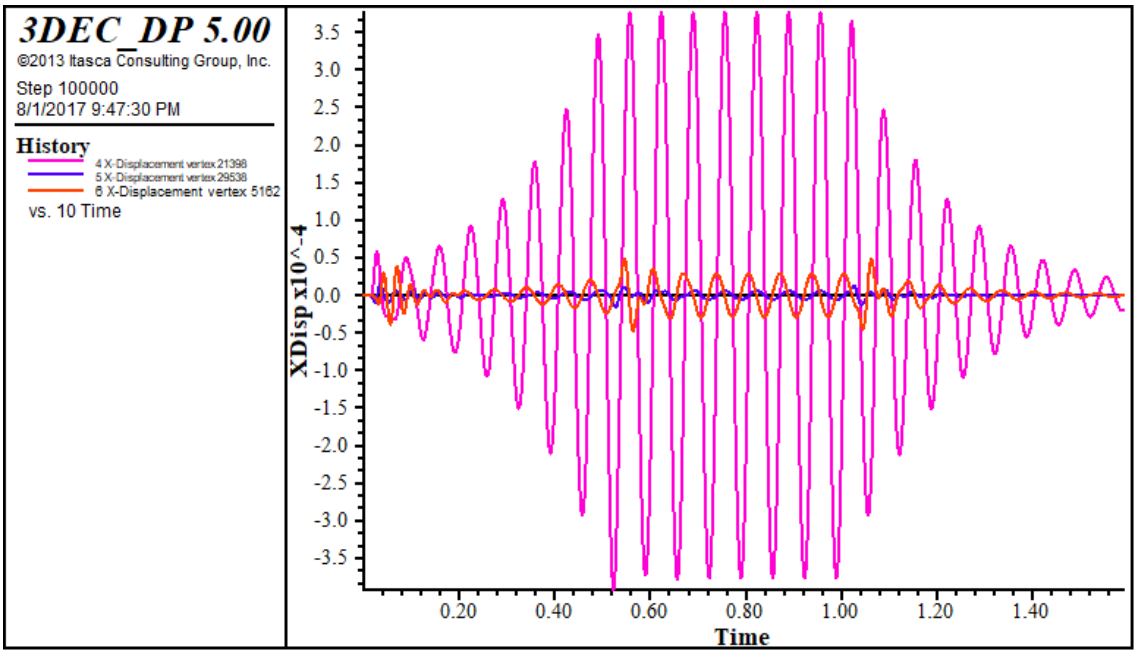

Figure C 7: The X-displacement time history for the 15 Hz stress wave on 100ft model

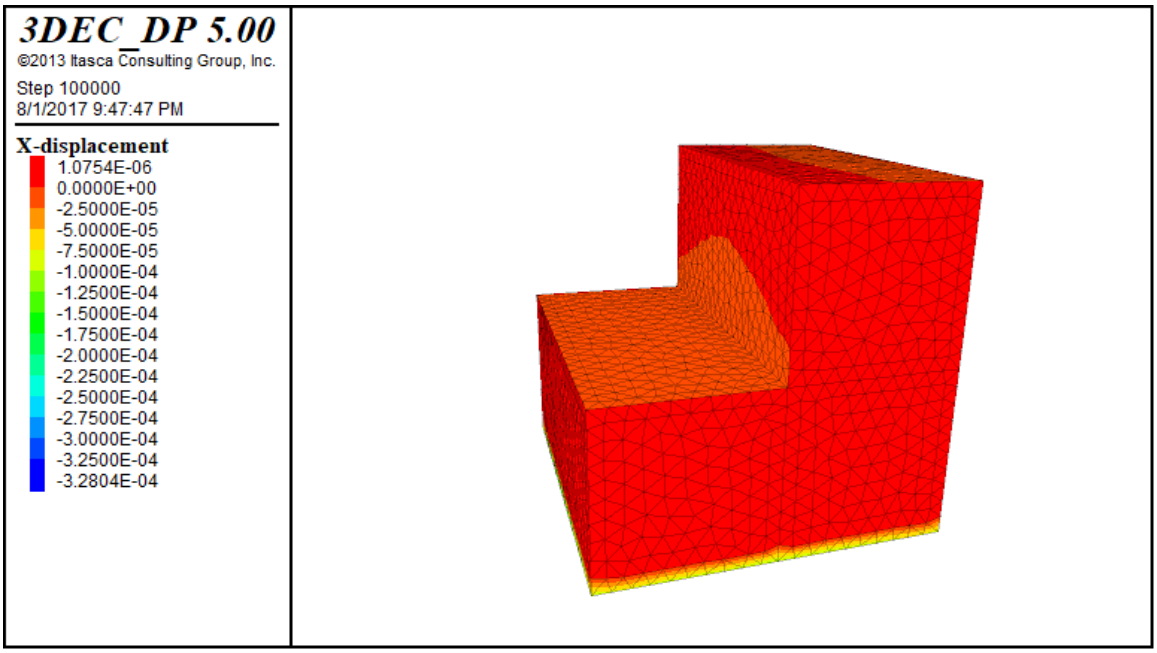

Figure C 8: The X-displacement contour for the 15 Hz stress wave on 100ft model

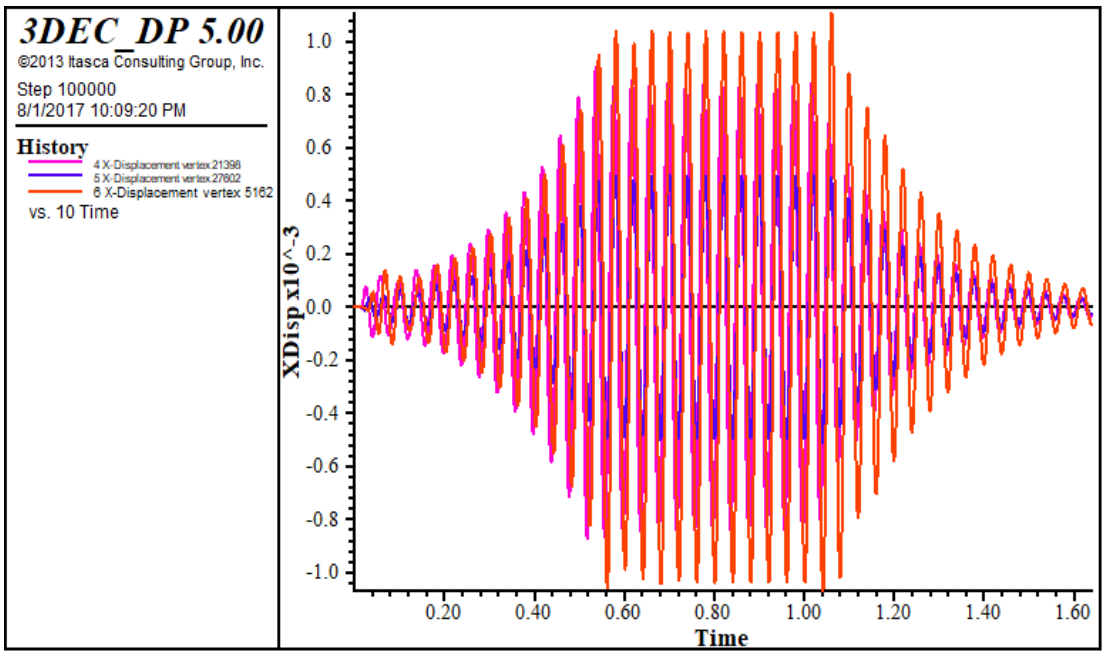

Figure C 9: The X-displacement time history for the 25 Hz stress wave on 100ft model

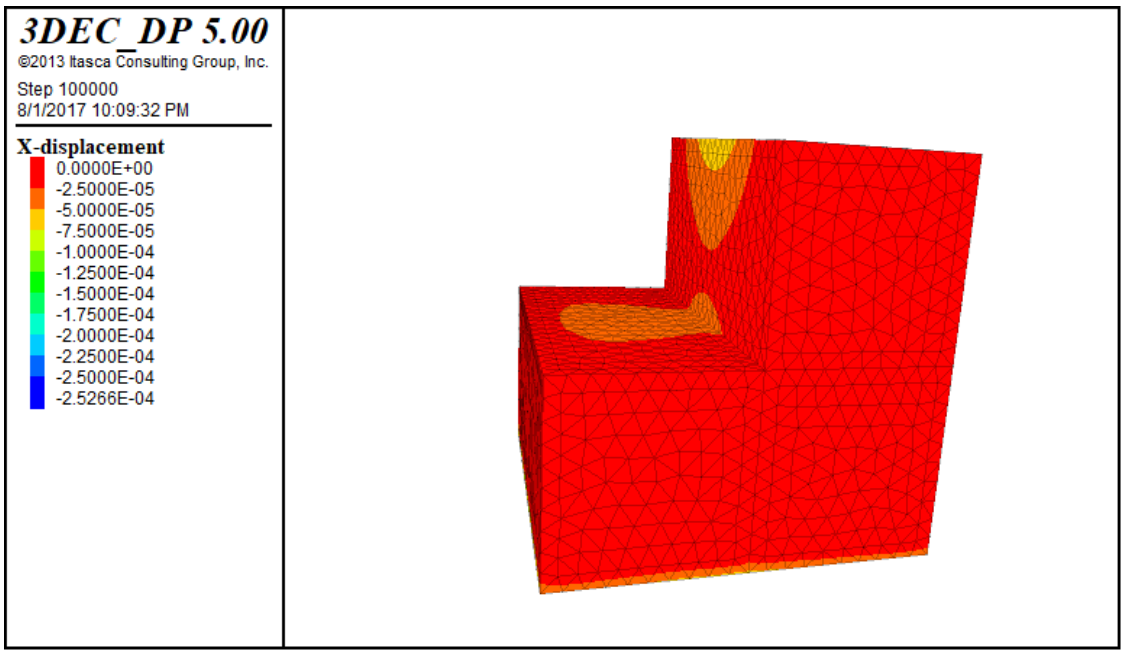

Figure C 10: The X-displacement contour for the 25 Hz stress wave on 100ft model

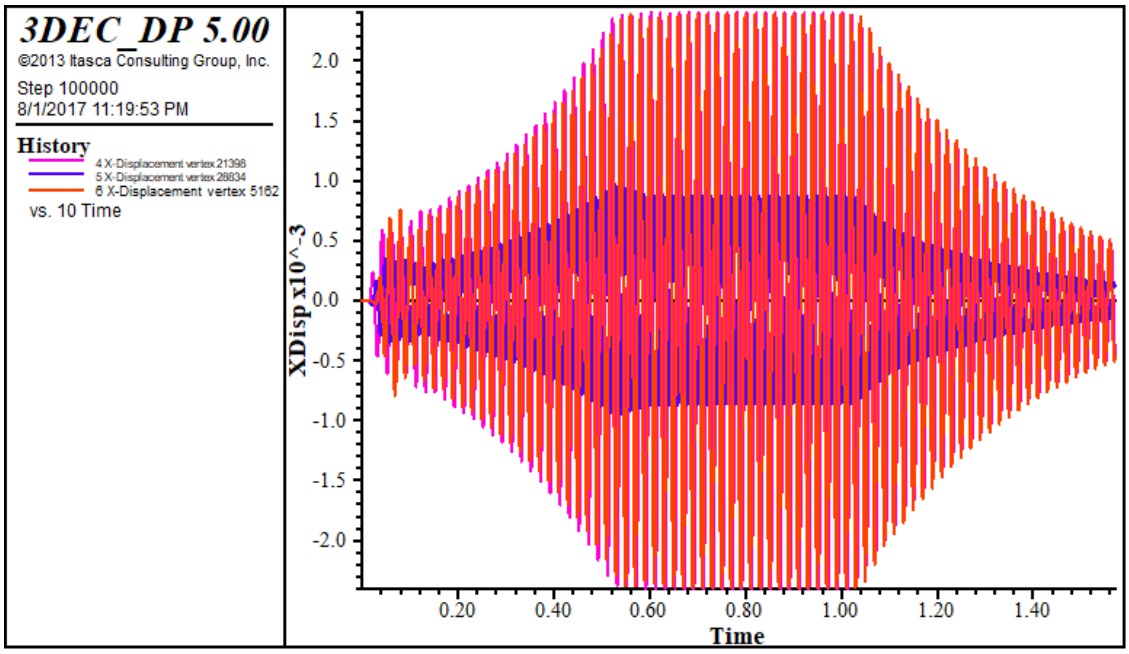

Figure C 11: The X-displacement time history for the 50 Hz stress wave on 100ft model

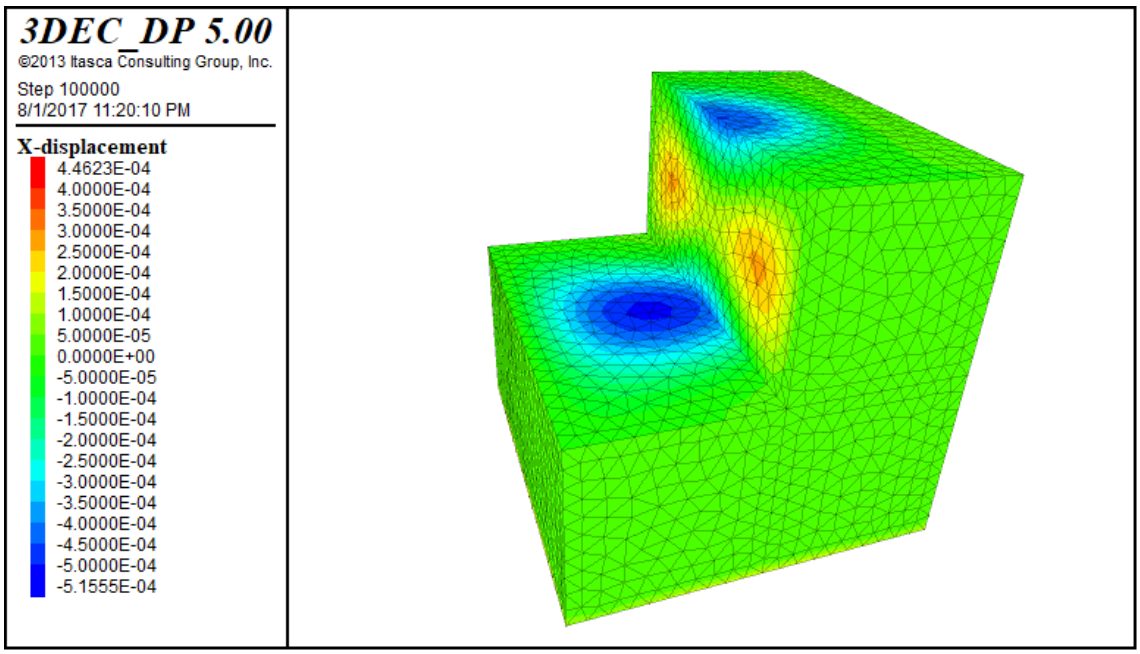

Figure C 12: The X-displacement contour for the 50 Hz stress wave on 100ft model

Bibliography

Ambraseys, N.N. and Menu J.M. (1998). Earthquake Induced Ground Displacements. *Journal of Earthquake Engineering 16,* 985-1006.

Anderson, D.A., Ritter, A.P., Winzer, S.R. and Reil, J.W. (1985). A method for site specific prediction and control of ground vibration from blasting. *Proceedings of the First Mini-Symposium on Explosives and Blasting Research, San Diego, CA,* 28-43.

Anderson, D.A. (1992g). Blast Vibration Frequencies What do they mean? *International Society of Explosives Engineers.*

Barla, G., Monacis, G., Perino, A. and Hatzor Y.H. (2010). Distinct element modelling in static and dynamic conditions with application to an underground archaeological site. *Rock Mechanics and Rock Engineering 43,* 877-890.

Christopherson, K.M. and Viterbo, V.C. (2011). Trim blasting designs in the Morenci Mine. *International Society of Explosives Engineers.*

Crum, S.V., Siskind, D.E. and Eltschlager K. (1992). Blast Vibration Measurements at Far Distances and Design Influences on Ground Vibrations. *International Society of Explosives Engineers,* 167-179.

Crum, S.V. and Pierce, W.E. (1995). House Responses to Low Frequency Ground Vibrations from Coal Mine Overburden Blasting: A Technical Update. *Proceedings of International Society of Explosives Engineers,* 76-88.

Crum, S.V. and Siskind, D.E. (2000). Response of Structures to Low-Frequency ground vibrations: A preliminary study. *International Society of Explosives Engineers.*

Damjanac, B., Varun and Lorig, L. (2013). Seismic Stability of Large Open Pit Slopes and Pseudo-Static Analysis. *Slope Stability, Australian Centre for Geomechanics, Perth,* 1203-1216.

Deng, X.F., Zhu, J.B., Chen, S.G. and Zhao, J. (2012). Some Fundamental Issues and Verification of 3DEC in Modeling Wave Propagation in Jointed Rock Masses. *Rock Mechanics and Rock Engineering,45,* 943-951.

Dowding, C.H. (1996). Construction Vibrations, *Prentice Hall*, 30-38.

Dunn, P. and Cocker, A. (1995). Pre-Splitting-Wall Control for Surface Coal Mines. *Proceedings Explo Conference*, 299-305.

Fang, H.Y. (1976). Field Studies of Structural Response to Blasting Vibrations and Environmental Effects. *Leigh University*.

Glass, C.E. (2000). The influence of seismic events on slope stability. *Slope Stability in Surface Mining, Society of Mining, Metallurgy and Exploration*, 97-105.

Halatchev, R. and Gabeva, D. (2017). Probabilistic analysis of seismic impact on open pit stability. *International Journal of Mining, Reclamation and Environment, 31:3*, 167-186.

Jiang, Q.H., Liu, X.H., Wei, W., et al. (2013). A new method for analyzing the stability of Rock Wedges. *International Journal of Rock Mechanics & Mining Sciences, 60*, 413-422

Jiao, Y.Y., Zhang, X.L., Zhao, J. (2007). Viscous Boundary of DDA for Modeling Stress Wave Propagation in Jointed Rock. *International Journal of Rock Mechanics and Mining Sciences, 44(7)*, 1070-1076.

Kramer, S.L. and Smith, M.W. (1997). Modified Newmark Model for Seismic Displacements of Compliant Slopes. *Journal of Geotechnical and Geoenvironmental Engineering*, 635-644.

Kuhlemeyer, R.L. and Lysmer, J. (1973). Finite element method accuracy for Wave Propagation Problems. *Journal of Soil Mechanics and Foundations Division, Proceedings of the American Society of Civil Engineers, Vol.99*, 421-427.

Lin, J.S. and Whitman, R. (1986). Earthquake Induced Displacements of Sliding Blocks. *Journal of Geotechnical Engineering*, 44-59.

Liu, H. L., Fei, K., and Gao, Y.F. (2003). Time History Analysis Method of Slope Seismic Stability. *Rock and Soil Mechanics, 24 (4)*, 553-557.

Lysmer, J. and Kuhlemeyer, R.L. (1969). Finite Dynamic Model for Infinite Media. *Journal of the Engineering Mechanics Division, American Society of Civil Engineers, Vol.95*, 859-877.

Ni, W., Tang, H., Liu, X., Yong, R. and Zou, Z. (2013). Dynamic Stability Analysis of Wedge in Rock Slope Based on Kinetic Vector Method. *Journal of Earth Science, 25 (4),* 749-756.

Pal, S., Kaynia, A.M., Bhasin, R.K., et.al., (2012). Earthquake Stability Analysis of Rock Slopes: A Case Study. *Rock Mechanics and Rock Engineering, 45 (2),* 205-215.

Preece, D.S., Pilz, J. and Zavodni, Z.M. (2010). Peak Particle velocity versus gravitational acceleration as a Stability Criterion for earth retaining walls subjected to production blast vibrations. *International Society of Explosives Engineers.*

Pierce, W.E., Crum, S.V. and Siskind, D.E. (1996). Assessment of Low-Frequency Blast Vibrations and Potential Impacts on Structures. *Contract Research Report by the U.S. Bureau of Mines for the office of Surface Mining, Reclamation and Enforcement,* 22.

Sarma, S. (1979). Stability analysis of embankments and slopes. *Journal of Geotechnical Engineering Division, ASCE 105(12),* 1511-1523.

Sharma, A., Pandey, S., Mishra, S. et al. (2013). Unlocking iron ore by controlling environmental using electronic blasting systems. *7th Congress-European Federation of Explosives Engineers.*

Shiguo, X., Wenkai, F. and Jianjing, Z. (2010). Analysis of the effects of Slope Geometry on the dynamic response of a near-field mountain from the Wenchuan Earthquake. *Science Press and Institute of Mountain Hazards and Environment, CAS and Springer*, 353-360.

Shipley, S.A., Leistner, H.G. and Jones, R.E. (1967). Elastic Wave Propagation-A comparison between Finite Element Predictions and Exact Solutions. *Proceedings International Symposium on Wave Propagation and Dynamic Properties of Earth Materials, University of New Mexico Press,* 509-519.

Siad, L. (2003). Seismic Stability Analysis of Fractured Rock Slopes by Yield Design Theory. *Soil Dynamics and Earthquake Engineering, 23(3),* 203-212.

Singh, V.K. and Singh, D.P. (1995). Controlled blasting in an Open-pit Mine for improved Slope Stability. *Geotechnical and Geological Engineering,* 51-57.

Siskind, D.E., Stagg, M.S, Kopp, J.W. and Dowding, C.H. (1980). Structure response and damage produced by ground vibration from surface mine blasting. *United States Bureau of Mines RI 8507*, 74.

Siskind, D.E., Stachura, V.J. and Nutting, M.J. (1987). Low-Frequency Vibrations Produced by Surface Mining Blasting over Abandoned Underground Mines. *United States Bureau of Mines RI 9078.*

Siskind, D.E. (1998). Ground Vibration effects on Structures. *International Society of Explosives Engineers.*

Stianson, J.R., Fredlund, D.G., Chan, D. (2011). Three-dimensional slope stability based on stresses from a stress-deformation analysis. *Canadian Geotechnical Journal, 48,* 891-904.

Tose, S.J. (2011). A review of the design criteria and practical aspects of developing a successful Pre-Split. *International Symposium on Stability of Rock Slopes in Open Pit Mining and Civil Engineering,* 525-546.

White, T., Farnfield, R. and Kelly, M. (1993b). The effects of Surface Mine Blasting on Buildings. *Proceedings 4th International Symposium on Rock Fragmentation by Blasting,* 105-111.

Vazquez, J.R. and Fernandez, E.G. (1986R). Progress in studying low frequency vibration waves caused by blasting. *International Society of Explosives Engineer*, 72-80.

Yang, R., Whitaker, T. and Kirkpatrick, S. (2009). PPV Management and frequency shifting in soft ground near high-walls to reduce blast damage. *International Society of Explosives Engineers.*

Zdazinsky, C. (2016). Preserving High-wall Stability by Shifting the Dominant Blast Vibration Frequency with Electronic Initiation. *International Society of Explosives Engineers.*

Zhao, T., Sun, J., Zhang, B. and Li, C. (2011). Analysis of Slope Stability with Dynamic Overloading from Earthquake. *Journal of Earth Science, Vol.23, No.3,* 285-296

VITA

Abhinav was born in the Jaipur City of the Rajasthan in India. He earned his Bachelors of Technology degrees in Mining Engineering with first class honors from the Indian Institute of Technology, Varanasi in 2010. He was then employed at the Orica-Mining Services, where he worked for more than five years in various capacities. Before, embarking on his journey with the Department of Mining Engineering with the University of Kentucky in 2015. He was working as Technical Services Lead, spearheading a team of engineers to execute mining projects. During his career, both in academic and industrial settings he published seven papers at national and international levels. In the department of Mining Engineering, he worked as a graduate research assistant under Dr. Jhon Silva-Castro. He expects to graduate with a Master of Science degrees in Mining Engineering in December 2017.